MODELING OF NANOCELLULOSE HYDROGEL COATINGS ON TEXTILE SUBSTRATES AND ENZYMATIC MODIFICATION OF NANOCELLULOSE COATINGS FOR SUSTAINABLE DYEING

by

RAHA SAREMI

(Under the Direction of Sergiy Minko and Suraj Sharma)

ABSTRACT

We have developed nanocellulose based thin films as functional coatings for textile materials. Nanocellulose thin films can incorporate many functionalities such as dye, antimicrobial, flame-retardant and stain-resistant molecules and transfer them to textile surfaces. To develop efficient and robust nanocellulose coatings, we studied multilayer model substrates of nanofibrillated cellulose (NFC) and nanocrystalline cellulose (NCC) on top of regenerated cellulose, polyester and nylon 66 on silicon wafers to mimic textile surfaces to investigate and improve the adhesion of nanocellulose toward natural and synthetic fibers. The thickness of the films and their surface morphology were studied by ellipsometry, Scanning Electron Microscopy, and Atomic Force Microscopy. The adhesion strength between the NFC and NCC gels and natural, synthetic and blended fabrics were investigated by using a T-Peel strength test.

We incorporated dye molecules to the nanocellulose coatings that we developed previously to create a sustainable and environmentally friendly dyeing technology with comparable dyeing performance to conventional dyeing technique. To enhance dyeability of nanocellulose, they were treated with cellulases from *Trichoderma reesei* and enzymogel nanoparticles. The enzymatic

treatments change surface area and crystallinity of the hydrogels by slowly degrading crystalline region and impurities in the primary cell wall and consequently improve dyeability of nanocellulose materials.

INDEX WORDS: Nanocellulose, Thin films, Coatings, Enzymatic treatment, Sustainable Dyeing Method

MODELING OF NANOCELLULOSE HYDROGEL COATINGS ON TEXTILE SUBSTRATES AND ENZYMATIC MODIFICATION OF NANOCELLULOSE COATINGS FOR SUSTAINABLE DYEING

by

RAHA SAREMI

B.S., Amirkabir University of Technology Tehran Polytechnic, Iran, 2007

M.S., Amirkabir University of Technology Tehran Polytechnic, Iran, 2009

A Dissertation Submitted to the Graduate Faculty of The University of Georgia in Partial Fulfillment of the Requirements for the Degree

DOCTOR OF PHILOSOPHY

ATHENS, GEORGIA

2017

MODELING OF NANOCELLULOSE HYDROGEL COATINGS ON TEXTILE SUBSTRATES AND ENZYMATIC MODIFICATION OF NANOCELLULOSE COATINGS FOR SUSTAINABLE DYEING

by

RAHA SAREMI

Major Professor:	Sergiy Minko Suraj Sharma
Committee:	Patricia A. Annis Jin Xie

Electronic Version Approved:

Suzanne Barbour
Dean of the Graduate School
The University of Georgia
December 2017

DEDICATION

This dissertation work is dedicated to my loving husband, M. Reza, for his unconditional love, remarkable patience and constant support. To the memory of my beloved grandmother, whom I love and miss every day, and to my dear parents, for their unconditional love and support.

ACKNOWLEDGEMENTS

Sincere appreciation and gratitude are extended to my advisor, Dr. Sergiy Minko, for his constructive criticism, insightful guidance and immense help and support throughout my Ph.D. studies. I am very grateful to my co-advisor Dr. Suraj Sharma, for his invaluable support, constant encouragement, and guidance throughout my doctoral work. I would also like to acknowledge the members of my committee: Dr. Patti Annis, and Dr. Jin Xie for providing valuable suggestions, ideas, and their support.

TABLE OF CONTENTS

Page

LIST OF TABLES viii

LIST OF FIGURES ix

CHAPTER 1 INTRODUCTION AND LITERATURE REVIEW 1

1.1 Production 2

1.2 Structure and properties 10

1.3 Application 16

1.4 Nanocellulose Coatings 17

1.5 Sustainable Textile Dyeing 17

1.6 Research Objectives 21

1.7 References 22

CHAPTER 2 NANOCELLULOSE THIN FILMS AS SUSTAINABLE FUNCTIONAL COATINGS FOR TEXTILE MATERIALS 39

2.1 Introduction 41

2.2 Experimental Section 43

2.3 Results and Discussion 48

2.4 Summary 51

2.5 References 53

2.6 Supporting Information 65

CHAPTER 3 ENZYMATIC TREATMENTS OF NANOCELLULOSE HYDROGELS FOR SUSTAINABLE DYEING TECHNOLOGY 97

3.1 Introduction 99

3.2 Experimental Section 101

3.3 Results and Discussion 105

3.4 References 111

CHAPTER 4 SUMMARY AND FUTTURE WORK 126

4.1 Summary 126

4.2 Future Work 127

LIST OF TABLES

Page

Table 1.1. Nanocellulose types, sources, and main production methods 2

Table 2.1. Thickness of regenerated cellulose films treated with PEI..... 61

Table 2.2. Thickness of polyester films treated with PEI and total area (%) of control film 61

Table 2.3. Thickness of Nylon films treated with PEI and total area (%) of control film..... 61

Table 2.4. Thickness of regenerated cellulose films treated with P(GMA-OEGMA)..... 61

Table 2.5. Thickness of polyester films treated with P(GMA-OEGMA) and total area (%) of control film..... 61

Table 2.6. Thickness of nylon films treated with P(GMA-OEGMA) and total area (%) of control film..... 62

Table 2.7. T-Peel test between fabrics and nanocellulose gels..... 63

Table 3.1. Color Strength and dye Fixation of NFC and NCC samples before and after washing 118

Table 3.2. Measurements of weight loss (%) after the enzyme and enzymogel treatments 119

Table 3.3. Methylene blue adsorption and specific surface areas of NFC and NCC samples.... 122

Table 3.4. XRD results of NFC and NCC samples..... 125

LIST OF FIGURES

Page

Fig. 1.1. Homogenizer system reproduced with permission from[46] 3

Fig. 1.2. Microfludics® microfluidizer System (http://www.microfluidicscorp.com/) 4

Fig. 1.3. Masuko ® grinder System[48] reproduced with permission from[47] 5

Fig. 1.4. Ultrasonication system for cellulose fibrillation reprinted with permission from[43] 7

Fig. 1.5. Scheme of TEMPO-mediated oxidation of cellulose reprinted with permission from[26] 8

Fig. 1.6. Chemical structure of cellulose 10

Fig. 1.7. The main steps to obtain polymorphs of cellulose reprinted with permission from[47] ... 11

Fig. 1.8. Hierarchical morphology of cellulose fiber and schematic illustration of NFC and NCC production. (a) Adapted with permission from[81], (b) adapted with permission from[24]. Copyright (2007) American Chemical Society 14

Fig. 1.9. (a) Bacterial Nanocellulose (BNC) produced by culture medium from rotten fruits reprinted with permission from[65]. (b) A typical water gel of bacterial cellulose reprinted with permission from[81] 15

Fig. 2.1. SEM images of polyester, cotton and nylon fibers coated with nanofibrillated cellulose (NFC) 59

Fig. 2.2. SEM images of thin films of NFC (a) and NCC (b) on silicon wafer 59

Fig. 2.3. AFM images of regenerated cellulose, nylon and polyester films on silicon wafers 59

Fig. 2.4. Nylon + PEI-NFC before (a) and after washing (b) 60

Fig. 2.5. Nylon + PEI+NCC before (a) and after washing (b) 60

Fig. 2.6. Step-by-step ellipsometric thickness map of Cellulose + P(GMA-OEGMA)-NFC 62

Fig. 2.7. Step-by-step ellipsometric thickness map of Cellulose + PEI-NCC 62

Fig. 2.8. T-PEEL test panel and test specimen 63

Fig. 2.9. Peeling load vs. peeling extension graph of NFC−natural/synthetic/blended fabrics ... 63

Fig. 2.10. Peeling load vs. peeling extension graph NCC−natural/synthetic/blended fabrics 64

Fig. 2.11. Topography image of the Si-Cellulose step after the scratch with a steel needle 65

Fig. 2.12. Topography image of the Si-Polyester steps after the scratch with a steel needle 65

Fig. 2.13. Topography image of the Si-Nylon step after the scratch with a steel needle 65

Fig. 2.14. Regenerated cellulose + NFC (control) before (a) and after washing (b) 66

Fig. 2.15. Topography image of the Si-Cellulose + NFC (Control, before washing) after the scratch with a steel needle..... 66

Fig. 2.16. Topography image of the Si-cellulose + NFC (Control, after washing) after the scratch with a steel needle..... 66

Fig. 2.17. Polyester + NFC (control) before (a) and after washing (b)..... 67

Fig. 2.18. Nylon + NFC (control) before (a) and after washing (b) 67

Fig. 2.19. Regenerated cellulose + NCC (control) before (a) and after washing (b)..... 68

Fig. 2.20. Topography image of the Si-Cellulose + NCC (Control, before washing) after the scratch with a steel needle..... 68

Fig. 2.21. Topography image of the Si-Cellulose + NCC (Control, after washing) after the scratch with a steel needle..... 68

Fig. 2.22. Polyester + NCC (control) before (a) and after washing (b) 69

Fig. 2.23. Topography image of the Si-Polyester + NCC (Control, before washing) after the scratch with a steel needle..... 69

Fig. 2.24. Nylon + NCC (control) before (a) and after washing (b) 70
Fig. 2.25. Topography image of the Si-Nylon + NCC (Control, before washing) after the scratch with a steel needle 70
Fig. 2.26. Regenerated cellulose + PEI-NFC before (a) and after washing (b) 71
Fig. 2.27. Topography image of the Si-Cellulose + PEI-NFC (before washing) after the scratch with a steel needle 71
Fig. 2.28. Topography image of the Si-Cellulose + PEI-NFC (after washing) after the scratch with a steel needle 71
Fig. 2.29. Polyester + PEI-NFC before (a) and after washing (b) 72
Fig. 2.30. Topography image of the Si-Polyester + PEI-NFC (before washing) after the scratch with a steel needle 72
Fig. 2.31. Topography image of the Si-Polyester + PEI-NFC (after washing) after the scratch with a steel needle 72
Fig. 2.32. Regenerated cellulose + PEI-NCC before (a) and after washing (b) 73
Fig. 2.33. Topography image of the Si-Cellulose + PEI-NCC (before washing) after the scratch with a steel needle 73
Fig. 2.34. Topography image of the Si-Cellulose + PEI-NCC (after washing) after the scratch with a steel needle 73
Fig. 2.35. Polyester + PEI-NCC before (a) and after washing (b) 74
Fig. 2.36. Topography image of the Si-Polyester + PEI-NCC (before washing) after the scratch with a steel needle 74
Fig. 2.37. Topography image of the Si-Polyester + PEI-NCC (after washing) after the scratch with a steel needle 74

Fig. 2.38. Nylon + PEI-NCC before (a) and after washing (b)..... 75
Fig. 2.39. Topography image of the Si-Nylon + PEI-NCC (after washing) after the scratch with a steel needle..... 75
Fig. 2.40. Regenerated cellulose + PEI+NFC before (a) and after washing (b)..... 76
Fig. 2.41. Topography image of the Si-Cellulose + PEI+NFC (before washing) after the scratch with a steel needle..... 76
Fig. 2.42. Topography image of the Si-Cellulose + PEI+NFC (after washing) after the scratch with a steel needle..... 76
Fig. 2.43. Polyester + PEI+NFC before (a) and after washing (b)..... 77
Fig. 2.44. Topography image of the Si-Polyester + PEI+NFC (before washing) after the scratch with a steel needle..... 77
Fig. 2.45. Topography image of the Si-Polyester + PEI+NFC (after washing) after the scratch with a steel needle..... 77
Fig. 2.46. Nylon + PEI+NFC before (a) and after washing (b)..... 78
Fig. 2.47 .Topography image of the Si-Nylon + PEI+NFC (before washing) after the scratch with a steel needle..... 78
Fig. 2.48. Topography image of the Si-Nylon + PEI+NFC (after washing) after the scratch with a steel needle..... 78
Fig. 2.49. Regenerated cellulose + PEI+NCC before (a) and after washing (b)..... 79
Fig. 2.50. Topography image of the Si-Cellulose + PEI+NCC (before washing) after the scratch with a steel needle..... 79
Fig. 2.51. Topography image of the Si-Cellulose + PEI+NCC (after washing) after the scratch with a steel needle..... 79

Fig. 2.52. Polyester + PEI+NCC before (a) and after washing (b) 80
Fig. 2.53. Topography image of the Si-Polyester + PEI+NCC (before washing) after the scratch with a steel needle 80
Fig. 2.54. Topography image of the Si-Polyester + PEI+NCC (after washing) after the scratch with a steel needle 80
Fig. 2.55. Nylon + PEI+NCC before (a) and after washing (b) 81
Fig. 2.56. Topography image of the Si-Nylon + PEI+NCC (before washing) after the scratch with a steel needle 81
Fig. 2.57. Topography image of the Si-Nylon + PEI+NCC (after washing) after the scratch with a steel needle 81
Fig. 2.58. Regenerated cellulose + P(GMA-OEGMA)-NFC before (a) and after washing (b) ... 82
Fig. 2.59. Topography image of the Si-Cellulose + P(GMA-OEGMA)-NFC (before washing) after the scratch with a steel needle 82
Fig. 2.60. Topography image of the Si-Cellulose + P(GMA-OEGMA)-NFC (after washing) after the scratch with a steel needle 83
Fig. 2.61. Polyester + P(GMA-OEGMA)-NFC before (a) and after washing (b) 83
Fig. 2.62. Nylon + P(GMA-OEGMA)-NFC before (a) and after washing (b) 84
Fig. 2.63. Topography image of the Si-Polyester + P(GMA-OEGMA)-NFC (after washing) after the scratch with a steel needle 84
Fig. 2.64. Regenerated cellulose + P(GMA-OEGMA)-NCC before (a) and after washing (b) .. 85
Fig. 2.65. Topography image of the Si-Cellulose + P(GMA-OEGMA)-NCC (before washing) after the scratch with a steel needle 85

Fig. 2.66. Topography image of the Si-Cellulose + P(GMA-OEGMA)-NCC (after washing) after the scratch with a steel needle 86
Fig. 2.67. Polyester + P(GMA-OEGMA)-NCC before (a) and after washing (b) 86
Fig. 2.68. Topography image of the Si-Polyester + P(GMA-OEGMA)-NCC (before washing) after the scratch with a steel needle 87
Fig. 2.69. Topography image of the Si-Polyester + P(GMA-OEGMA)-NCC (after washing) after the scratch with a steel needle 87
Fig. 2.70. Nylon + P(GMA-OEGMA)-NCC before (a) and after washing (b) 88
Fig. 2.71. Topography image of the Si-Nylon + P(GMA-OEGMA)-NCC (after washing) after the scratch with a steel needle..... 88
Fig. 2.72. Regenerated cellulose + P(GMA-OEGMA)+NFC before (a) and after washing (b).. 89
Fig. 2.73. Topography image of the Si-Cellulose + P(GMA-OEGMA)+NFC (before washing) after the scratch with a steel needle 89
Fig. 2.74. Topography image of the Si-Cellulose + P(GMA-OEGMA)+NFC (after washing) after the scratch with a steel needle 90
Fig. 2.75. Polyester + P(GMA-OEGMA)+NFC before (a) and after washing (b)..... 90
Fig. 2.76. Topography image of the Si-Polyester + P(GMA-OEGMA)+NFC (after washing) after the scratch with a steel needle 90
Fig. 2.77. Nylon + P(GMA-OEGMA)+NFC before (a) and after washing (b)..... 91
Fig. 2.78. Topography image of the Si-Nylon + P(GMA-OEGMA)+NFC (before washing) after the scratch with a steel needle..... 91
Fig. 2.79. Topography image of the Si-Nylon + P(GMA-OEGMA)+NFC (after washing) after the scratch with a steel needle..... 92

Fig. 2.80. Regenerated cellulose + P(GMA-OEGMA)+NCC before (a) and after washing (b) . 92
Fig. 2.81. Topography image of the Si-Cellulose + P(GMA-OEGMA)+NCC (before washing) after the scratch with a steel needle 93
Fig. 2.82. Topography image of the Si-Cellulose + P(GMA-OEGMA)+NCC (after washing) after the scratch with a steel needle 93
Fig. 2.83. Polyester + P(GMA-OEGMA)+NCC before (a) and after washing (b)..... 93
Fig. 2.84. Topography image of the Si-Polyester + P(GMA-OEGMA)+NCC (before washing) after the scratch with a steel needle 94
Fig. 2.85. Topography image of the Si-Polyester + P(GMA-OEGMA)+NCC (after washing) after the scratch with a steel needle 94
Fig. 2.86. Nylon + P(GMA-OEGMA)+NCC before (a) and after washing (b) 95
Fig. 2.87. Topography image of the Si-Nylon + P(GMA-OEGMA)+NCC (before washing) after the scratch with a steel needle..... 95
Fig. 2.88. Topography image of the Si-Nylon + P(GMA-OEGMA)+NCC (after washing) after the scratch with a steel needle..... 96
Fig. 3.1. Hierarchical morphology of cellulose fiber and schematic illustration of NFC and NCC production 116
Fig. 3.2. Dyeing protocol of NFC and NCC with reactive red 120 116
Fig. 3.3. Chemical structure of cellulase from Trichoderma reesei ATCC 26921 (a), reactive red dye 120 (b), cellulose (c), and methylene blue (d) 117
Fig. 3.4. Dyed enzyme-treated NFC and NCC (a) dyed cotton fabric with enzyme-treated NFC (b), and dyed cotton fabric with enzyme-treated NCC (c)..... 117

Fig. 3.5. (a) Schematic of the enzymogel nanoparticle consists of a silica core, and a PAA brush shell loaded with cellulase enzyme; (b, c, d) cryo-TEM images of the particle with a silica core (b) swollen, (c) shrunken PAA brush, and (d) uniformly loaded with enzymes at pH 4.5 reproduced with permission from[32] 118

Fig. 3.6. Color strength spectra of NFC and NCC before washing 119

Fig. 3.7. Color strength spectra of NFC and NCC after washing 119

Fig. 3.8. TGA (a) and DTG (b) curves of NFC before and after the enzyme treatment..... 120

Fig. 3.9. TGA (a) and DTG (b) curves of NCC before and after the enzyme treatment 121

Fig. 3.10. Calibration curve of absorbance vs. concentration of methylene blue..... 122

Fig. 3.11. Langmuir adsorption isotherm of Methylene blue on NFC 123

Fig. 3.12. Langmuir adsorption isotherm of Methylene blue on NCC..... 124

Fig. 3.13. X-ray diffraction patterns of NFC samples 125

Fig. 3.14. X-ray diffraction patterns of NCC samples..... 125

CHAPTER 1

INTRODUCTION AND LITERATURE REVIEW

Cellulose is the most abundant, renewable, biodegradable, and environmentally friendly organic compound found in nature. Cellulose is widely found in plants (e.g., wood[1], bamboo[2-3], pineapple leaf[4-5], coconut husk[6], sugarcane bagasse[7-8], kenaf[9], soy hull[10], sisal[11], rice husk[12], cotton pulp[13], and potato residue[14]), in several marine animals (e.g., tunicate[15]), in algae[16], and bacteria[17]. However, wood is the most common source of cellulose for industrial projects. As such bleached Kraft pulp[18-22] and bleached sulfite pulp[23-25] are mainly used to produce nanocellulose fibers.[13] Nanocellulose, due to its unique properties such as high aspect ratio (length to width ratio), crystallinity, shear thinning behavior and mechanical properties, is a subject of many studies and investigations. In this chapter, production methods, structure, and properties of nanocellulose hydrogels, as well as nanocellulose coatings and sustainable textile dyeing methods, will be discussed in detail.

1.1 Production

In the production of nanocellulose materials, depending on the desired properties and final application of nanocellulose, different chemical, and mechanical processes have been used. The sources and the most commonly used production methods of nanocellulose are summarized in Table *1.1*.

Table 1.1. Nanocellulose types, sources, and main production methods

Nanocellulose Type	Typical Sources	Main Preparation Method
Nanofibrillated Cellulose (NFC)	Wood, Plant	Mechanical Treatments
Nanocrystalline Cellulose (NCC)	Wood, Plant, Animal (Tunicate), algae and bacteria	Acid hydrolysis
Bacterial Nanocellulose (BNC)	Low molecular weight sugars and alcohols[13]	Bacterial synthesis Static and stirring cultivations

1.1.1 Production of Nanofibrillated cellulose (NFC)

Nanocellulose fibrils are isolated from wood and plant-based fibers using mechanical treatment, such as a homogenizer, microfluidizer, and grinder to delaminate the cell walls of fibers and free the nanosized fibrils from the microfiber bundles to prepare nanofibrillated cellulose. The first production of nanofibrillated cellulose was reported in the 80s[26-27] and since then several methods of mechanical treatment have been used to increase the quality and quantity of NFC[13]. In recent studies, nanofibrillated cellulose has been manufactured from different cellulosic sources in two steps. The first step is a homogenization pretreatment to purify the original cellulose and make it ready for subsequent treatments. This pretreatment depends on the cellulose source and the morphology needed for the subsequent treatment in the second step. For example, for wood[28] and plants[29], the pretreatment occurs by removing partial or complete hemicellulose, lignin, and other matrix materials as well isolating individual fibers. For animal source cellulose such as tunicate[29], the objective of this step is to isolate the mantle from animal and separate the individual microfibrils by removing the protein matrix. Cellulose from algae can be pretreated by first

culturing and then washing methods to remove the algal cell wall components[29-32]. For bacterial cellulose, the pretreatment involves culturing process to grow microfibrils and then washing process to eliminate the bacteria[29, 33-35].

The second step is to separate these cellulose materials into nanofibrils using mechanical treatments such as homogenizer[27, 36-37], microfluidizer[38-39], grinders[40], cryo-crushing[36, 41-42], and high-intensity ultrasonic treatments[43-44].

Mechanical Treatment

Homogenizer System

In a homogenizer system, the slurry from a cellulose fiber suspension is pumped through valves with high pressure and low velocity. Then the velocity and pressure quickly increases and decreases respectively resulting in strong mechanical shearing which causes the homogenizing effect resulting in fibrillation of fibers[13] (Fig. *1.1*). Although the homogenization treatment is a straightforward and easy method for the fibrillation of nanocellulose fibers and can be scaled to industrial production, it can be an energy-intensive process. Another disadvantage of the homogenization of nanofibrillated cellulose is that long fibers frequently clog the instrument, usually at the moving parts (in-line valves)[45].

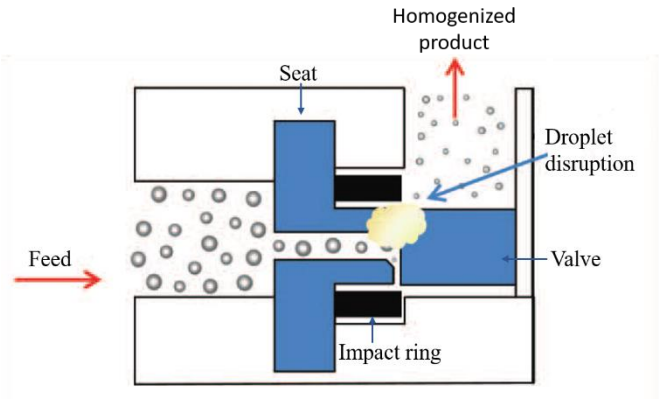

Fig. 1.1. Homogenizer system reproduced with permission from[46]

Microfluidizer System

In microfluidizer, the slurry goes through a high-pressure chamber and passes through microchannels with very high velocity allowing the fibrillation of cellulosic pulps. The higher degree of fibrillation in microfluidizer can be achieved by reducing the chamber size[13] because the chamber can be designed with different sizes[45] (Fig. *1.2*). Microfluidization compared to the homogenization process, overcomes the problem of clogging because it does not have any in-line moving parts. Moreover, this system operates at a constant shear rate, unlike the homogenizer system which runs at a constant processing volume[45].

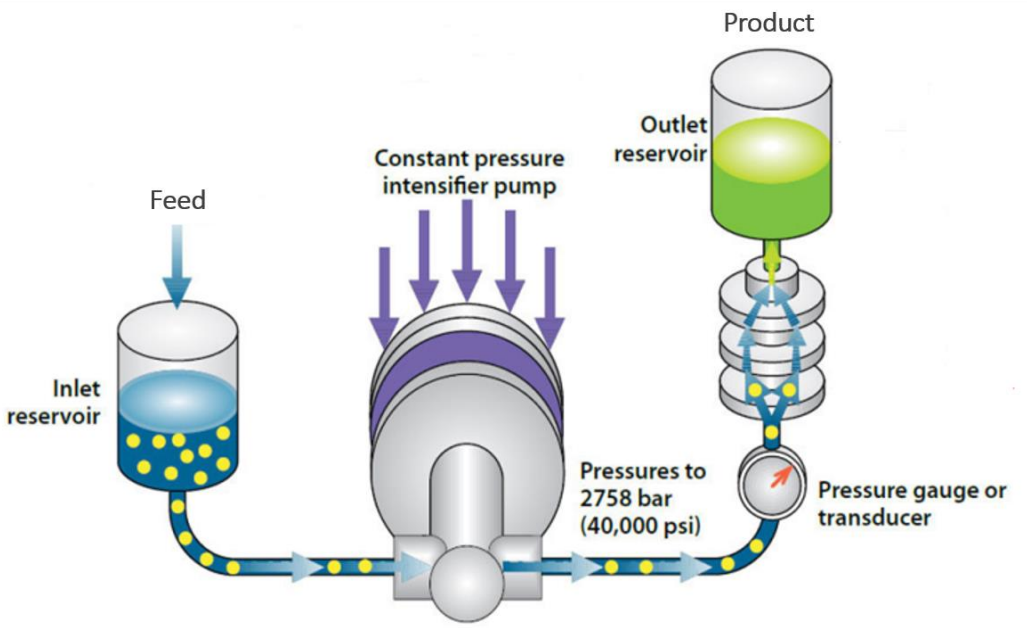

Fig. 1.2. Microfludics® microfluidizer System (http://www.microfluidicscorp.com/)

Grinder System

In a grinder system, due to the shearing forces produced by the static and rotating grinding stones, the system can break down the cell wall structure helping the nanofibers to individualize from the pulp[13, 28] (Fig. *1.3*). The stones are made of non-porous resins containing silicon carbide. They can be produced with different grit classes and groove configurations to change flow patterns

during the process[45]. In this system, it was observed that the size of fibers was decreased as the number of passes increased, but the fiber morphology did not change significantly, and at five passes, most of the fibers turned into the nanosized fibers. Therefore, they concluded that five passes through the grinder system were enough to produce NFC fibers without any homogenization process[47]. The disadvantage of this system is the disk maintenance and replacement because pulp fibers can wear down the grooves on the disks. The benefit of using grinders is that compare to the homogenization system; the grinding system needs less number of passes. However, this process can decrease the length of fibrils resulting in less strength of nanofibrils that might change the physical properties of NFC[47].

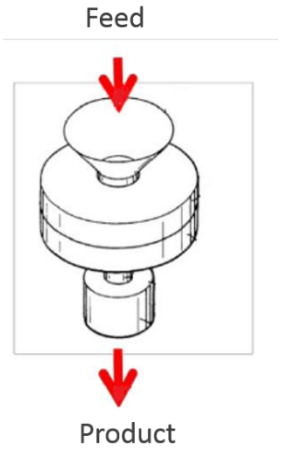

Fig. 1.3. Masuko ® grinder System[48] reproduced with permission from[47]

Cryo-crushing System

Cryo-crushing is a less commonly used system for the fibrillation of NFC since it cannot produce very fine fibrils, and cannot be used in large-scale production. In this method, pulp, frozen by liquid nitrogen, goes under a high impact grinding with a mortar and pestle[45] to break down the cell wall and isolate the fibrils[42].

High-Intensity Ultrasonication (HIUS)

High-intensity ultrasonication (HIUS) is also used to isolate nanofibrils. Ultrasound (in the range of 20 kHz–10 MHz) converts mechanical or electrical energy into high-frequency acoustical energy. HIUS waves can produce a powerful mechanical oscillating power when the molecules in a liquid absorb the ultrasonic energy. This mechanical oscillating power is directly applied to the suspension of cellulose fibers in distilled water and forces the cellulose fibrils to isolate from its biomass (Fig. 1.4)[43-44]. Ultrasonic radiation can be used in many experiments such as emulsification, catalysis, homogenization, disaggregation, scission, and dispersion. The benefit of this system compared to the other mechanical treatments is that it reduces the shortening of the nanofibrils length during the process[44].

Pretreatment

As a large number of mechanical passes needed to achieve the desired nanofibrillated cellulose, and each pass requires a high amount of energy, enzymatic or TEMPO (2,2,6,6-tetramethylpyperidine-1-oxy radical) pretreatment of cellulose are suggested to save time and money[13].

Enzymatic Pretreatment

Enzymatic pretreatment by limiting the interactions between microfibrils significantly reduces the energy consumption of the mechanical treatments. This pretreatment is based on the idea that cellulases, the set of enzymes found in nature, can degrade cellulose structure. Therefore, to modify the cellulose structure, isolated cellulases can be added to the microfibrils before the mechanical treatment[13].

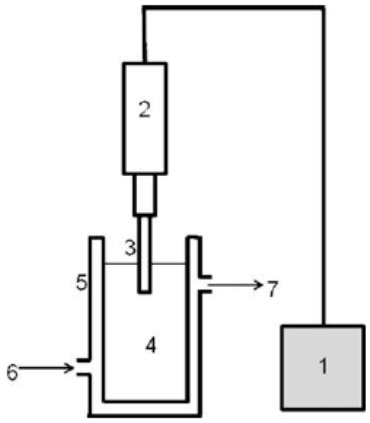

Fig. 1.4. Ultrasonication system for cellulose fibrillation reprinted with permission from[43]
1. power control, 2. piezoelectric converter, 3. ultrasonic probe, 4. cellulose suspension, 5. double-walled glass beaker, 6. ice water inlet and 7. Outlet

TEMPO-Mediated Oxidation

TEMPO-mediated oxidation is a method of oxidizing cellulose fibers by adding NaClO to cellulose suspensions containing 2,2,6,6-tetramethylpyperidine-1-oxy radical (TEMPO) and sodium bromide at pH 10.5 at room temperature[19-20, 26]. As a result, carboxylate and aldehyde are introduced at the primary hydroxyl groups of cellulose at C-6, causing the degradation of microfibrils, and it also decreases the degree of polymerization (DP). As a result, nanofibrils can be isolated more easily by the mechanical forces due to the higher repulsive forces of the ionized carboxylate groups than the hydrogen bonds between them[13, 26, 49-50].

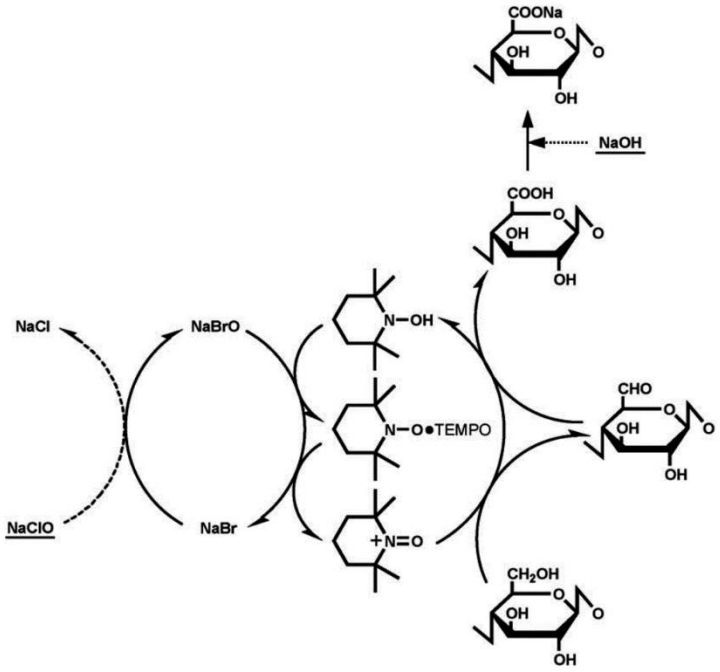

Fig. 1.5. Scheme of TEMPO-mediated oxidation of cellulose reprinted with permission from[26]

As TEMPO-mediated oxidation reaction of cellulose (Fig. *1.5*) shows that two moles of NaClO are consumed to form one mole of a carboxylate group, and one mole of NaClO is consumed to form one mole of aldehyde, Saito et al. [26] defined the oxidation efficiency by Equation (1.1):

$$\textit{Oxidation efficiency (\%)} = 100 \times (2 \times (C_T - C_O) + (A_T - A_O))/M_{NaClO} \quad (1.1)$$

Where M_{NaClO} is the quantity of NaClO added to the cellulose suspension (mmol/g), C_O and C_T are carboxylate contents (mmol/g) before and after oxidation, A_T and A_O are the corresponding aldehyde contents. They also calculated the oxidation efficiency values for cotton linters, ramie and spruce holocellulose 62%, 85%, and 96%, respectively.[26]

There are also other TEMPO-mediated oxidation systems with different conditions to the above system[50-51]. Other pretreatments such as carboxymethylation[52] or acetylation[53] are also suggested by some studies[13]. Carboxymethylation treatment introduces charged groups into the cellulose pulps causes the pulps to swell. As a result, they have lower cell wall cohesion and are

easier to be delaminated[47, 54]. In acetylation treatment, the grafted acetyl groups onto the inner crystalline regions of MFC decrease the hydrophilicity of microfibrils and improve the chemical affinity between MFC and a nonpolar solvent. They also reduce the hydrogen bonding between microfibrils and allow for a better delamination during the mechanical treatments[53, 55].

1.1.2 Production of Nanocrystalline cellulose (NCC)

Acid hydrolysis has been used to make nanocrystalline cellulose (NCC) by extracting crystalline particles from a variety of sources such as plant, wood, tunicate, algae, and bacteria[47]. This process removes (hydrolyzes) the amorphous part of cellulose microfibrils to free crystalline rodlike particles[56] when the material is mixed with deionized water and sulfuric acid[28, 57]. Other acids such as hydrochloric[58-59] and maleic[60] were also used. After the appropriate amount of depolymerization, the mixture is diluted with deionized water. Then it goes under a series of centrifugation, washing, and dialysis to remove the remaining acid and salt[15, 35, 61-63]. The dialysis usually followed by a mechanical treatment typically sonication to disperse the nanocrystals as a uniform suspension[54].

1.1.3 Production of Bacterial Nanocellulose (BNC)

Unlike NFC and NCC productions via mechanical and chemical processes, BNC is formed as a polymer through biotechnology-based methods to build up microfibrils bundles from a low molecular weight sugars and alcohols[64-65]. The two most common methods of producing BNC are static and stirring cultures. Static culture leads to a thick, leather-like pellicle while the stirring culture which takes place in the dispersed culture medium results in irregular pellets. Since mechanical properties and morphology of bacterial cellulose from these two cultivation methods are different, the choice of these production methods depends on the final application of BNC. Moreover, static culture method needs a larger area and longer time but produces a higher amount

of BNC. Therefore, this method is costly for industrial production[66]. The fermentation medium in the production of BNC must contain carbon, nitrogen and other macro and micro nutrients such as phosphorus, sulfur, potassium, and magnesium salts[65, 67-70].

1.2 Structure and properties

Regardless of its source, cellulose consists of glucose units linearly linked together by β 1–4 glucosidic bonds. It means that there is a covalent bond that connects an oxygen to C1 of one glucose ring and C4 of the other glucose ring. The repeat segment, which is a dimer of glucose, is known as cellobiose. Depending on the source of cellulose material, the degree of polymerization (n) can be from 10000 to 15000[1-3]. In cellulose, each monomer has three hydroxyl groups that can form strong intermolecular hydrogen bonds with oxygens of the adjacent ring which lead to parallel cellulose chains forming elementary fibrils. These elementary fibrils aggregate into larger microfibrils due to both inter and intra-molecular hydrogen bonds and van der Waals forces. These hydrogen bonds give cellulose stability, high axial stiffness, the ability to form crystalline and amorphous regions, and a glass transition temperature higher than its degradation temperature[35, 47, 57, 71-72].

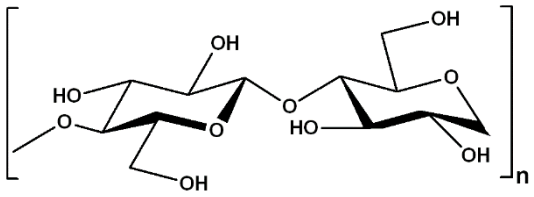

Fig. 1.6. Chemical structure of cellulose

Cellulose at least has four different forms or polymorphs. Cellulose I, II, III, and IV. Cellulose I and II are the main forms of cellulose. Cellulose I or native cellulose is the crystalline cellulose that consists of crystallites and amorphous regions that can be found in plants, tunicates, bacteria, and algae. This form of cellulose is metastable and can convert to cellulose II or III.

Cellulose I consists of the mixture of cellulose Iα and Iβ. Iβ is the most stable form of cellulose I and can be achieved by annealing treatment. Cellulose II is the most thermodynamically stable form of cellulose, which can be achieved through either mercerization or dissolution and regeneration out of solutions. Cellulose III_I, III_{II} can be produced from cellulose I or II through treatment with liquid ammonia respectively, and cellulose III can be converted to cellulose IV by subsequent thermal treatment with glycerol[64, 73-78] (Fig. *1.7*)[47].

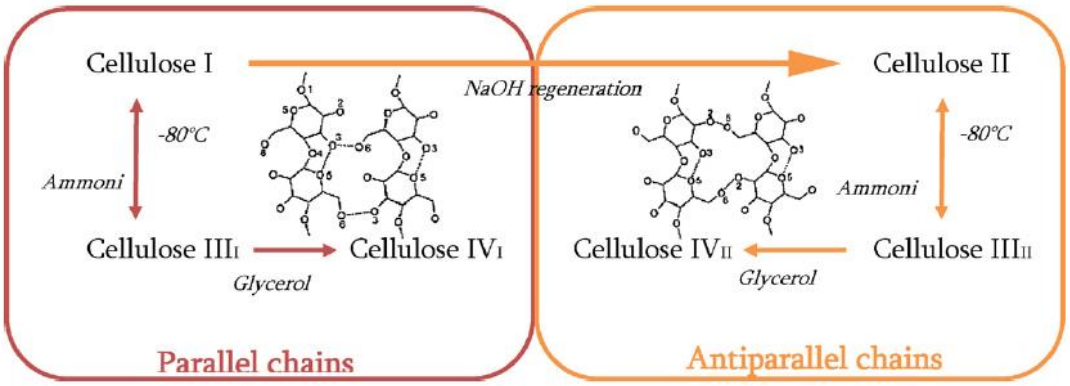

Fig. 1.7. The main steps to obtain polymorphs of cellulose reprinted with permission from[47]

In cellulose thirty-six elementary fibrils (individual units) bundle together to form microfibrils. These fibrils are composed of crystals (ordered regions) and amorphous regions (disordered regions) that can be separated from the original cellulose fibers by mechanical treatment[28, 37, 79-80], acid hydrolysis[28, 79], and enzymatic hydrolysis[28, 79]. By applying these methods, nanofibrillated cellulose (NFC) also called microfibrillated cellulose (MFC), and nanocrystalline cellulose (NCC) can be produced (Fig. 1.8). Although these treatments can be done separately, multiple of these treatments are required to achieve the desired form and structure[35]. Another type of nanocellulose materials is nanocellulose secreted by various bacteria cultured in sugars and alcohols. This type of nanocellulose fibrils is called bacterial nanocellulose (BNC) (Fig. *1.9*)[65, 81].

Crystallinity, crystal structure, morphology, size, dimensions, shape and aspect ratio of nanocellulose materials to a certain extent depend on the source of the cellulose and method of extraction[57, 82]. Algea and tunicate yield 100 nm to several micrometers nanocellulose in length with high crystallinity[83-85] compared to nanocellulose from wood which has lower crystallinity and yield 100 nm to 300 nm nanocrystals in length[61, 86].

1.2.1 Structure and Properties of Nanofibrillated Cellulose (NFC)

NFC is composed of fibrils (Fig. *1.8*) with a high aspect ratio (length to width ratio), these fibrils have lengths and widths in the micrometer and nanometer scales[57, 87-89]. Depending on the technique of production, they can also be 4–20 nm wide, and 500–2000 nm long[35]. Nanofibrillated cellulose fibers from different sources and different production methods have similar morphology but different dimensions[42, 47]. Instruments such as scanning electron microscopy (SEM), Transmission Electron Microscopy (TEM), and Atomic Force Microscopy (AFM) can be used to observe and measure NFC diameter[47]. NFC contains both amorphous and crystalline regions. X-ray diffraction measurement is a common method to measure the NFC degree of crystallinity[47]. The degree of crystallinity depends on the source of cellulose materials. For instance, the degree of crystallinity is around 78%, 70%, 90%, and 30-40% for NFC obtained from wheat straw, soy hull[41], sisal[90-91], and beet pulp[31] respectively. Another important property of NFC is its high specific area. This property is usually hard to measure due to the aggregation of NFC fibers after drying. Therefore, the measurement is an approximation and is based on modeling tools that use the length or diameter. Siqueira et al.[92] measured the specific area of sisal NFC around 50 m2/g, which is about ten times greater than the original sisal fiber[47, 92].

In the case of toxicity, according to the results of the initial investigations, NFC is safe and environmentally friendly[93-94]. However, Catalán et al.[95] in a recent study showed that TEMPO-

oxidized NFC administrated by a single pharyngeal aspiration caused an inflammatory response and DNA damage into the lungs of mice, but they did not find any systematic genotoxicity in the bone marrow. Therefore, to investigate the toxicity of NFC, the source of cellulose, types of pretreatments, mechanical processes, and final applications should be taken into account since they result in different characteristics, properties, and toxicity of NFC. Another important property of nanofibrillated cellulose is rheology. Regardless of the source of cellulose, NFC shows specific rheological properties regarding pseudo-plasticity and shear thinning behavior meaning that with increasing shear rate, NFC shows a significant decrease in viscosity[96-98]. Later studies showed that regardless of the concentration of NFC in suspensions, the NFC suspensions show a gel-like behavior and even at the lowest concentration, they form a strong network[24].

1.2.2 Structure and Properties of Nanocrystalline Cellulose (NCC)

NCC is composed of nanosized crystals, and as a result of the acid hydrolysis treatment, they look like whiskers (Fig. *1.8*). These whiskers have a high aspect ratio (3–5 nm wide, 50–500 nm in length), and they are highly crystalline (54–88%)[12]. The structure and properties of NCC, such as dimension and morphology, depend on the source of cellulose, acid hydrolysis conditions (a type of acid, the concentration of acid, temperature, and time), and the intensity of the sonication process. However, their lengths usually range between 100 and 300 nm[49, 61, 75, 99-101]. For example, NCC produced with HCL[101-102] has poor colloidal stability, compared to those hydrolyzed with sulfuric acid[103]. The NCC fibers generated from the highly crystalline tunicate and algae have several microns long nanocrystals compared to the less crystalline wood fiber NCC that has shorter nanocrystals[54, 83, 104-105].

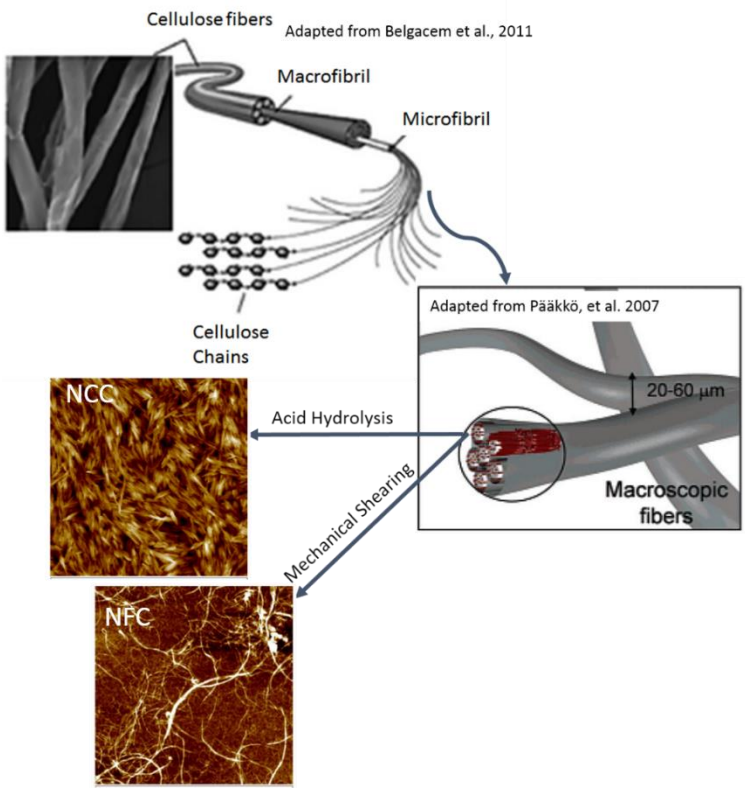

Fig. 1.8. Hierarchical morphology of cellulose fiber and schematic illustration of NFC and NCC production. (a) Adapted with permission from[81], (b) adapted with permission from[24]. Copyright (2007) American Chemical Society

In the case of toxicity, the first report considered NCC to be safe with low environmental risk[106]. Current studies of NCC toxicity also have shown no adverse health effects. However, the toxicity of NCC strongly depends on its physical and chemical properties, such as particle shape, dimensions, surface chemistry, and particle charge. These properties also depend on the source of cellulose, methods of preparation, and post-treatments such as sonication[107].

Rheology is also one of the critical properties of nanocrystalline cellulose. Rheological properties of NCC suspensions show shear thinning behavior. This behavior increases as the concentration increases. However, NCC shows a little concentration dependence at a high shear rate[108-111]. Urena-Benavides et al.[112] concluded that the rheological properties of NCC depend on the concentration of NCC and the temperature[112-113]. Another important property of NCC is its liquid crystalline characteristic. NCC suspensions show a birefringent and liquid crystalline

behavior, because of their asymmetric rod-like particles, which can display nematic behavior when the rods align under specific conditions[99, 113-114].

1.2.3 Structure and Properties of Bacterial Nanocellulose (BNC)

BNC is composed of microfibrils secreted by various bacteria from low-molecular-weight sugars and alcohols[54] (Fig. 1.9)[65, 81]. These microfibrils are 20-100 nm wide and 1-5 μm long[35, 72]. BNC is similar to plant-based nanofibers regarding chemical composition. However, it does not have any impurities such as hemicelluloses, lignin, or pectin[64]. BNC has a high degree of polymerization (2000-8000) and a high degree of crystallinity (60-90%), therefore, it has excellent mechanical properties[64]. However, morphology, structure, physical and mechanical properties can be different depending upon the preparation condition and also the chemical agents present in the medium[68, 115-116]. For example, the static method yields a regular shape with better morphology than the stirring condition[66]. Moreover, BNC produced by static culture has higher mechanical strength than the product from stirring culture[65]. Other properties of BNC include a high degree of crystallinity, high density, ability to retain its shape, high water-binding capacity, and higher surface area than native cellulose[65].

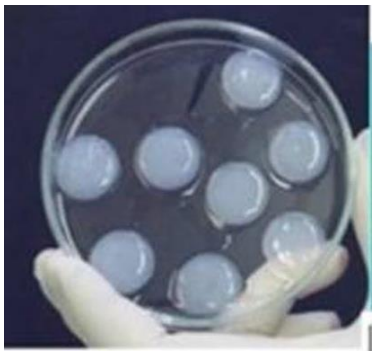

Fig. 1.9. (a) Bacterial Nanocellulose (BNC) produced by culture medium from rotten fruits reprinted with permission from[65]. (b) A typical water gel of bacterial cellulose reprinted with permission from[81]

1.3 Application

Nanocellulose gels either in the form of fibrils (nanofibrillated cellulose (NFC) and Bacterial nanocellulose (BNC)) or the form of crystals (nanocrystalline cellulose (NCC)), due to their abundant natural resources and their unique properties, are widely used to develop environmentally friendly materials.

1.3.1 Application of Nanocellulose Fibers (NFC)

NFC has a variety of applications in flexible displays, optical devices, automobile industry (e.g., automobile windows)[117-118], edible coatings and packaging materials[118-119], infrastructure, and energy (e.g., lightweight and high-performance composites)[118, 120]. NFC also can be used as a binder or viscosity modifier in paper and packaging industry[47]. It also has a potential application to be used as a coating element in printing applications[47, 121].

1.3.2 Application of Nanocrystalline Fibers (NCC)

NCC, because of its distinctive properties, safety, and efficiency, has the potential of becoming part of many different products in personal care, food, pharmaceuticals (drug carriers), nanocellulose-based hydrogels[118, 122], air permeable and resistant paper[118, 123], packaging[118, 124], photonic devices[118, 125], conductive materials[118, 126], tissue engineering[118, 127] and optical devices[118, 128] to name a few.

1.3.3 Application of Bacterial Nanocellulose (BNC)

BNC has many applications in pharmaceuticals, textiles, food, cosmetics, papers, and electronics. In medical care, it can be used for external wound dressings. However, pure BNC does not show any benefit in the process of chronic wound healing. Therefore, different types of BNC based composites have been introduced and investigated to address this issue. Unlike plant-based celluloses, BNC can also be used in medical implants incorporated into living bodies[129]. In the

case of textile application, BNC can be used in sports clothing, tents, and camping equipment (e.g., nanocomposites for smart fabrics)[65]. Another application of BNC is a dietary fiber which offers a variety of benefits such as reducing the risk of diabetes, obesity, and cardiovascular disease[66]. In cosmetic industry, BNC can be incorporated into creams, tonics, conditioners, and nail polishes as a stabilizer[65]. Because of the excellent mechanical properties, BNC has a potential to use as a reinforcing agent in paper and fiber production. It is also a superior option for headphone and loudspeaker membranes (Sony Corp.)[64].

1.4 Nanocellulose Coatings

Nanocellulose coatings/films have been used for food[130] and Flexible packages[130-133] in different studies. They are effective in protecting food substances and products, from various types of processing damages.[130] Nanocellulose coatings with moisture barrier[134] and gas barrier[135] properties have a potential to be used for high-performance paper-based packaging. Nanocellulose coatings can also be used for artificial blood vessels by combining a textile vessel with nanocellulose coatings to form a new type of small artificial blood vessel in a composite structure.[136] Nanocellulose fibers offer significant advantages to use as reinforcing coatings for polymer composites compared to their synthetic counterparts such as glass and carbon fibers with regards to the environment, economy and lower energy consumption.[137] In this study, nanocellulose coatings/films developed to transfer dye molecules to textile surfaces for sustainable textile dyeing (chapter 3).

1.5 Sustainable Textile Dyeing

Conventional textile dyeing technology requires copious amount of water and releases a massive amount of wastewater consists of harmful and toxic chemicals to the environment which causes health, safety, and environmental concerns and increases the cost of treating effluent as

well as the cost of producing water supply. One of the reasons to use synthetic dyes over natural dyes despite all the problems associated with toxicity and safety are synthetic dyes in various hues and colors which cannot be achieved or hard to produce with natural dyes. Synthetic dyes are also free of insoluble impurities compared to natural dyes. Therefore, dyeing with natural dyes is harder because it is difficult to create a dyebath free of insoluble materials. Moreover, reproducing the same shade of color with natural dyes is very hard while there are standardized methods to reproduce different shades of colors with synthetic dyes. Synthetic dyes can also be mixed in a single dyeing process, while to achieve the ideal color from natural dyes if different natural dyes are not compatible and they need specific dyeing process, we cannot use a single dyeing process. Therefore, dyeing with synthetic dyes is more, time, water and energy efficient. Moreover, synthetic Dyes do not need mordants to fix dyes on textile surfaces while we need to use mordants for dyeing cotton with natural dyes. Therefore, there is a need for additional application step, and, using heavy metals in the process (iron and aluminum). And most importantly some synthetic fibers that we mostly use such as polyester are not dyeable with natural dyes. Overall, despite the sustainability of natural dyes reported by a vast number of research papers, the use of natural dyes in textile dyeing technology on a global scale is minimal.[138] Regarding sustainability, toxicity, and environmental impacts are two important factors. Measurements of effluent toxicity revealed that salt and metals were the major sources of toxicity in dyeing process and most of the synthetic dyes with regard to sustainability do not harm the user or the environment. However, particular dyes are not acceptable to use because of their ability to break down to harmful components unacceptable based on their ability to break down into hazardous materials. But regarding environmental impact, dyeing technology has an adverse effect on the environment.[138] One of the most important action to increase sustainability and decrease environmental impact, is to improve

color fastness and increase dye exhaustion in dyeing process which consequently decrease the amount of dye in the wastewater.[138]

Reactive dyes were introduced originally in 1956. They are the most common dyes used for dyeing of cellulose fibers because of the straightforward method of application, and good color fastness. Dye and salt are first added to the dyebath following with alkali. Salt helps promote dye exhaustion and the functional groups in dye with the addition of alkali result in the covalent bonding between dye and fibers which causes good color fastness.[138] The first reactive dyes had poor dye exhaustion, requiring a lot of salt for the reaction. It was also inefficient in the dyeing of cotton fibers leaving a significant amount of unfixed dye which needed to be removed by intensive rinsing after the dyeing step. Reactive dyes have been improved and have high dye fixation by using two or more reactive groups of the same (homo-) or different (heterobifunctional) types resulting in using less amount of salt (so-called ‘‘low salt’’).[139-140] These dyes can be used in continuous, and especially semicontinuous (pad-batch) processes, where salt can be omitted altogether, and the efficiencies of reactions between fiber and dye are high resulting in less intensive rinsing step. The rinsing step in the dyeing of cellulosic fibers with reactive dyes takes up a substantial proportion of the wet processing cycle. There have been studies to improve the efficiency of the rinsing process to save time, reduce the amount of water used in the process, and consequently decrease the cost by for example combining cooling and rinsing which uses a high starting temperature and reduces time and consumption of water in the process.[138, 141]

Decolorizing of wastewater is also a popular approach to remove color-causing compounds; however, the colorless waste may still have compounds that could be more toxic than the original colored waste. Therefore, the disappearance of the color in the wastewater means merely the decoloration and not the degradation of the dye molecules. Commonly a combination

of physical, chemical, electrical, and biological processes is needed to remove the chemicals significantly. However, some studies reported that the new intermediates are generated in different treatment processes of decolorization. The complicated dye structure makes the decolorization as well as removal of organic molecules from these wastes a challenging task, and yet none of the processes alone has been able to remove all the remaining compounds from the wastewater completely.[142] A synthetic origin of dyes and their complex aromatic molecular structures make them stable and very hard to biodegrade. However, A wide range of microorganisms such as bacteria, fungi, and algae can efficiently decolorize a variety of dyes. But Most of the studies to date have focused on living fungi for biodegradation of dyes.[138, 143]

Waterless dyeing technology such as ColorZen[144] and DyeCoo[145] is also another approach to tackle wastewater problem of the textile dyeing process. One study proposed a process consists of a dyestuff dissolved, suspended or dispersed in a boiling organic liquid at a relatively high temperature followed by a cooling and washing with a low boiling organic liquid, and finally drying the dyed materials. The remaining dyestuff from the dyeing step can be recycled and used for the further materials to be dyed.[146] There are also wet-processing technologies, such as enzymatic treatments that activate and accelerate chemical reaction and as a result, reduces the amount of water needed for the rinsing steps and saves energy, and ultrasonic treatments that reduced consumption of dyes and chemicals and consumes around 20% less water.[147] Although there have been some improvements in textile dyeing methods, the problems of toxicity and environmental impacts still exists. Therefore, there is a need to develop new sustainable, and environmentally friendly textile dyeing methods.

1.6 Research Objectives

Paper 1. Nanocellulose Thin Films as Sustainable Functional Coatings for Textile Materials

The second chapter of this dissertation focuses on the development of stable and smooth textile coatings from nanocellulose hydrogels. The primary goal of this study was to develop sustainable and environmentally friendly nanocellulose based coatings that can transfer functional molecules or particles such as dye molecules to textile materials. The specific objectives of the study were as follows:

1. Increasing the adhesion between nanocellulose materials and textile surfaces (natural and synthetic fibers) to make stable coatings after washing with water.
2. Measuring peel strength between natural, synthetic and blended fabrics to investigate the adhesion strength between nanocellulose coatings and textile fibers.

Paper 2. Enzymatic Treatments of Nanocellulose Hydrogels for Sustainable Textile Dyeing Technology

In chapters 3, we develop new sustainable and environmentally friendly textile dyeing technique based on the nanocellulose coatings that we developed previously (chapter 2). Some of the specific objectives of this study were as follows:

1. Incorporating the dyeing molecules with nanocellulose coatings and measure the color strength and dye fixation of the colored nanocellulose coatings.
2. Increasing the dye performance of nanocellulose coatings by conducting enzymatic treatments on nanocellulose hydrogels before the dyeing step
3. Investigating the effect of enzymatic treatments on the structure and properties of nanocellulose hydrogels such as the degree of crystallinity and thermal stability.

1.7 References

1. Chen, L.; Wang, Q.; Hirth, K.; Baez, C.; Agarwal, U. P.; Zhu, J., Tailoring the yield and characteristics of wood cellulose nanocrystals (CNC) using concentrated acid hydrolysis. *Cellulose* **2015,** *22* (3), 1753-1762.

2. Brito, B. S.; Pereira, F. V.; Putaux, J.-L.; Jean, B., Preparation, morphology and structure of cellulose nanocrystals from bamboo fibers. *Cellulose* **2012,** *19* (5), 1527-1536.

3. Zhang, Y.; Lu, X.-B.; Gao, C.; Lv, W.-J.; Yao, J.-M., Preparation and characterization of nano crystalline cellulose from bamboo fibers by controlled cellulase hydrolysis. *Journal of Fiber Bioengineering and Informatics* **2012,** *5* (3), 263-271.

4. dos Santos, R. M.; Neto, W. P. F.; Silvério, H. A.; Martins, D. F.; Dantas, N. O.; Pasquini, D., Cellulose nanocrystals from pineapple leaf, a new approach for the reuse of this agro-waste. *Industrial Crops and Products* **2013,** *50*, 707-714.

5. Cherian, B. M.; Leão, A. L.; de Souza, S. F.; Thomas, S.; Pothan, L. A.; Kottaisamy, M., Isolation of nanocellulose from pineapple leaf fibres by steam explosion. *Carbohydrate Polymers* **2010,** *81* (3), 720-725.

6. Rosa, M.; Medeiros, E.; Malmonge, J.; Gregorski, K.; Wood, D.; Mattoso, L.; Glenn, G.; Orts, W.; Imam, S., Cellulose nanowhiskers from coconut husk fibers: Effect of preparation conditions on their thermal and morphological behavior. *Carbohydrate Polymers* **2010,** *81* (1), 83-92.

7. Mandal, A.; Chakrabarty, D., Isolation of nanocellulose from waste sugarcane bagasse (SCB) and its characterization. *Carbohydrate Polymers* **2011,** *86* (3), 1291-1299.

8. Maddahy, N.; Ramezani, O.; Kermanian, H. In *Production of nanocrystalline cellulose from sugarcane bagasse*, Proceedings of the 4th International Conference on Nanostructures (ICNS4), 2012; pp 12-14.

9. Kargarzadeh, H.; Ahmad, I.; Abdullah, I.; Dufresne, A.; Zainudin, S. Y.; Sheltami, R. M., Effects of hydrolysis conditions on the morphology, crystallinity, and thermal stability of cellulose nanocrystals extracted from kenaf bast fibers. *Cellulose* **2012,** *19* (3), 855-866.

10. Neto, W. P. F.; Silvério, H. A.; Dantas, N. O.; Pasquini, D., Extraction and characterization of cellulose nanocrystals from agro-industrial residue–soy hulls. *Industrial Crops and Products* **2013,** *42*, 480-488.

11. Morán, J. I.; Alvarez, V. A.; Cyras, V. P.; Vázquez, A., Extraction of cellulose and preparation of nanocellulose from sisal fibers. *Cellulose* **2008,** *15* (1), 149-159.

12. Johar, N.; Ahmad, I.; Dufresne, A., Extraction, preparation and characterization of cellulose fibres and nanocrystals from rice husk. *Industrial Crops and Products* **2012,** *37* (1), 93-99.

13. Missoum, K.; Belgacem, M. N.; Bras, J., Nanofibrillated cellulose surface modification: a review. *Materials* **2013,** *6* (5), 1745-1766.

14. Lu, H.; Gui, Y.; Zheng, L.; Liu, X., Morphological, crystalline, thermal and physicochemical properties of cellulose nanocrystals obtained from sweet potato residue. *Food research international* **2013,** *50* (1), 121-128.

15. Elazzouzi-Hafraoui, S.; Nishiyama, Y.; Putaux, J.-L.; Heux, L.; Dubreuil, F.; Rochas, C., The shape and size distribution of crystalline nanoparticles prepared by acid hydrolysis of native cellulose. *Biomacromolecules* **2007,** *9* (1), 57-65.

16. Sugiyama, J.; Vuong, R.; Chanzy, H., Electron diffraction study on the two crystalline phases occurring in native cellulose from an algal cell wall. *Macromolecules* **1991,** *24* (14), 4168-4175.

17. Roman, M.; Winter, W. T., Effect of sulfate groups from sulfuric acid hydrolysis on the thermal degradation behavior of bacterial cellulose. *Biomacromolecules* **2004,** *5* (5), 1671-1677.

18. Iwamoto, S.; Nakagaito, A.; Yano, H.; Nogi, M., Optically transparent composites reinforced with plant fiber-based nanofibers. *Applied Physics A* **2005,** *81* (6), 1109-1112.

19. Saito, T.; Kimura, S.; Nishiyama, Y.; Isogai, A., Cellulose nanofibers prepared by TEMPO-mediated oxidation of native cellulose. *Biomacromolecules* **2007,** *8* (8), 2485-2491.

20. Saito, T.; Nishiyama, Y.; Putaux, J.-L.; Vignon, M.; Isogai, A., Homogeneous suspensions of individualized microfibrils from TEMPO-catalyzed oxidation of native cellulose. *Biomacromolecules* **2006,** *7* (6), 1687-1691.

21. Spence, K. L.; Venditti, R. A.; Rojas, O. J.; Habibi, Y.; Pawlak, J. J., The effect of chemical composition on microfibrillar cellulose films from wood pulps: water interactions and physical properties for packaging applications. *Cellulose* **2010,** *17* (4), 835-848.

22. Taipale, T.; Österberg, M.; Nykänen, A.; Ruokolainen, J.; Laine, J., Effect of microfibrillated cellulose and fines on the drainage of kraft pulp suspension and paper strength. *Cellulose* **2010,** *17* (5), 1005-1020.

23. Stenstad, P.; Andresen, M.; Tanem, B. S.; Stenius, P., Chemical surface modifications of microfibrillated cellulose. *Cellulose* **2008,** *15* (1), 35-45.

24. Pääkkö, M.; Ankerfors, M.; Kosonen, H.; Nykänen, A.; Ahola, S.; Österberg, M.; Ruokolainen, J.; Laine, J.; Larsson, P. T.; Ikkala, O., Enzymatic hydrolysis combined with

mechanical shearing and high-pressure homogenization for nanoscale cellulose fibrils and strong gels. *Biomacromolecules* **2007,** *8* (6), 1934-1941.

25. Ahola, S.; Österberg, M.; Laine, J., Cellulose nanofibrils—adsorption with poly (amideamine) epichlorohydrin studied by QCM-D and application as a paper strength additive. *Cellulose* **2008,** *15* (2), 303-314.

26. Saito, T.; Okita, Y.; Nge, T.; Sugiyama, J.; Isogai, A., TEMPO-mediated oxidation of native cellulose: Microscopic analysis of fibrous fractions in the oxidized products. *Carbohydrate polymers* **2006,** *65* (4), 435-440.

27. Zimmermann, T.; Bordeanu, N.; Strub, E., Properties of nanofibrillated cellulose from different raw materials and its reinforcement potential. *Carbohydrate Polymers* **2010,** *79* (4), 1086-1093.

28. Hubbe, M. A.; Rojas, O. J.; Lucia, L. A.; Sain, M., Cellulosic nanocomposites: a review. *BioResources* **2008,** *3* (3), 929-980.

29. Sugiyama, J.; Persson, J.; Chanzy, H., Combined infrared and electron diffraction study of the polymorphism of native celluloses. *Macromolecules* **1991,** *24* (9), 2461-2466.

30. Horikawa, Y.; Sugiyama, J., Localization of crystalline allomorphs in cellulose microfibril. *Biomacromolecules* **2009,** *10* (8), 2235-2239.

31. Heux, L.; Dinand, E.; Vignon, M., Structural aspects in ultrathin cellulose microfibrils followed by 13 C CP-MAS NMR. *Carbohydrate Polymers* **1999,** *40* (2), 115-124.

32. Hanley, S. J.; Revol, J.-F.; Godbout, L.; Gray, D. G., Atomic force microscopy and transmission electron microscopy of cellulose from Micrasterias denticulata; evidence for a chiral helical microfibril twist. *Cellulose* **1997,** *4* (3), 209-220.

33. Jonas, R.; Farah, L. F., Production and application of microbial cellulose. *Polymer Degradation and Stability* **1998,** *59* (1), 101-106.

34. Iguchi, M.; Yamanaka, S.; Budhiono, A., Bacterial cellulose—a masterpiece of nature's arts. *Journal of Materials Science* **2000,** *35* (2), 261-270.

35. Moon, R. J.; Martini, A.; Nairn, J.; Simonsen, J.; Youngblood, J., Cellulose nanomaterials review: structure, properties and nanocomposites. *Chemical Society Reviews* **2011,** *40* (7), 3941-3994.

36. Dufresne, A.; Cavaille, J.-Y.; Vignon, M. R., Mechanical behavior of sheets prepared from sugar beet cellulose microfibrils. *Journal of applied polymer science* **1997,** *64* (6), 1185-1194.

37. Stelte, W.; Sanadi, A. R., Preparation and characterization of cellulose nanofibers from two commercial hardwood and softwood pulps. *Industrial & engineering chemistry research* **2009,** *48* (24), 11211-11219.

38. Naderi, A.; Lindström, T.; Sundström, J.; Pettersson, T.; Flodberg, G.; Erlandsson, J., Microfluidized carboxymethyl cellulose modified pulp: a nanofibrillated cellulose system with some attractive properties. *Cellulose* **2015,** *22* (2), 1159-1173.

39. Ferrer, A.; Filpponen, I.; Rodríguez, A.; Laine, J.; Rojas, O. J., Valorization of residual Empty Palm Fruit Bunch Fibers (EPFBF) by microfluidization: production of nanofibrillated cellulose and EPFBF nanopaper. *Bioresource Technology* **2012,** *125*, 249-255.

40. Iwamoto, S.; Nakagaito, A.; Yano, H., Nano-fibrillation of pulp fibers for the processing of transparent nanocomposites. *Applied Physics A* **2007,** *89* (2), 461-466.

41. Alemdar, A.; Sain, M., Isolation and characterization of nanofibers from agricultural residues–Wheat straw and soy hulls. *Bioresource technology* **2008,** *99* (6), 1664-1671.

42. Chakraborty, A.; Sain, M.; Kortschot, M., Cellulose microfibrils: a novel method of preparation using high shear refining and cryocrushing. *Holzforschung* **2005,** *59* (1), 102-107.

43. Johnson, R. K.; Zink-Sharp, A.; Renneckar, S. H.; Glasser, W. G., A new bio-based nanocomposite: fibrillated TEMPO-oxidized celluloses in hydroxypropylcellulose matrix. *Cellulose* **2009,** *16* (2), 227-238.

44. Wang, S.; Cheng, Q., A novel process to isolate fibrils from cellulose fibers by high-intensity ultrasonication, Part 1: Process optimization. *Journal of applied polymer science* **2009,** *113* (2), 1270-1275.

45. Spence, K. L.; Venditti, R. A.; Rojas, O. J.; Habibi, Y.; Pawlak, J. J., A comparative study of energy consumption and physical properties of microfibrillated cellulose produced by different processing methods. *Cellulose* **2011,** *18* (4), 1097-1111.

46. McClements, D. J.; Rao, J., Food-grade nanoemulsions: formulation, fabrication, properties, performance, biological fate, and potential toxicity. *Critical reviews in food science and nutrition* **2011,** *51* (4), 285-330.

47. Lavoine, N.; Desloges, I.; Dufresne, A.; Bras, J., Microfibrillated cellulose–Its barrier properties and applications in cellulosic materials: A review. *Carbohydrate polymers* **2012,** *90* (2), 735-764.

48. Matsuda, Y.; Hirose, M.; Ueno, K., Super microfibrillated cellulose, process for producing the same, and coated paper and tinted paper using the same. Google Patents: 2001.

49. Eichhorn, S. J.; Dufresne, A.; Aranguren, M.; Marcovich, N.; Capadona, J.; Rowan, S. J.; Weder, C.; Thielemans, W.; Roman, M.; Renneckar, S., Review: current international research into cellulose nanofibres and nanocomposites. *Journal of Materials Science* **2010,** *45* (1), 1-33.

50. Isogai, T.; Saito, T.; Isogai, A., Wood cellulose nanofibrils prepared by TEMPO electro-mediated oxidation. *Cellulose* **2011,** *18* (2), 421-431.

51. Sbiai, A.; Kaddami, H.; Sautereau, H.; Maazouz, A.; Fleury, E., TEMPO-mediated oxidation of lignocellulosic fibers from date palm leaves. *Carbohydrate polymers* **2011,** *86* (4), 1445-1450.

52. Aulin, C.; Johansson, E.; Wågberg, L.; Lindström, T., Self-organized films from cellulose I nanofibrils using the layer-by-layer technique. *Biomacromolecules* **2010,** *11* (4), 872-882.

53. Okahisa, Y.; Yoshida, A.; Miyaguchi, S.; Yano, H., Optically transparent wood–cellulose nanocomposite as a base substrate for flexible organic light-emitting diode displays. *Composites Science and Technology* **2009,** *69* (11), 1958-1961.

54. Klemm, D.; Kramer, F.; Moritz, S.; Lindström, T.; Ankerfors, M.; Gray, D.; Dorris, A., Nanocelluloses: A new family of nature-based materials. *Angewandte Chemie International Edition* **2011,** *50* (24), 5438-5466.

55. Tingaut, P.; Zimmermann, T.; Lopez-Suevos, F., Synthesis and characterization of bionanocomposites with tunable properties from poly (lactic acid) and acetylated microfibrillated cellulose. *Biomacromolecules* **2009,** *11* (2), 454-464.

56. Islam, M. T.; Alam, M. M.; Patrucco, A.; Montarsolo, A.; Zoccola, M., Preparation of Nanocellulose: A Review. *AATCC Journal of Research* **2014,** *1* (5), 17-23.

57. Habibi, Y.; Lucia, L. A.; Rojas, O. J., Cellulose nanocrystals: chemistry, self-assembly, and applications. *Chemical reviews* **2010,** *110* (6), 3479-3500.

58. Wang, B.; Sain, M., Isolation of nanofibers from soybean source and their reinforcing capability on synthetic polymers. *Composites Science and Technology* **2007,** *67* (11), 2521-2527.

59. Montanari, S.; Roumani, M.; Heux, L.; Vignon, M. R., Topochemistry of carboxylated cellulose nanocrystals resulting from TEMPO-mediated oxidation. *Macromolecules* **2005,** *38* (5), 1665-1671.

60. Filson, P. B.; Dawson-Andoh, B. E., Sono-chemical preparation of cellulose nanocrystals from lignocellulose derived materials. *Bioresource Technology* **2009,** *100* (7), 2259-2264.

61. Beck-Candanedo, S.; Roman, M.; Gray, D. G., Effect of reaction conditions on the properties and behavior of wood cellulose nanocrystal suspensions. *Biomacromolecules* **2005,** *6* (2), 1048-1054.

62. Bondeson, D.; Mathew, A.; Oksman, K., Optimization of the isolation of nanocrystals from microcrystalline cellulose by acid hydrolysis. *Cellulose* **2006,** *13* (2), 171-180.

63. Bai, W.; Holbery, J.; Li, K., A technique for production of nanocrystalline cellulose with a narrow size distribution. *Cellulose* **2009,** *16* (3), 455-465.

64. Klemm, D.; Heublein, B.; Fink, H. P.; Bohn, A., Cellulose: fascinating biopolymer and sustainable raw material. *Angewandte Chemie International Edition* **2005,** *44* (22), 3358-3393.

65. Jozala, A. F.; de Lencastre-Novaes, L. C.; Lopes, A. M.; de Carvalho Santos-Ebinuma, V.; Mazzola, P. G.; Pessoa-Jr, A.; Grotto, D.; Gerenutti, M.; Chaud, M. V., Bacterial nanocellulose production and application: a 10-year overview. *Applied microbiology and biotechnology* **2016,** *100* (5), 2063-2072.

66. Shi, Z.; Zhang, Y.; Phillips, G. O.; Yang, G., Utilization of bacterial cellulose in food. *Food Hydrocolloids* **2014,** *35*, 539-545.

67. Krystynowicz, A.; Czaja, W.; Wiktorowska-Jezierska, A.; Gonçalves-Miśkiewicz, M.; Turkiewicz, M.; Bielecki, S., Factors affecting the yield and properties of bacterial cellulose. *Journal of Industrial Microbiology and Biotechnology* **2002,** *29* (4), 189-195.

68. Mohammadkazemi, F.; Azin, M.; Ashori, A., Production of bacterial cellulose using different carbon sources and culture media. *Carbohydrate polymers* **2015,** *117*, 518-523.

69. Kuo, C.-H.; Chen, J.-H.; Liou, B.-K.; Lee, C.-K., Utilization of acetate buffer to improve bacterial cellulose production by Gluconacetobacter xylinus. *Food Hydrocolloids* **2016,** *53*, 98-103.

70. Czaja, W.; Romanovicz, D.; Malcolm Brown, R., Structural investigations of microbial cellulose produced in stationary and agitated culture. *Cellulose* **2004,** *11* (3-4), 403-411.

71. Andresen, M.; Johansson, L.-S.; Tanem, B. S.; Stenius, P., Properties and characterization of hydrophobized microfibrillated cellulose. *Cellulose* **2006,** *13* (6), 665-677.

72. Kalia, S.; Dufresne, A.; Cherian, B. M.; Kaith, B.; Avérous, L.; Njuguna, J.; Nassiopoulos, E., Cellulose-based bio-and nanocomposites: a review. *International Journal of Polymer Science* **2011,** *2011*.

73. Kroon-Batenburg, L.; Kroon, J., The crystal and molecular structures of cellulose I and II. *Glycoconjugate journal* **1997,** *14* (5), 677-690.

74. O'SULLIVAN, A. C., Cellulose: the structure slowly unravels. *Cellulose* **1997,** *4* (3), 173-207.

75. Azizi Samir, M. A. S.; Alloin, F.; Dufresne, A., Review of recent research into cellulosic whiskers, their properties and their application in nanocomposite field. *Biomacromolecules* **2005,** *6* (2), 612-626.

76. Nishiyama, Y., Structure and properties of the cellulose microfibril. *Journal of Wood Science* **2009,** *55* (4), 241-249.

77. Dufresne, A., Polymer nanocomposites from biological sources. *Encyclopedia of nanoscience and nanotechnology* **2007,** *21*, 219-250.

78. Saxena, I. M.; Brown, R. M., Cellulose biosynthesis: current views and evolving concepts. *Annals of botany* **2005,** *96* (1), 9-21.

79. Siró, I.; Plackett, D., Microfibrillated cellulose and new nanocomposite materials: a review. *Cellulose* **2010,** *17* (3), 459-494.

80. Platikanov, D.; Exerowa, D., *Highlights in colloid science*. John Wiley & Sons: 2009.

81. Belgacem, M. N.; Gandini, A., Production, chemistry and properties of cellulose-based materials. *Biopolymers-New Materials for Sustainable Films and Coatings* **2011**, 151-178.

82. Marchessault, R.; Morehead, F.; Koch, M. J., Some hydrodynamic properties of neutral suspensions of cellulose crystallites as related to size and shape. *Journal of Colloid Science* **1961,** *16* (4), 327-344.

83. Terech, P.; Chazeau, L.; Cavaille, J., A small-angle scattering study of cellulose whiskers in aqueous suspensions. *Macromolecules* **1999,** *32* (6), 1872-1875.

84. Sassi, J.-F.; Chanzy, H., Ultrastructural aspects of the acetylation of cellulose. *Cellulose* **1995,** *2* (2), 111-127.

85. Revol, J.-F., On the cross-sectional shape of cellulose crystallites in Valonia ventricosa. *Carbohydrate Polymers* **1982,** *2* (2), 123-134.

86. Fengel, D.; Wegener, G., *Wood: chemistry, ultrastructure, reactions*. Walter de Gruyter: 1983.

87. Salas, C.; Nypelö, T.; Rodriguez-Abreu, C.; Carrillo, C.; Rojas, O. J., Nanocellulose properties and applications in colloids and interfaces. *Current Opinion in Colloid & Interface Science* **2014,** *19* (5), 383-396.

88. Turbak, A. F.; Snyder, F. W.; Sandberg, K. R. In *Microfibrillated cellulose, a new cellulose product: properties, uses, and commercial potential*, J. Appl. Polym. Sci.: Appl. Polym. Symp.;(United States), ITT Rayonier Inc., Shelton, WA: 1983.

89. Zhang, Y.; Carbonell, R. G.; Rojas, O. J., Bioactive cellulose nanofibrils for specific human IgG binding. *Biomacromolecules* **2013,** *14* (12), 4161-4168.

90. Siqueira, G.; Bras, J.; Dufresne, A., Luffa cylindrica as a lignocellulosic source of fiber, microfibrillated cellulose and cellulose nanocrystals. *BioResources* **2010,** *5* (2), 727-740.

91. Siqueira, G.; Tapin-Lingua, S.; Bras, J.; da Silva Perez, D.; Dufresne, A., Morphological investigation of nanoparticles obtained from combined mechanical shearing, and enzymatic and acid hydrolysis of sisal fibers. *Cellulose* **2010,** *17* (6), 1147-1158.

92. Siqueira, G.; Bras, J.; Dufresne, A., New process of chemical grafting of cellulose nanoparticles with a long chain isocyanate. *Langmuir* **2009,** *26* (1), 402-411.

93. Pitkänen, M.; Sneck, A.; Hentze, H.; Sievänen, J.; Hiltunen, J.; Hellén, E.; Honkalampi, U.; von Wright, A. In *Nanofibrillar cellulose—Assessment of cytotoxic and genotoxic properties in vitro*, 2010 Tappi International conference on nanotechnology for the forest products industry, 2010.

94. Vartiainen, J.; Pöhler, T.; Sirola, K.; Pylkkänen, L.; Alenius, H.; Hokkinen, J.; Tapper, U.; Lahtinen, P.; Kapanen, A.; Putkisto, K., Health and environmental safety aspects of friction grinding and spray drying of microfibrillated cellulose. *Cellulose* **2011,** *18* (3), 775-786.

95. Catalán, J.; Rydman, E.; Aimonen, K.; Hannukainen, K.-S.; Suhonen, S.; Vanhala, E.; Moreno, C.; Meyer, V.; da Silva Perez, D.; Sneck, A., Genotoxic and inflammatory effects of nanofibrillated cellulose in murine lungs. *Mutagenesis* **2016**, gew035.

96. Herrick, F. W.; Casebier, R. L.; Hamilton, J. K.; Sandberg, K. R. In *Microfibrillated cellulose: morphology and accessibility*, J. Appl. Polym. Sci.: Appl. Polym. Symp.;(United States), ITT Rayonier Inc., Shelton, WA: 1983.

97. Lowys, M.-P.; Desbrieres, J.; Rinaudo, M., Rheological characterization of cellulosic microfibril suspensions. Role of polymeric additives. *Food Hydrocolloids* **2001,** *15* (1), 25-32.

98. Siqueira, G.; Bras, J.; Dufresne, A., Cellulose whiskers versus microfibrils: influence of the nature of the nanoparticle and its surface functionalization on the thermal and mechanical properties of nanocomposites. *Biomacromolecules* **2008,** *10* (2), 425-432.

99. Dong, X. M.; Kimura, T.; Revol, J.-F.; Gray, D. G., Effects of ionic strength on the isotropic-chiral nematic phase transition of suspensions of cellulose crystallites. *Langmuir* **1996,** *12* (8), 2076-2082.

100. Marchessault, R.; Morehead, F.; Walter, N., Liquid crystal systems from fibrillar polysaccharides. **1959**.

101. Araki, J.; Wada, M.; Kuga, S.; Okano, T., Flow properties of microcrystalline cellulose suspension prepared by acid treatment of native cellulose. *Colloids and Surfaces A: Physicochemical and Engineering Aspects* **1998,** *142* (1), 75-82.

102. Araki, J.; Wada, M.; Kuga, S.; Okano, T., Influence of surface charge on viscosity behavior of cellulose microcrystal suspension. *Journal of wood science* **1999,** *45* (3), 258-261.

103. Revol, J.-F.; Godbout, L.; Dong, X.-M.; Gray, D. G.; Chanzy, H.; Maret, G., Chiral nematic suspensions of cellulose crystallites; phase separation and magnetic field orientation. *Liquid Crystals* **1994,** *16* (1), 127-134.

104. Favier, V.; Canova, G.; Cavaillé, J.; Chanzy, H.; Dufresne, A.; Gauthier, C., Nanocomposite materials from latex and cellulose whiskers. *Polymers for Advanced Technologies* **1995,** *6* (5), 351-355.

105. Hanley, S. J.; Giasson, J.; Revol, J.-F.; Gray, D. G., Atomic force microscopy of cellulose microfibrils: comparison with transmission electron microscopy. *Polymer* **1992,** *33* (21), 4639-4642.

106. Kovacs, T.; Naish, V.; O'Connor, B.; Blaise, C.; Gagné, F.; Hall, L.; Trudeau, V.; Martel, P., An ecotoxicological characterization of nanocrystalline cellulose (NCC). *Nanotoxicology* **2010,** *4* (3), 255-270.

107. Roman, M., Toxicity of cellulose nanocrystals: a review. *Industrial Biotechnology* **2015,** *11* (1), 25-33.

108. Azizi Samir, M. A. S.; Alloin, F.; Sanchez, J.-Y.; El Kissi, N.; Dufresne, A., Preparation of cellulose whiskers reinforced nanocomposites from an organic medium suspension. *Macromolecules* **2004,** *37* (4), 1386-1393.

109. Bercea, M.; Navard, P., Shear dynamics of aqueous suspensions of cellulose whiskers. *Macromolecules* **2000,** *33* (16), 6011-6016.

110. Liu, D.; Chen, X.; Yue, Y.; Chen, M.; Wu, Q., Structure and rheology of nanocrystalline cellulose. *Carbohydrate Polymers* **2011,** *84* (1), 316-322.

111. Lu, P.; Hsieh, Y.-L., Preparation and properties of cellulose nanocrystals: rods, spheres, and network. *Carbohydrate Polymers* **2010,** *82* (2), 329-336.

112. Ureña-Benavides, E. E.; Ao, G.; Davis, V. A.; Kitchens, C. L., Rheology and phase behavior of lyotropic cellulose nanocrystal suspensions. *Macromolecules* **2011,** *44* (22), 8990-8998.

113. Lin, N.; Huang, J.; Dufresne, A., Preparation, properties and applications of polysaccharide nanocrystals in advanced functional nanomaterials: a review. *Nanoscale* **2012,** *4* (11), 3274-3294.

114. Shopsowitz, K. E.; Qi, H.; Hamad, W. Y.; MacLachlan, M. J., Free-standing mesoporous silica films with tunable chiral nematic structures. *Nature* **2010,** *468* (7322), 422-425.

115. Jung, H.-I.; Lee, O.-M.; Jeong, J.-H.; Jeon, Y.-D.; Park, K.-H.; Kim, H.-S.; An, W.-G.; Son, H.-J., Production and characterization of cellulose by Acetobacter sp. V6 using a cost-effective molasses–corn steep liquor medium. *Applied biochemistry and biotechnology* **2010,** *162* (2), 486-497.

116. Ruka, D. R.; Simon, G. P.; Dean, K. M., Altering the growth conditions of Gluconacetobacter xylinus to maximize the yield of bacterial cellulose. *Carbohydrate polymers* **2012,** *89* (2), 613-622.

117. Xiao, S.; Gao, R.; Gao, L.; Li, J., Poly (vinyl alcohol) films reinforced with nanofibrillated cellulose (NFC) isolated from corn husk by high intensity ultrasonication. *Carbohydrate polymers* **2016,** *136*, 1027-1034.

118. Abitbol, T.; Rivkin, A.; Cao, Y.; Nevo, Y.; Abraham, E.; Ben-Shalom, T.; Lapidot, S.; Shoseyov, O., Nanocellulose, a tiny fiber with huge applications. *Current opinion in biotechnology* **2016,** *39*, 76-88.

119. Oun, A. A.; Rhim, J.-W., Preparation and characterization of sodium carboxymethyl cellulose/cotton linter cellulose nanofibril composite films. *Carbohydrate polymers* **2015,** *127*, 101-109.

120. Mukherjee, T.; Czaka, M.; Kao, N.; Gupta, R. K.; Choi, H. J.; Bhattacharya, S., Dispersion study of nanofibrillated cellulose based poly (butylene adipate-co-terephthalate) composites. *Carbohydrate polymers* **2014,** *102*, 537-542.

121. Ankerfors, M.; Lindstrom, T.; Song, H.; Hoc, M., Composition for coating of printing paper. Google Patents: 2012.

122. McKee, J. R.; Hietala, S.; Seitsonen, J.; Laine, J.; Kontturi, E.; Ikkala, O., Thermoresponsive nanocellulose hydrogels with tunable mechanical properties. *ACS Macro Letters* **2014,** *3* (3), 266-270.

123. Yang, S.; Tang, Y.; Wang, J.; Kong, F.; Zhang, J., Surface treatment of cellulosic paper with starch-based composites reinforced with nanocrystalline cellulose. *Industrial & Engineering Chemistry Research* **2014,** *53* (36), 13980-13988.

124. Slavutsky, A. M.; Bertuzzi, M. A., Water barrier properties of starch films reinforced with cellulose nanocrystals obtained from sugarcane bagasse. *Carbohydrate polymers* **2014,** *110*, 53-61.

125. Wang, B.; Walther, A., Self-Assembled, Iridescent, Crustacean-Mimetic Nanocomposites with Tailored Periodicity and Layered Cuticular Structure. *ACS nano* **2015,** *9* (11), 10637-10646.

126. Montes, S.; Carrasco, P. M.; Ruiz, V.; Cabañero, G.; Grande, H. J.; Labidi, J.; Odriozola, I., Synergistic reinforcement of poly (vinyl alcohol) nanocomposites with cellulose nanocrystal-stabilized graphene. *Composites Science and Technology* **2015,** *117*, 26-31.

127. Zhou, C.; Shi, Q.; Guo, W.; Terrell, L.; Qureshi, A. T.; Hayes, D. J.; Wu, Q., Electrospun bio-nanocomposite scaffolds for bone tissue engineering by cellulose nanocrystals reinforcing maleic anhydride grafted PLA. *ACS applied materials & interfaces* **2013,** *5* (9), 3847-3854.

128. Mariano, M.; El Kissi, N.; Dufresne, A., Melt processing of cellulose nanocrystal reinforced polycarbonate from a masterbatch process. *European Polymer Journal* **2015,** *69*, 208-223.

129. Klemm, D.; Schumann, D.; Kramer, F.; Heßler, N.; Koth, D.; Sultanova, B. In *Nanocellulose materials–Different cellulose, different functionality*, Macromolecular symposia, Wiley Online Library: 2009; pp 60-71.

130. Zhao, Y.; Simonsen, J.; Cavender, G.; Jung, J.; Fuchigami, L. H., Nano-cellulose coatings to prevent damage in foodstuffs. Google Patents: 2014.

131. Vilarinho, F.; Sanches-Silva, A.; Vaz, M. F.; Farinha, J. P., Nanocellulose: a benefit for green food packaging. *Critical Reviews in Food Science and Nutrition* **2016,** (just-accepted), 00-00.

132. RAMPAZZO, R.; MASCHERONI, E.; FASANO, F.; MARI, M.; PIERGIOVANNI, L., STRATEGIES FOR IMPLEMENTING NANO-CELLULOSE COATINGS IN FLEXIBLE PACKAGING. *Italian Journal of Food Science* **2015**.

133. Li, F.; Biagioni, P.; Bollani, M.; Maccagnan, A.; Piergiovanni, L., Multi-functional coating of cellulose nanocrystals for flexible packaging applications. *Cellulose* **2013,** *20* (5), 2491-2504.

134. Aulin, C.; Ström, G. r., Multilayered alkyd resin/nanocellulose coatings for use in renewable packaging solutions with a high level of moisture resistance. *Industrial & Engineering Chemistry Research* **2013,** *52* (7), 2582-2589.

135. Herrera, M. A.; Sirviö, J. A.; Mathew, A. P.; Oksman, K., Environmental friendly and sustainable gas barrier on porous materials: Nanocellulose coatings prepared using spin-and dip-coating. *Materials & Design* **2016,** *93*, 19-25.

136. Wang, C.; Li, Y. L.; Hong, F.; Tang, S. J.; Wang, Y. Y. In *Nano-Cellulose Coating Small-Caliber Artificial Blood Vessel*, Advanced Materials Research, Trans Tech Publ: 2011; pp 1794-1798.

137. Jabbar, A.; Militký, J.; Wiener, J.; Kale, B. M.; Ali, U.; Rwawiire, S., Nanocellulose coated woven jute/green epoxy composites: Characterization of mechanical and dynamic mechanical behavior. *Composite Structures* **2017,** *161*, 340-349.

138. Muthu, S. S., *Roadmap to Sustainable Textiles and Clothing: Eco-friendly Raw Materials, Technologies, and Processing Methods*. Springer: 2014.

139. GIROD, K.; GALAFASSI, P., The genuine low salt reactive dyes. *Colourage* **2004,** *51* (7), 100-104.

140. Kitamura, S.; Washimi, T.; Yamamoto, K. In *Low salt dyeing using fibre reactive dyes on cotton. Book of papers*, AATCC International Conference and Exhibition, Philadelphia, 1998.

141. Bradbury, M.; Collishaw, P.; Moorhouse, S., Smart Rinsing: A Step Change in Reactive Dye Application Technology. *AATCC Review* **2001,** *1* (11).

142. Hao, O. J.; Kim, H.; Chiang, P.-C., Decolorization of wastewater. *Critical reviews in environmental science and technology* **2000,** *30* (4), 449-505.

143. Fu, Y.; Viraraghavan, T., Removal of CI Acid Blue 29 from an aqueous solution by Aspergillus niger. *Aatcc Review* **2001,** *1* (1), 36-40.

144. ColorZen, 2012. ColorZen: How it Works/the Benefits. Available at: http://www.colorzen.com/.

145. DyeCoo CO2 Dyeing Technology. Available at: http://www.dyecoo.com/.

146. Hermes, J. Process for the rapid, continuous and waterless dyeing of textile and plastic materials. 1977.

147. Hasanbeigi, A.; Price, L., A technical review of emerging technologies for energy and water efficiency and pollution reduction in the textile industry. *Journal of Cleaner Production* **2015,** *95*, 30-44.

CHAPTER 2

NANOCELLULOSE THIN FILMS AS SUSTAINABLE FUNCTIONAL COATINGS FOR TEXTILE MATERIALS[1]

[1] Saremi, R., N., Borodinov, A., Laradgi, S., Sharma, I., Lusinov, and S., Minko. To be submitted to Cellulose.

Abstract

We have developed nanocellulose based thin films as functional coatings for textile materials. Nanocellulose thin films can incorporate many functionalities such as dye, antimicrobial, flame-retardant and stain-resistant molecules and transfer them to textile surfaces. To develop efficient and robust nanocellulose coatings, we prepared multilayer model surfaces of nanofibrillated cellulose (NFC) and nanocrystalline cellulose (NCC) on top of regenerated cellulose, polyester and nylon 66 on silicon wafers using a spin coating process to investigate and improve the adhesion of nanocellulose toward natural and synthetic fibers. The multilayer surfaces were made by using modified NFC and NCC gels with a polyelectrolyte and a copolymer synthesized from oligo [ethylene glycol] methyl ether methacrylate and Glycidyl methacrylate to improve the adhesion between nanocellulose fibers and textile fibers and make stable, smooth, thin films. The thickness of the films and their surface morphology were studied by ellipsometry, Scanning Electron Microscopy (SEM), and Atomic Force Microscopy (AFM). The adhesion strength between the NFC and NCC gels and natural, synthetic and blended fabrics were investigated by using a T-Peel strength test for sandwich-like specimens consisting of two layers of fabrics adhered with nanocellulose hydrogels.

2.1 Introduction

Due to current health, safety and environmental concerns associated with the textile industry, and growing need for advanced generation of smart textiles[1] it is necessary to focus on the development of more environmentally sustainable and renewable materials that have a potential to transfer various functionalities to textile surfaces. In this context, cellulose is the most abundant,[2-3] renewable, biodegradable and environmentally friendly organic compound found in nature and has a potential to be used in the development of natural resource-based materials with minimum health, environmental, or safety concerns.[4] Cellulose-based materials have been used in many applications by taking advantages of the hierarchical structure design within these elements. However, to achieve the properties, functionality, and quality needed for high-performance materials, cellulose should be extracted at the nanoscale level to remove the majority of the defects associated with the hierarchical structure. Cellulose is composed of fibrils that are formed by the process of biosynthesis and stabilized by the intra/inter chain hydrogen bonds and van der Waals forces.[5] These fibrils consisting of crystalline and amorphous regions[6] can be separated by mechanical,[7-12] chemical[13-15] or a combination of both treatments[16] to make cellulose nanoparticles in the form of fibrils (nanofibrillated cellulose [NFC]) or the form of crystals/whiskers (nanocrystalline cellulose [NCC]).[17-18] These nanoparticles present low density, high length-to-width ratio, and high mechanical stability, which make them ideal for developing new materials.[16, 19-21] Cellulose has a natural affinity toward self-adhesion, which relies primarily on inter/intra-molecular hydrogen bonding between the adjacent hydroxyl groups that occurs in the wet state. Mechanical entanglements, specifically for nanofibrillated cellulose (NFC). Van der Waals forces which contribute to the parallel stacking of cellulose chains in one plane. And covalent linkages between repeat units.[22-23] These forces/interactions have significant impacts on the mechanical

stability and stiffness of nanocellulose materials. Cellulose also has many surface hydroxyl groups[5] that can form hydrogen bonds with other electronegative groups such as hydroxyl, amine, and halide in addition to the covalent bonds and physical entanglement of the cellulose fibrillar network, polymer surfaces[22] or textiles structures that anchor nanocellulose materials to other surfaces for coating application. Functional molecules, added to the nanocellulose materials, are also covalently bonds or physically entrapped into the fibrillar network and can be anchored to textile surfaces along with the nanocellulose materials. Nanocellulose particles also have a large surface area that allows for the high uptake of functional molecules which make them the ideal substrate for incorporating functionalities to other surfaces.

Nanocellulose coatings/films have been used for food[24] and Flexible packages[24-27] in different studies. They are effective in protecting food substances and products, from various types of processing damages.[24] Nanocellulose coatings can also be used for reinforcing polymer composites[28] as well as in medical applications such as artificial blood vessels by combining a textile vessel with nanocellulose coatings to form a new type of small artificial blood vessel.[29] In this study, we used thin films of natural and synthetic fibers to mimic textile surfaces[30] to investigate and improve the adhesion strength between nanocellulose and textile fibers in the nanoscale system. Nanocellulose particles have been used in many studies to develop thin films of nanocelluose using spin coating and spin casting processes.[31-34] In this work, we developed stable thin films of NFC and NCC by using the spin coating method. These coatings can be further used to transfer different functionalities to textile surfaces.

2.2 Experimental Section

2.2.1 Materials

Nanocellulose Hydrogels. Nanofibrillated cellulose gel (NFC) (2%) was prepared as previously reported,[35] and nanocrystalline cellulose gel (NCC) (11.9%) was purchased from the Process Development Center, University of Maine.

Solvents for polymer solutions. m-Cresol (MW 108.14), Lithium chloride (MW 42.39), N,N-Dimethylacetamide (MW 87.12) Chlorobenzene (MW 112.56) and Phenol (MW 94.11) were purchased from Sigma-Aldrich.

Anchoring Substances. Polyethylenimine (PEI) (average Mn 60,000) was used as an anchoring substance and was received from Sigma-Aldrich. 1% PEI solution was prepared in 60°C deionized water (DI) and stirred for 30 min. Glycidyl methacrylate (97%), azoisobutyronitrile (AIBN), oligo (ethylene glycol) methyl ether methacrylate (average Mn 950, containing 100 ppm MEHQ and 300 ppm BHT as inhibitor) and inhibitor removers (replacement packing for removing hydroquinone and monomethyl ether hydroquinone [MEHQ] and replacement packing for removing tert-butylcatechol [BHT]) were purchased from Sigma-Aldrich. All solvents used in this study were purchased from VWR International and used as received.

Substrates. Silicon wafers with a natural oxide surface and orientation 100 were purchased from University Wafer (South Boston, MA).

2.2.2 Synthesis of the copolymer

P(GMA-OEGMA) was synthesized by solution radical polymerization. According to NMR analysis, the copolymer had 66 mol % OEGMA and 34 mol % GMA. Due to the large molecular mass of OEGMA, it composed 93% of the copolymer by weight. The typical overall value of molecular weight measured by DLS and calculated from NMR data was about 2 000 kDa. While

the product of the reaction was a random copolymer, the strong polar nature of PEG units made the crystal formation possible. This composition had a glass transition at -50°C and well-pronounced melting at 35°C and was remarkably well soluble in water.

Synthesis of the copolymer. P(GMA-OEGMA) copolymer used here was synthesized using solution free-radical copolymerization. MEHQ inhibitor removers were added to GMA, MEHQ and BHT inhibitor removers were added to OEGMA dissolved in MEK. After 45 minutes, the beads were filtered, and the resulting solutions were mixed with AIBN and MEK. The GMA/OEGMA molar ratio was 1:4. Overall monomer concentration was set at 0.5 M, and AIBN concentration was 0.01 M. The solution was placed in a round-bottom flask and purged with nitrogen for 45 minutes. Afterward, the flask was placed in a water bath preheated to 50°C for 1.5 hours. The flask was then opened to the atmosphere, and its solution was precipitated in diethyl ether. Dissolution in MEK and precipitation in diethyl ether was repeated three times. The copolymer was stored in MEK solution in the absence of light

Analysis of the copolymer composition. Nuclear magnetic resonance was done using Bruker AVANCE-300 spectrometer and TopSpin 1.3 PL4 software and analyzed with Delta 5.0.4 software.

Analysis of the copolymer thermal properties. Differential scanning calorimetry (Model 2920; TA Instruments) was carried out at a heating/cooling rate of 20 °C/min. The temperature range of the experiment was set from -100 °C to 100 °C. The samples were heated, cooled and then reheated again. The second heating was used to measure the glass transition temperature and melting point. The glass transition is reported as the inflection point on the heat flow graph.

Analysis of the copolymer molecular weight. Dynamic light scattering was used to estimate the molecular weight of the synthesized polymers. A Malvern Zetasizer ZS Dynamic Light

Scattering and Zeta Potential instrument were utilized to characterize the size of polymer coil in methyl ethyl ketone and to estimate the molecular weight. A set of monodisperse polystyrene standards with molecular weights ranging from 200 up to 3000 kDa dissolved in MEK were used for calibration. The resulting data were fitted with a linear function in $MW^{0.5}$-size coordinates. It was further recalculated into the molecular weight using NMR data regarding copolymer composition.

2.2.3 Preparation of Substrates

Silicon Wafers. Si wafers were cut into square pieces (1 × 1 cm^2) and then cleaned in a solution of 28% NH4OH/30% H2O2/H2O (1:1:1) at 65 °C for 1 hour. They were rinsed with DI water and dried under a flux of argon gas. The cleaned wafers were dipped into the solution of PEI (1%) for 15 min and rinsed with DI water and dried with argon gas. The resulting modified silicon wafers were kept at room temperature in a clean desiccator for later use.

Preparation of Regenerated Cellulose Films. Thin cellulose films were prepared by heating a mixture of cellulose in a solution of lithium chloride (LiCl, 1-3%) and N,N-dimethylacetamide (DMAc, 3-9%) to 150 °C then allowing the solution to cool slowly to room temperature.[36-37] Afterward, 20 μl of the cellulose solution was spin coated (3000 rpm for 10 s) onto the cleaned silicon wafers. The samples were submerged in DI water for 20 min to remove the remaining LiCl; They were dried with argon gas and heated for 20 min at 180 °C to allow for the evaporation of any residual solvent. Finally, they were stored at room temperature in a clean chamber for further use.

Preparation of Polyester Films. Polyester fibers were dissolved in a solution of phenol-chlorobenzene (1:1) in a boiling water bath (temperature held at approximately 100 °C). Once fully dissolved, 20 μl of the solution was spin coated (3000 rpm for 20 s) on the silicon wafers. The

substrates were transferred to an oven heated at 180 °C and left for 24 hours to remove the residual solvent.

Preparation of Nylon Films. The solution was made by dissolving nylon 66 fibers in m-cresol at 100 °C for several hours until complete dissolution. The nylon films were prepared by spin-coating (3000 rpm for 20 s) 20 μl of the solution on the silicon wafers. The substrates were immediately transferred to an oven and dried at 180°C for 24 hours.

2.2.4 Preparation of Multilayer Films

Nanocellulose films on Model Surfaces. NFC and NCC multilayer films were prepared by spin-coating (3000 rpm for 30 s) 20 μl of the diluted NFC and NCC hydrogels (1%) onto the substrates (cellulose, polyester and nylon films) and annealed at 120 °C for 24 hours.

PEI-Modified Nanocellulose films on Model Surfaces. The PEI-modification was performed using two different approaches: Treatment of the substrates (PEI-NFC/NCC) and treatment of the NFC/NCC hydrogels (PEI+NFC/NCC). In the PEI-NFC/NCC method, substrates were submerged into the 1% PEI solution for 30 min, then rinsed with DI water and dried with argon gas before spin-coating (30 rpm 10 s) 20 μl of the solution of NFC/NCC (1%). Then the substrates annealed at 120 °C for 1 hour. In the PEI+NFC/NCC method, NFC (0.1%) and NCC (1%) were mixed with the PEI solution (1%) (20:1 by volume) and stirred for 1 hour. Then 20 μl of the PEI-modified hydrogels were spin-coated onto the model surfaces. Finally, they were transferred to an oven and dried at 120 °C for 1 hour.

P(GMA-OEGMA)-Modified Nanocellulose Films on Model Surfaces. The P(GMA-OEGMA)-modification was also performed using both substrates (P(GMA-OEGMA)-NFC/NCC) and NFC/NCC hydrogels (P(GMA-OEGMA)+NFC/NCC) treatments with the copolymer. In the P(GMA-OEGMA)-NFC/NCC method, the model films were submerged in the solution of the

copolymer for 30 min, then rinsed with DI water and dried with argon gas before spin-coating (30 rpm 10 s) 20 µl of the NFC/NCC (1%) hydrogels. Then the substrates annealed at 120 °C for 1 hour. In the PEI+NFC/NCC method, NFC (0.1%) and NCC (1%) were mixed with P(GMA-OEGMA) (20:1 by volume) and stirred for 1 hour. Then 20 µl of the P(GMA-OEGMA)-modified hydrogels were spin-coated (30 rpm 10 s) on the model surfaces. Finally, they were transferred to an oven and dried at 120 °C for 1 hour.

2.2.5 Characterization Techniques

Scanning Electron Microscopy (SEM). SEM imaging was carried out using an FEI Teneo (FEI Co., Hillsboro, OR), a Field Emission Scanning Electron Microscope.

Atomic Force Microscopy (AFM). Atomic force microscopy (AFM) images were taken using Bruker Multimode Nanoscope instrument with the ScanAssyst-Air probe (Bruker, spring constant 0.4 N/n, a silicon oxide tip).

Ellipsometry. The thickness of the films at three different locations of each sample after the deposition of each layer on the substrates was measured by A spectrometric ellipsometer from Accurion (Germany) with a fixed angle of incidence of 70°. Ellipsometry thickness maps were generated using the Accurion software package, DataStudio.

2.2.6 T-Peel Test

The peel test is a standard mechanical test to measure adhesion, and it can be performed at different angles. In a T-peel test (the specimen forms a T-shape), two thin flexible laminates are bonded together by a layer of adhesive and are pulled apart at 90° angle while recording the peeling force (the force needed to separate these two layers from each other), which is related to the adhesion strength.[38] In this study, T-peel tests were performed according to ASTM D1876-08 test method using an Instron tensile compression tester. For these tests, cotton (100%, plain weave),

nylon (100%, spun, plain weave), polyester/cotton (50%/50%, plain weave), polyester (100%, spun, plain weave) (purchased from Testafabrics, INC., USA), and cotton/polyester (35%/65%) (provided by Burlington Labs, USA) fabrics were cut into 50 mm × 152 mm along the warp direction. The test panel (Fig. 2.8) consisted of two layers of fabrics were bonded together with 5 g of NFC/NCC hydrogels (2%) over approximately 127 mm of their length. A 2-kg load was applied on top of the test panels while drying. Then the specimens were placed in a conditioning chamber (Macbeth SpectraLight®) for 7 days at a relative humidity of 50 ± 2 % at 23 ± 1°C. Finally, cut the bonded panels into 25-mm-wide test specimens with a sharp cutter. During the tests, the peeling force was recorded at a constant head speed of 254 mm/min.

2.3 Results and Discussion

As shown in Fig. 2.1, we successfully coated a thin layer of nanocellulose hydrogels on a single fiber of polyester, cotton, and nylon. Fig. 2.2 shows the difference of NFC and NCC coatings related to the surface morphology in a microscale. While NFC coating has a higher roughness due to the fibrillated structure, NCC coating is smoother and more uniform. Therefore, NFC hydrogel may result in more efficient and stable coating in the case of incorporating functionalities into the NFC fibrillated network and further bind them to textile surfaces using physical entanglement and mechanical interlocking throughout its mesh-like and fibrillated network. In our next study (chapter 3), we further investigate how to modify the NFC/NCC coatings to increase the number of functional molecules that can survive during the rinsing and drying steps on textile surfaces.

2.3.1 Thickness/Surface Area Measurement

Film thicknesses were measured by ellipsometry as well as AFM at three different locations before and after washing the films with 50°C water to measure the stability of the films. For AFM images, the thickness was estimated using AFM imaging of the topography of the samples after

scratching off parts of the films with the sharp steel needle. The thickness was measured along the scratch at three different points by subtracting the thickness of the deposited layers from the thickness of silicon wafers. Table 2.1-Table 2.6 show thicknesses and total area (%) of the control (without any modifications) and modified films before and after washing. Fig. 2.3 shows the AFM images of regenerated cellulose, nylon and polyester films on silicon wafers with the estimated root mean square (RMS) roughness of 6.59 nm, 1.17 nm, and 2.19 nm. For regenerated cellulose films, the thickness of pure cellulose is 83.9 nm, and the thickness of NFC layer is about 50 nm, but after washing, it decreased to 16 nm which shows low adhesion between cellulose films and NFC layer. On the other hand, the thickness of NCC-cellulose film shows almost no difference before and after washing (105 nm). For polyester and nylon films (55.2 nm and 30 nm respectively), the amount of NFC and NCC gels before and after washing make it easier to measure the total areas of NFC/NCC gels on top of polyester and nylon films by ImageJ software. The total area of NFC for polyester before and after washing are 14.05% and 3.95% and for NCC are 84.81% and 5.39% respectively. The similar trend happened for nylon-NFC/NCC films which show a very weak adhesion between NFC/NCC layers and nylon film (AFM images are available in the supporting information-Fig. 2.17 and Fig. 2.18) with the total area of NFC 14.05% and 8.43% and NCC 75.13% and 1.97% for before and after washing respectively. This show a very weak adhesion between NFC/NCC layers and polyester and nylon substrates. To increase the adhesion between NFC/NCC layer and cotton, polyester and nylon films, we proposed the use of anchoring substances that would provide additional adhesion between model surfaces and the nanocellulose hydrogels. In this study we used, PEI and P(GMA-OEGMA) to increase the adhesion between the layers. Cationic anchoring polymers have been used in many studies to treat mineral substrates before the surfaces are exposed to cellulose solutions.[32-33, 39-46] The anchoring polymers provide

cationic surface layers on the mineral substrates and interact with cellulose through electrostatic attraction.[39] Since nanocellulose, cotton, and polyester fibers are anionic, and nylon 66 possesses a zwitterion structure and has both positive and negative electrical charges. Adhesion between nanocellulose and these fibers can be counteracted by repulsive forces resulting from the electrostatic interaction. These repulsive forces can be overcome by employing PEI containing cationic polyelectrolytes. Cationic PEI anchors anionic cellulose through its branched structure.

P(GMA-OEGMA), on the other hand, contains epoxy groups which provide crosslinking between nanocellulose and the substrates resulting in stronger adhesion and higher thickness and coverage. As shown in Table 2.1-Table 2.6 both nanocellulose and substrate treated films show higher thicknesses and more stability than control films after washing with 50°C water. These results are consistent with the previous studies on model films of cellulose. The thickness and coverage of the cellulose films are much higher with PEI than without PEI.[45] Both treatments also show comparable results except for PEI treated NCC for all three substrates, and Nylon+NFC, PEI treated substrate which the thicknesses are much higher compared to nanocellulose treated films. Therefore, both methods of modifications can be used to improve the adhesion between nanocellulose gels and textile surfaces. Fig. 2.4 and Fig. 2.5 show AFM images of nylon+PEI-treated nanocellulose gels (NFC/NCC) model films before and after washing. The step-by-step ellipsometric thickness map of cellulose + P(GMA-OEGMA)-NFC (Fig. 2.6) and cellulose + PEI-NCC (Fig. 2.7) further confirms the efficiency of PEI and P(GMA-OEGMA) treatments of nanocellulose gel and substrate in making smooth, thin coatings for textile surfaces.

2.3.2 T-peel test

Finally, for T-peel test, five samples were tested for each experimental measurement, and the mean value of peel strength was calculated from S = F/W, where F is the peeling force applied

to the specimens in Newtons and W is the width of the strips in mm.[47] Table 2.7 compares the average peel strength (N/25mm) and peel extension (mm) for cotton, polyester, nylon, cotton/polyester (35/65) and cotton/polyester (50/50) adhered with NFC and NCC gels. Fig. 2.9 and Fig. 2.10 show peeling load vs. peeling extension graphs for NFC-fabrics and NCC-fabrics respectively.

For all NFC/NCC-fabric samples, the debonding of the structures occurred primarily at the NFC/NCC-fabrics interface. The average forces to part the two bonded fabrics to NCC were determined to be higher than NFC because the NCC whisker-like particles are smaller than the fibrils in NFC and can be better-trapped and entangled into the structure of fabrics. During the sample preparation and drying steps for the peel test, NCC particles in hydrogels are likely to migrate and subsequently entrapped into the fibers in the fabrics and made stronger bonds. The NFC/NCC- nylon samples also show higher peel strength than the other samples which is consistent with the result from the model surfaces. For model surfaces, the thickness of the nanocellulose layer on NFC/NCC-nylon films after the washing step is up to 140 nm which is substantially higher than the thickness of NCC on the cellulose and polyester films. Since nanocellulose, cotton, and polyester fibers are anionic, there will be repulsive forces between their negative electrical charges. However, nylon 66 possesses a zwitterion structure and has both positive as well as negative electrical charges. These positive charges may contribute to the higher adhesion between nylon and nanocellulose gels.

2.4 Summary

Stable, thin and smooth nanocellulose coatings were developed using two different methods of modifying nanocellulose gels and modifying substrates. The stability of the coatings was analyzed by measuring the thicknesses of the films with AFM and ellipsometry before and

after the washing step. Before the modification with the anchoring substances, only cellulose films showed stability after the washing step. After the modification, all the samples had excellent stability, and thicknesses up to 431 nm were achieved. T peel test was conducted to investigate the adhesion between nanocellulose hydrogels and fabrics. And nylon fabrics showed higher peel strength compared to cotton, polyester, and blended fabrics. It was anticipated that the developed nanocellulose coatings could be applied to textile surfaces to transfer different functionalities such as dye molecules to textile materials. This matter will be further investigated in chapter 3.

2.5 References

1. Tao, X., *Handbook of smart textiles*. Springer Singapore: 2015.

2. Henriksson, M.; Berglund, L. A., Structure and properties of cellulose nanocomposite films containing melamine formaldehyde. *Journal of Applied Polymer Science* **2007,** *106* (4), 2817-2824.

3. Iwamoto, S.; Nakagaito, A.; Yano, H., Nano-fibrillation of pulp fibers for the processing of transparent nanocomposites. *Applied Physics A: Materials Science & Processing* **2007,** *89* (2), 461-466.

4. Azzam, F.; Moreau, C. l.; Cousin, F.; Menelle, A.; Bizot, H.; Cathala, B., Cellulose nanofibril-based multilayered thin films: Effect of ionic strength on porosity, swelling, and optical properties. *Langmuir* **2014,** *30* (27), 8091-8100.

5. Kalia, S.; Dufresne, A.; Cherian, B. M.; Kaith, B.; Avérous, L.; Njuguna, J.; Nassiopoulos, E., Cellulose-based bio-and nanocomposites: a review. *International Journal of Polymer Science* **2011,** *2011*.

6. Atalla, R., The individual structures of native celluloses. **1999**.

7. Chakraborty, A.; Sain, M.; Kortschot, M., Cellulose microfibrils: a novel method of preparation using high shear refining and cryocrushing. *Holzforschung* **2005,** *59* (1), 102-107.

8. Iwamoto, S.; Nakagaito, A.; Yano, H., Nano-fibrillation of pulp fibers for the processing of transparent nanocomposites. *Applied Physics A* **2007,** *89* (2), 461-466.

9. Johnson, R. K.; Zink-Sharp, A.; Renneckar, S. H.; Glasser, W. G., A new bio-based nanocomposite: fibrillated TEMPO-oxidized celluloses in hydroxypropylcellulose matrix. *Cellulose* **2009,** *16* (2), 227-238.

10. Lavoine, N.; Desloges, I.; Dufresne, A.; Bras, J., Microfibrillated cellulose–Its barrier properties and applications in cellulosic materials: A review. *Carbohydrate polymers* **2012,** *90* (2), 735-764.

11. Nishiyama, Y., Structure and properties of the cellulose microfibril. *Journal of Wood Science* **2009,** *55* (4), 241-249.

12. Wang, S.; Cheng, Q., A novel process to isolate fibrils from cellulose fibers by high-intensity ultrasonication, Part 1: Process optimization. *Journal of applied polymer science* **2009,** *113* (2), 1270-1275.

13. Missoum, K.; Belgacem, M. N.; Bras, J., Nanofibrillated cellulose surface modification: a review. *Materials* **2013,** *6* (5), 1745-1766.

14. Saito, T.; Kimura, S.; Nishiyama, Y.; Isogai, A., Cellulose nanofibers prepared by TEMPO-mediated oxidation of native cellulose. *Biomacromolecules* **2007,** *8* (8), 2485-2491.

15. Saito, T.; Nishiyama, Y.; Putaux, J.-L.; Vignon, M.; Isogai, A., Homogeneous suspensions of individualized microfibrils from TEMPO-catalyzed oxidation of native cellulose. *Biomacromolecules* **2006,** *7* (6), 1687-1691.

16. Moon, R. J.; Martini, A.; Nairn, J.; Simonsen, J.; Youngblood, J., Cellulose nanomaterials review: structure, properties and nanocomposites. *Chemical Society Reviews* **2011,** *40* (7), 3941-3994.

17. Klemm, D.; Kramer, F.; Moritz, S.; Lindström, T.; Ankerfors, M.; Gray, D.; Dorris, A., Nanocelluloses: A new family of nature-based materials. *Angewandte Chemie International Edition* **2011,** *50* (24), 5438-5466.

18. Atalla, R. H.; Brady, J. W.; Matthews, J. F.; Ding, S. Y.; Himmel, M. E., Structures of plant cell wall celluloses. *Biomass recalcitrance: deconstructing the plant cell wall for bioenergy* **2008**, 188-212.

19. Salas, C.; Nypelö, T.; Rodriguez-Abreu, C.; Carrillo, C.; Rojas, O. J., Nanocellulose properties and applications in colloids and interfaces. *Current Opinion in Colloid & Interface Science* **2014,** *19* (5), 383-396.

20. Habibi, Y.; Lucia, L. A.; Rojas, O. J., Cellulose nanocrystals: chemistry, self-assembly, and applications. *Chem. Rev* **2010,** *110* (6), 3479-3500.

21. Johar, N.; Ahmad, I.; Dufresne, A., Extraction, preparation and characterization of cellulose fibres and nanocrystals from rice husk. *Industrial Crops and Products* **2012,** *37* (1), 93-99.

22. Gardner, D. J.; Oporto, G. S.; Mills, R.; Samir, M. A. S. A., Adhesion and surface issues in cellulose and nanocellulose. *Journal of Adhesion Science and Technology* **2008,** *22* (5-6), 545-567.

23. Sinko, R.; Qin, X.; Keten, S., Interfacial mechanics of cellulose nanocrystals. *MRS Bulletin* **2015,** *40* (4), 340-348.

24. Zhao, Y.; Simonsen, J.; Cavender, G.; Jung, J.; Fuchigami, L. H., Nano-cellulose coatings to prevent damage in foodstuffs. Google Patents: 2014.

25. Vilarinho, F.; Sanches-Silva, A.; Vaz, M. F.; Farinha, J. P., Nanocellulose: a benefit for green food packaging. *Critical Reviews in Food Science and Nutrition* **2016,** (just-accepted), 00-00.

26. RAMPAZZO, R.; MASCHERONI, E.; FASANO, F.; MARI, M.; PIERGIOVANNI, L., STRATEGIES FOR IMPLEMENTING NANO-CELLULOSE COATINGS IN FLEXIBLE PACKAGING. *Italian Journal of Food Science* **2015**.

27. Li, F.; Biagioni, P.; Bollani, M.; Maccagnan, A.; Piergiovanni, L., Multi-functional coating of cellulose nanocrystals for flexible packaging applications. *Cellulose* **2013,** *20* (5), 2491-2504.

28. Jabbar, A.; Militký, J.; Wiener, J.; Kale, B. M.; Ali, U.; Rwawiire, S., Nanocellulose coated woven jute/green epoxy composites: Characterization of mechanical and dynamic mechanical behavior. *Composite Structures* **2017,** *161*, 340-349.

29. Wang, C.; Li, Y. L.; Hong, F.; Tang, S. J.; Wang, Y. Y. In *Nano-Cellulose Coating Small-Caliber Artificial Blood Vessel*, Advanced Materials Research, Trans Tech Publ: 2011; pp 1794-1798.

30. Song, J.; Liang, J.; Liu, X.; Krause, W. E.; Hinestroza, J. P.; Rojas, O. J., Development and characterization of thin polymer films relevant to fiber processing. *Thin Solid Films* **2009,** *517* (15), 4348-4354.

31. Luner, P. E.; Oh, E., Characterization of the surface free energy of cellulose ether films. *Colloids and Surfaces A: Physicochemical and Engineering Aspects* **2001,** *181* (1), 31-48.

32. Fält, S.; Wågberg, L.; Vesterlind, E.-L.; Larsson, P. T., Model films of cellulose ID–improved preparation method and characterization of the cellulose film. *Cellulose* **2004,** *11* (2), 151-162.

33. Sczech, R.; Riegler, H., Molecularly smooth cellulose surfaces for adhesion studies. *Journal of colloid and interface science* **2006,** *301* (2), 376-385.

34. Kontturi, E.; Thüne, P.; Niemantsverdriet, J., Novel method for preparing cellulose model surfaces by spin coating. *Polymer* **2003,** *44* (13), 3621-3625.

35. Kim, Y.; McCoy, L. T.; Lee, E.; Lee, H.; Saremi, R.; Feit, C.; Hardin, I. R.; Sharma, S.; Mani, S.; Minko, S., Environmentally sound textile dyeing technology with nanofibrillated cellulose. *Green Chemistry* **2017,** *19* (17), 4031-4035.

36. McCormick, C. L., Novel cellulose solutions. Google Patents: 1981.

37. McCormick, C. L.; Callais, P. A.; Hutchinson Jr, B. H., Solution studies of cellulose in lithium chloride and N, N-dimethylacetamide. *Macromolecules* **1985,** *18* (12), 2394-2401.

38. Kim, K. S.; Aravas, N., Elastoplastic analysis of the peel test. *International Journal of Solids and Structures* **1988,** *24* (4), 417-435.

39. Ahola, S.; Salmi, J.; Johansson, L.-S.; Laine, J.; Österberg, M., Model films from native cellulose nanofibrils. Preparation, swelling, and surface interactions. *Biomacromolecules* **2008,** *9* (4), 1273-1282.

40. Aulin, C.; Ahola, S.; Josefsson, P.; Nishino, T.; Hirose, Y.; Österberg, M.; Wågberg, L., Nanoscale Cellulose Films with Different Crystallinities and Mesostructures□ Their Surface Properties and Interaction with Water. *Langmuir* **2009,** *25* (13), 7675-7685.

41. Eriksson, M.; Notley, S. M.; Wågberg, L., Cellulose thin films: Degree of cellulose ordering and its influence on adhesion. *Biomacromolecules* **2007,** *8* (3), 912-919.

42. Gunnars, S.; Wågberg, L.; Stuart, M. C., Model films of cellulose: I. Method development and initial results. *Cellulose* **2002,** *9* (3-4), 239-249.

43. Hoeger, I.; Rojas, O. J.; Efimenko, K.; Velev, O. D.; Kelley, S. S., Ultrathin film coatings of aligned cellulose nanocrystals from a convective-shear assembly system and their surface mechanical properties. *Soft Matter* **2011,** *7* (5), 1957-1967.

44. Notley, S. M.; Eriksson, M.; Wågberg, L.; Beck, S.; Gray, D. G., Surface forces measurements of spin-coated cellulose thin films with different crystallinity. *Langmuir* **2006,** *22* (7), 3154-3160.

45. Wågberg, L.; Decher, G.; Norgren, M.; Lindström, T.; Ankerfors, M.; Axnäs, K., The build-up of polyelectrolyte multilayers of microfibrillated cellulose and cationic polyelectrolytes. *Langmuir* **2008,** *24* (3), 784-795.

46. Yokota, S.; Kitaoka, T.; Wariishi, H., Surface morphology of cellulose films prepared by spin coating on silicon oxide substrates pretreated with cationic polyelectrolyte. *Applied Surface Science* **2007,** *253* (9), 4208-4214.

47. Zhang, Z.-z.; Zhang, H.-j.; Guo, F.; Wang, K.; Jiang, W., Enhanced wear resistance of hybrid PTFE/Kevlar fabric/phenolic composite by cryogenic treatment. *Journal of materials science* **2009,** *44* (22), 6199-6205.

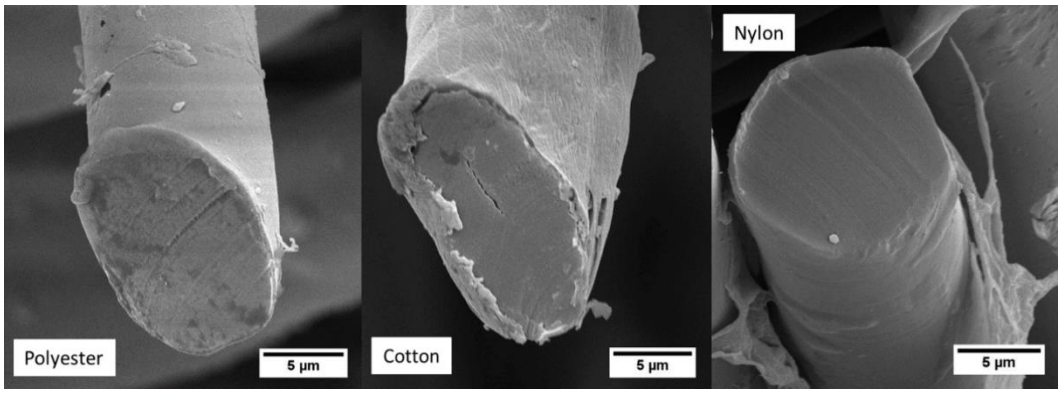

Fig. 2.1. SEM images of polyester, cotton and nylon fibers coated with nanofibrillated cellulose (NFC)

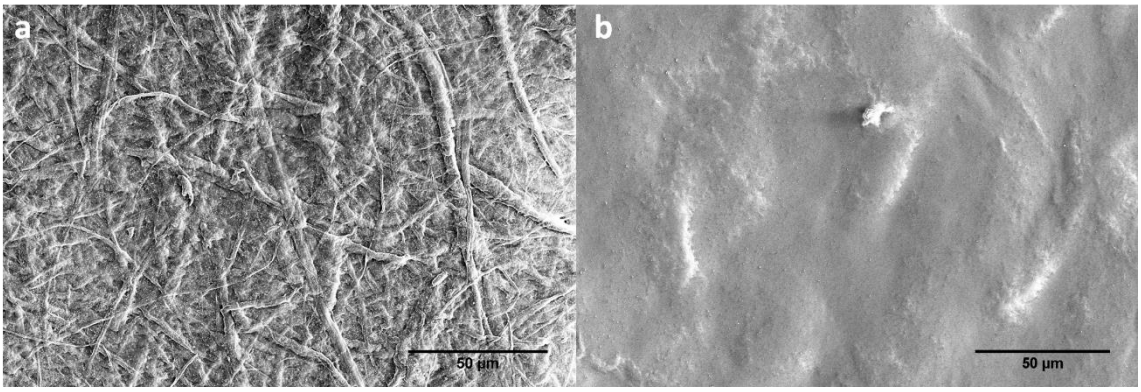

Fig. 2.2. SEM images of thin films of NFC (a) and NCC (b) on silicon wafer

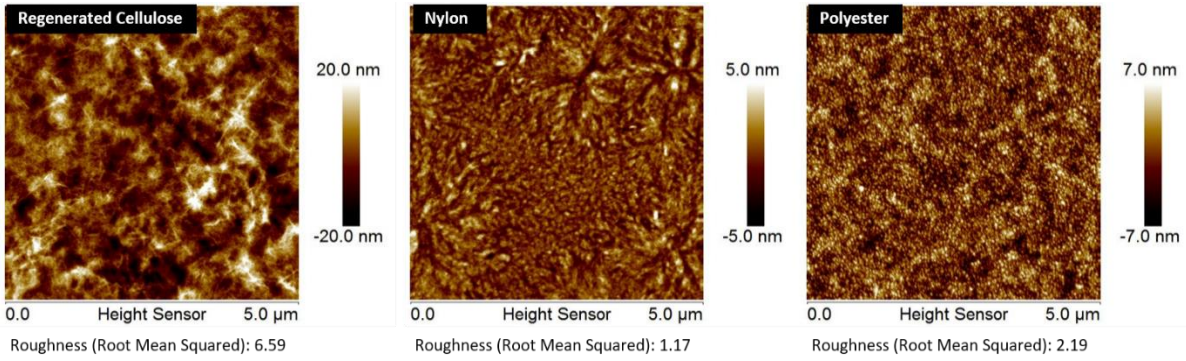

Fig. 2.3. AFM images of regenerated cellulose, nylon and polyester films on silicon wafers

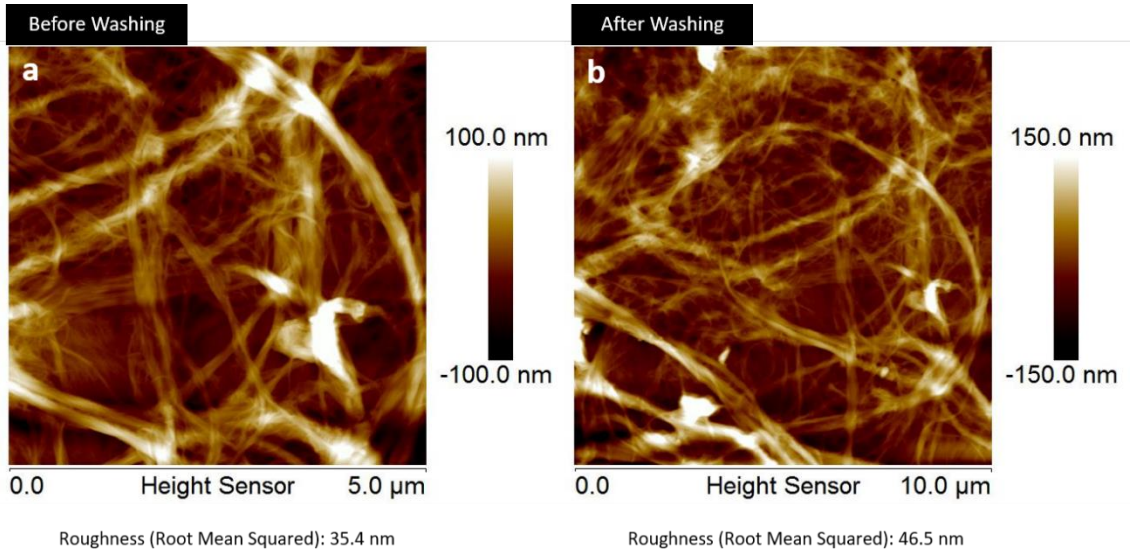

Fig. 2.4. Nylon + PEI-NFC before (a) and after washing (b)

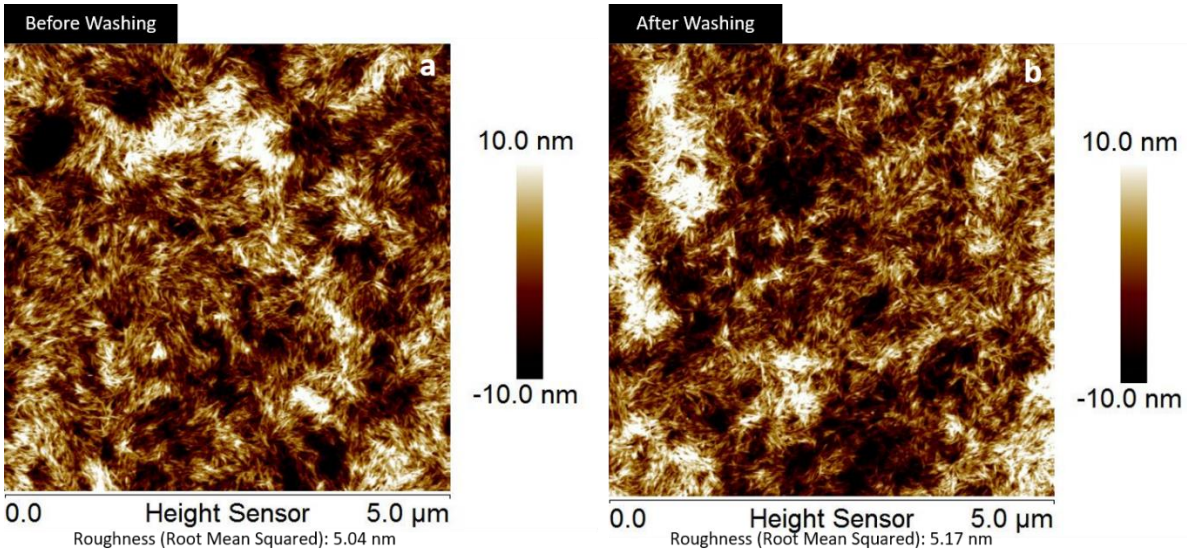

Fig. 2.5. Nylon + PEI+NCC before (a) and after washing (b)

Table 2.1. Thickness of regenerated cellulose films treated with PEI

Thickness	Cellulose	Cellulose + NFC (Control)	Cellulose + PEI+NFC	Cellulose + PEI-NFC	Cellulose + NCC (Control)	Cellulose + PEI+NCC	Cellulose + PEI-NCC
Before Washing	83.90 nm (1.00)	134.00 nm (0.58)	104.00 nm (1.25)	130.00 nm (1.20)	105.00 nm (0.60)	124.00 nm (0.75)	173.00 nm (0.90)
After Washing	-	100.00 nm (0.81)	90.00 nm (1.13)	120.00 nm (1.44)	104.00 nm (0.55)	114.00 nm (0.88)	126.00 nm (1.60)

Table 2.2. Thickness of polyester films treated with PEI and total area (%) of control film

Thickness	Polyester	Polyester + NFC (Control)	Polyester + PEI+NFC	Polyester + PEI-NFC	Polyester + NCC (Control)	Polyester + PEI+NCC	Polyester + PEI-NCC
Before Washing	55.20 nm (1.60)	14.05%	73.60 nm (0.68)	97.50 nm (1.56)	78.40 nm (0.56) 84.81%	132.00 nm (1.23)	168.00 nm (0.77)
After Washing	-	3.95%	69.60 nm (1.31)	90.00 nm (0.88)	5.39%	123.00 nm (0.80)	100.00 nm (0.33)

Table 2.3. Thickness of Nylon films treated with PEI and total area (%) of control film

Thickness	Nylon	Nylon + NFC (Control)	Nylon + PEI+NFC	Nylon + PEI-NFC	Nylon + NCC (Control)	Nylon + PEI+NCC	Nylon + PEI-NCC
Before Washing	30.00 nm (0.16)	14.05%	82.50 nm (0.21)	*	95.10 nm (1.66) 75.13%	94.90 nm (0.45)	*
After Washing	-	8.43%	63.00 nm (0.69)	*	1.97%	45.70 nm (0.84)	172.00 nm (1.00)

Table 2.4. Thickness of regenerated cellulose films treated with P(GMA-OEGMA)

Thickness	Cellulose	Cellulose + NFC (Control)	Cellulose + P(GMA-OEGMA)+NFC	Cellulose + P(GMA-OEGMA)-NFC	Cellulose + NCC (Control)	Cellulose + P(GMA-OEGMA)+NCC	Cellulose + P(GMA-OEGMA)-NCC
Before Washing	83.90 nm (1.00)	134.00 nm (0.58)	117.00 nm (1.11)	206.00 nm (0.77)	105.00 nm (0.60)	91.50 nm (0.66)	94.30 nm (1.33)
After Washing	-	100.00 nm (0.81)	91.50 nm (2.32)	205.00 nm (0.28)	104.00 nm (0.55)	90.70 nm (0.08)	88.30 nm (0.90)

Table 2.5. Thickness of polyester films treated with P(GMA-OEGMA) and total area (%) of control film

Thickness	Polyester	Polyester + NFC (Control)	Polyester + P(GMA-OEGMA)+NFC	Polyester + P(GMA-OEGMA)-NFC	Polyester + NCC (Control)	Polyester + P(GMA-OEGMA)+NCC	Polyester + P(GMA-OEGMA)-NCC
Before Washing	55.20 nm (1.60)	14.05%	*	*	78.40 nm (0.56) 84.81%	135.00 nm (1.47)	133.00 nm (0.54)
After Washing	-	3.95%	400.00 nm (2.63)	*	5.39%	134.00 nm (0.32)	131.00 nm (1.33)

Table 2.6. Thickness of nylon films treated with P(GMA-OEGMA) and total area (%) of control film

Thickness	Nylon	Nylon + NFC (Control)	Nylon + P(GMA-OEGMA)+NFC	Nylon + P(GMA-OEGMA)-NFC	Nylon + NCC (Control)	Nylon + P(GMA-OEGMA)+NCC	Nylon + P(GMA-OEGMA)-NCC
Before Washing	30.00 nm (0.16)	14.05%	431.00 nm (2.23)	*	95.10 nm (1.66) 75.13%	163.00 nm (0.87)	*
After Washing	-----	8.43%	329.00 nm (1.88)	268.00 nm (2.45)	1.97%	161.00 nm (0.62)	168.00 nm (1.10)

* Due to the high thickness of the film, thickness measurement was not possible.
Standard deviations are shown in parenthesis.

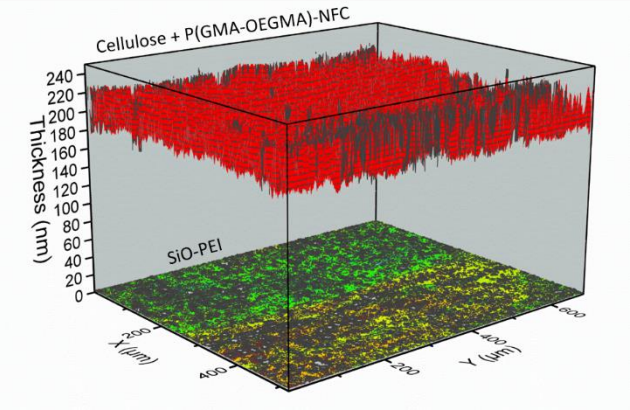

Fig. 2.6. Step-by-step ellipsometric thickness map of Cellulose + P(GMA-OEGMA)-NFC

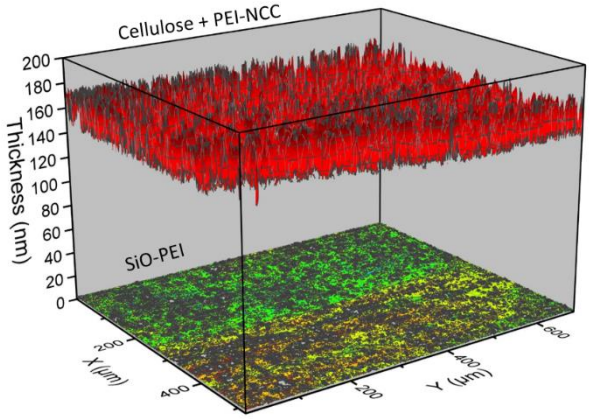

Fig. 2.7. Step-by-step ellipsometric thickness map of Cellulose + PEI-NCC

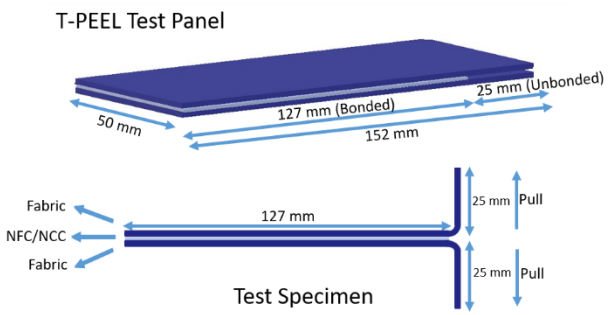

Fig. 2.8. T-PEEL test panel and test specimen

Table 2.7. T-Peel test between fabrics and nanocellulose gels

Fabrics	Adhesive Layers	Avg Peel Strength (N/25mm)	Avg Peel Extension (mm)
Cotton	NFC	0.06 (0.01)	124.76 (0.68)
Polyester	NFC	0.06 (0.03)	125.22 (0.30)
Nylon	NFC	0.14 (0.02)	126.66 (1.20)
Cotton/Polyester (35/65)	NFC	0.08 (0.02)	125.22 (0.75)
Cotton/Polyester (50/50)	NFC	0.06 (0.01)	137.69 (0.66)
Cotton	NCC	0.17 (0.04)	109.92 (1.12)
Polyester	NCC	0.14 (0.03)	126.86 (0.73)
Nylon	NCC	0.19 (0.04)	122.65 (0.45)
Cotton/Polyester (35/65)	NCC	0.11 (0.01)	128.11 (1.44)
Cotton/Polyester (50/50)	NCC	0.20 (0.04)	124.96 (0.77)

Standard deviations are shown in parenthesis.

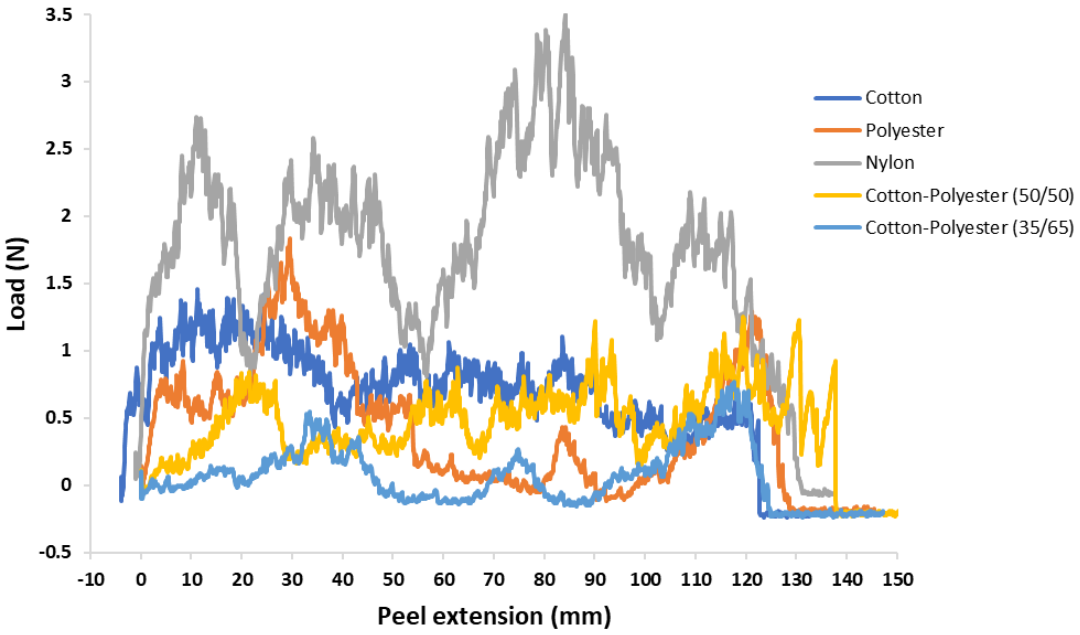

Fig. 2.9. Peeling load vs. peeling extension graph of NFC−natural/synthetic/blended fabrics

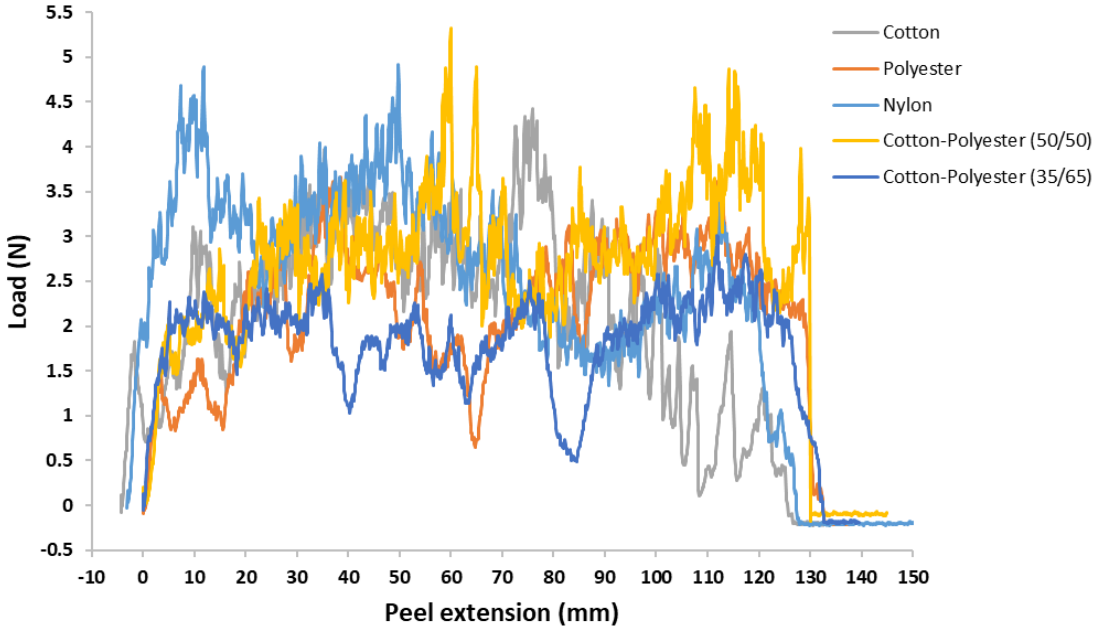

Fig. 2.10. Peeling load vs. peeling extension graph NCC−natural/synthetic/blended fabrics

2.6 Supporting Information

Atomic Force Microscopy (AFM).

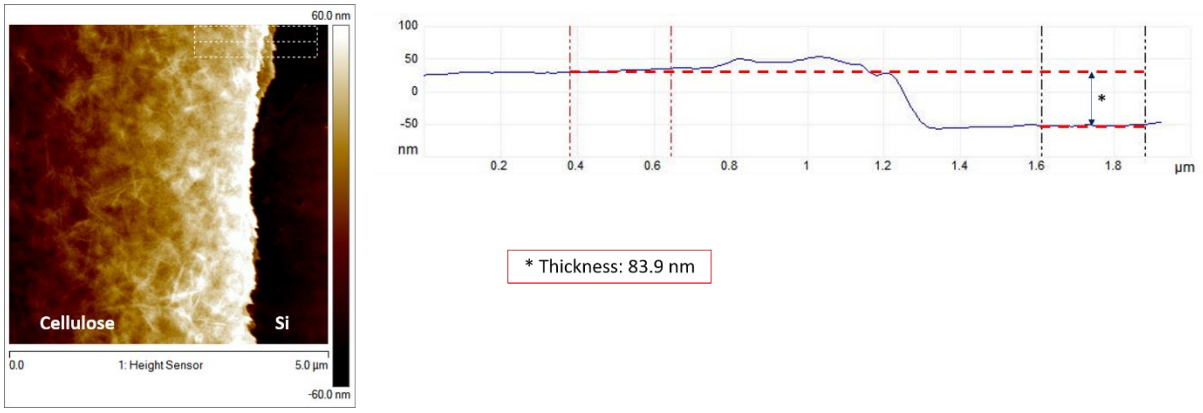

Fig. 2.11. Topography image of the Si-Cellulose step after the scratch with a steel needle

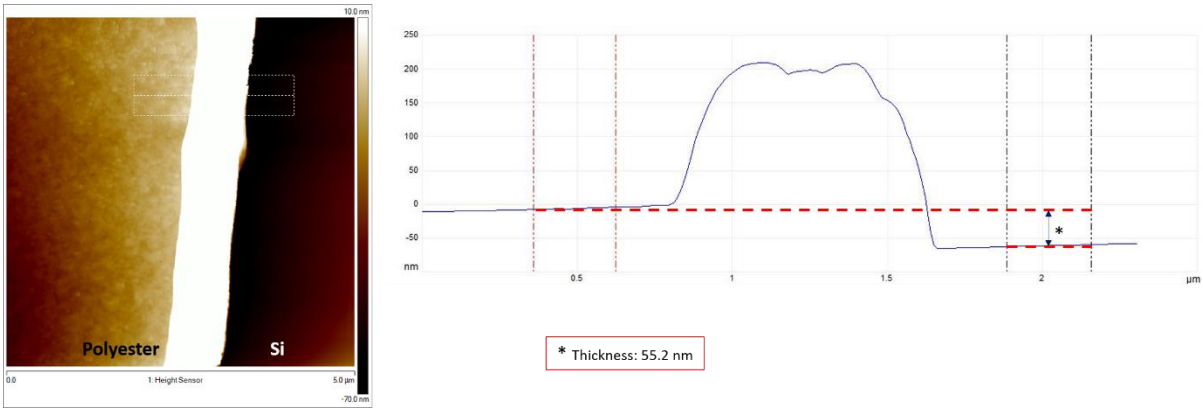

Fig. 2.12. Topography image of the Si-Polyester steps after the scratch with a steel needle

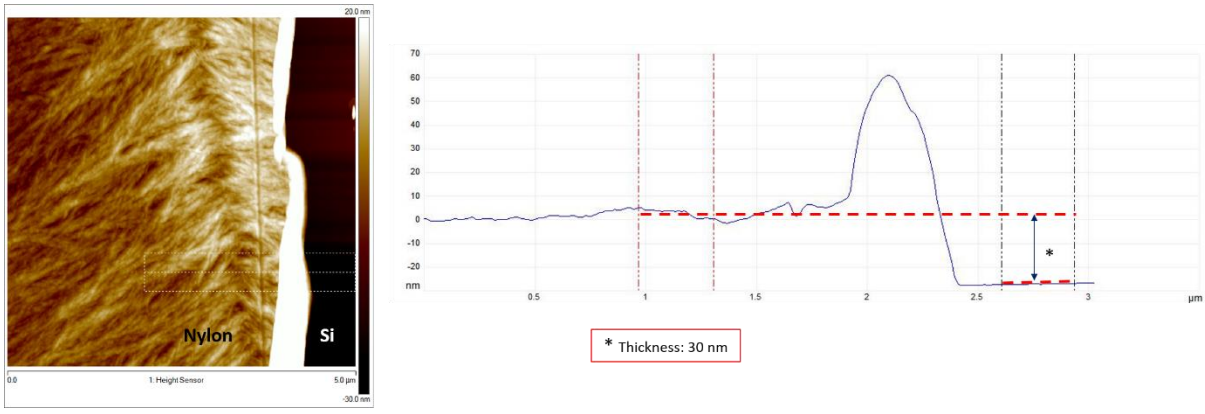

Fig. 2.13. Topography image of the Si-Nylon step after the scratch with a steel needle

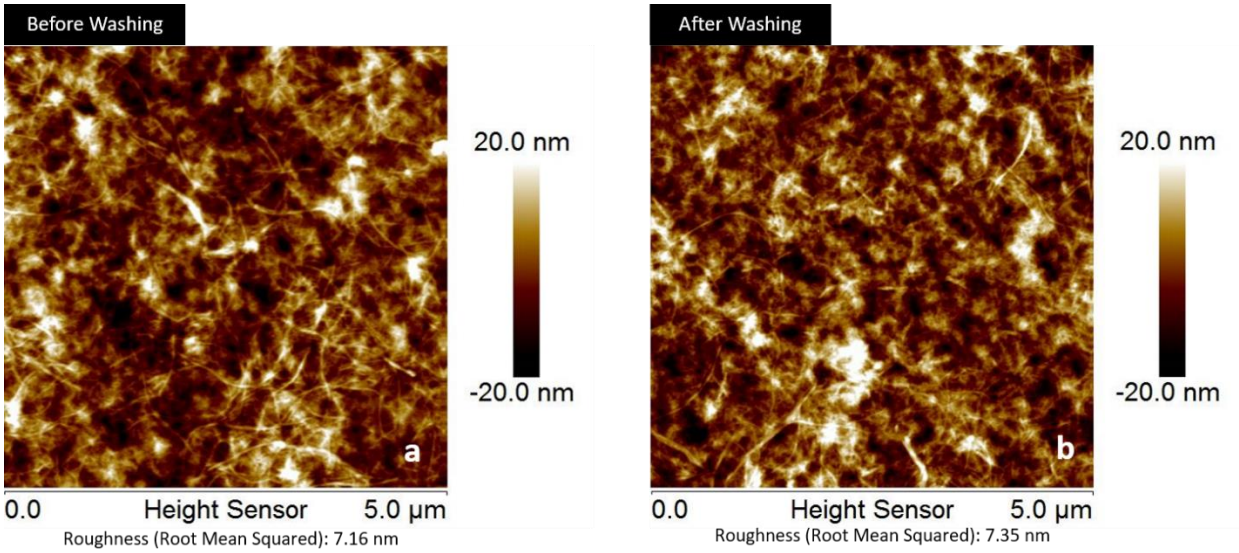

Fig. 2.14. Regenerated cellulose + NFC (control) before (a) and after washing (b)

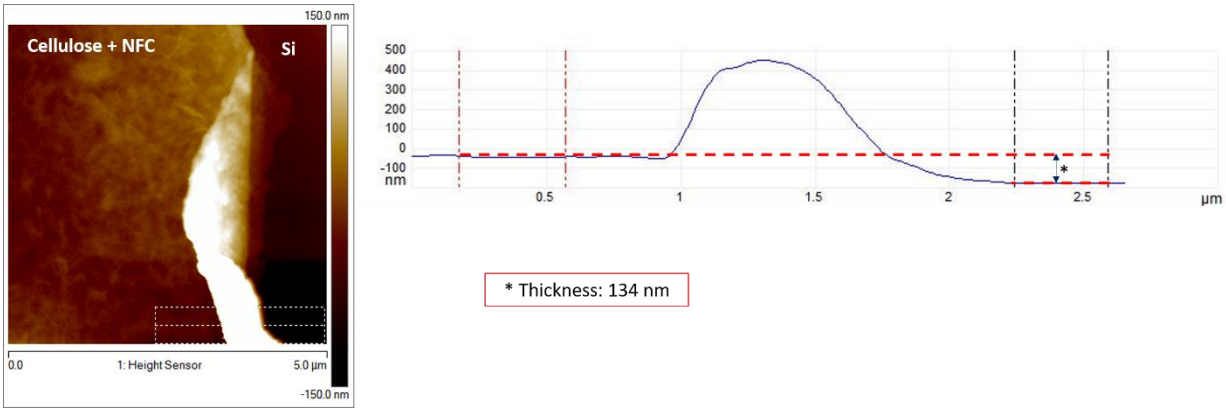

Fig. 2.15. Topography image of the Si-Cellulose + NFC (Control, before washing) after the scratch with a steel needle

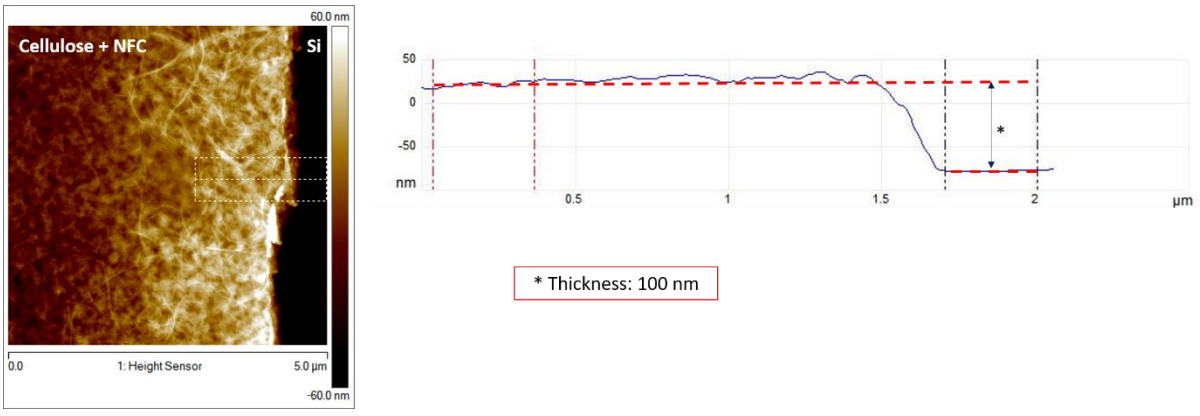

Fig. 2.16. Topography image of the Si-cellulose + NFC (Control, after washing) after the scratch with a steel needle

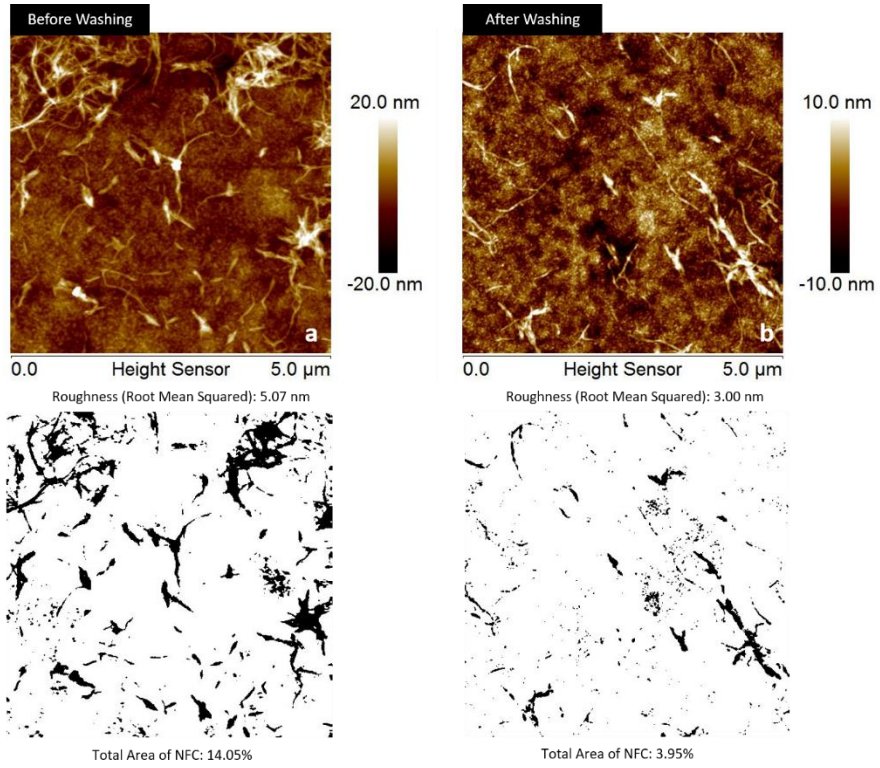

Fig. 2.17. Polyester + NFC (control) before (a) and after washing (b)

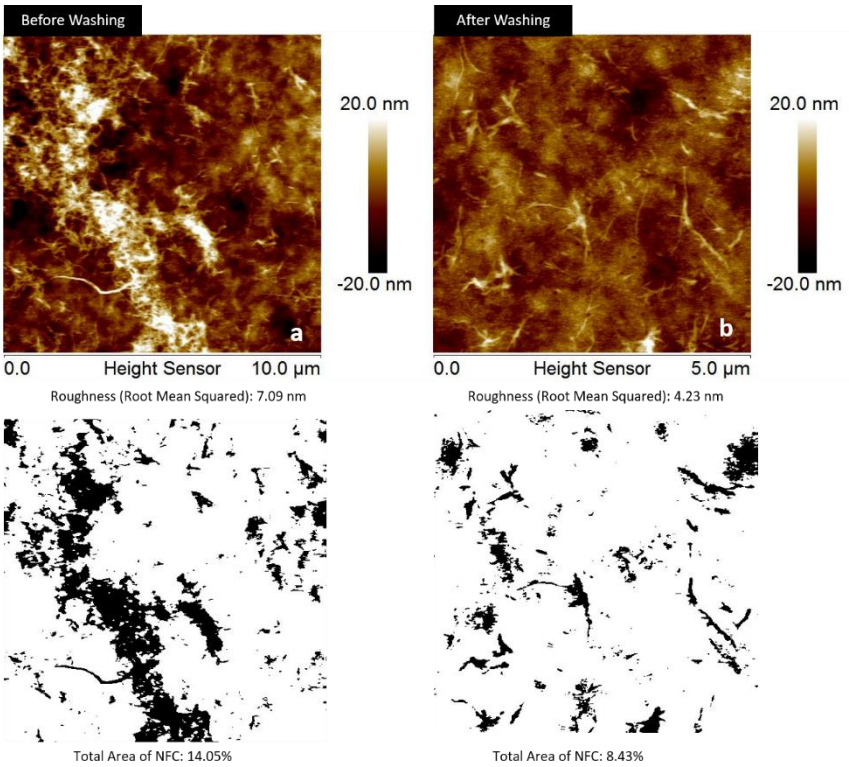

Fig. 2.18. Nylon + NFC (control) before (a) and after washing (b)

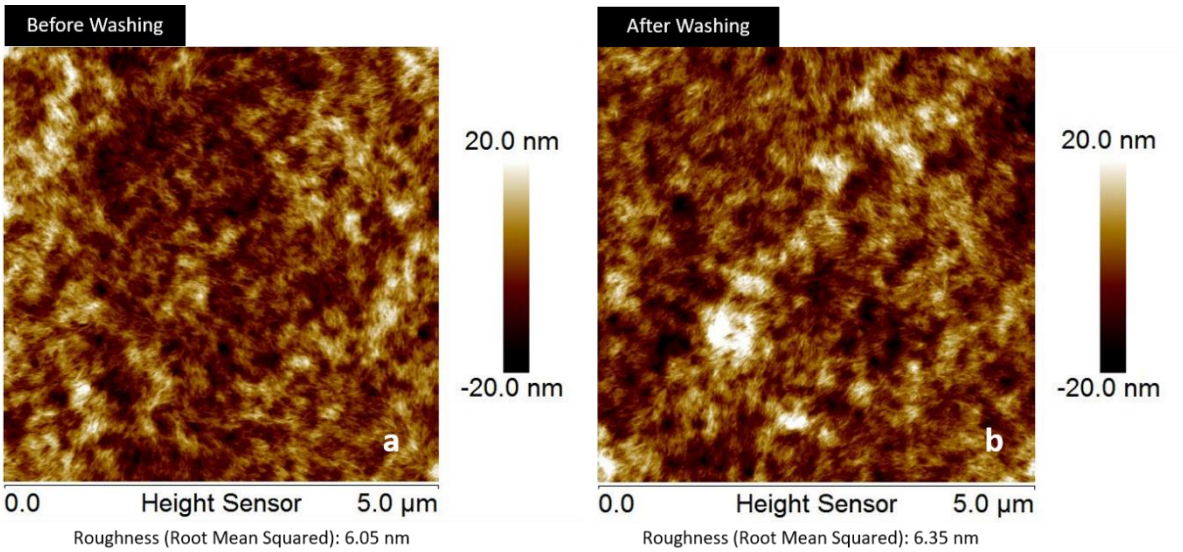

Fig. 2.19. Regenerated cellulose + NCC (control) before (a) and after washing (b)

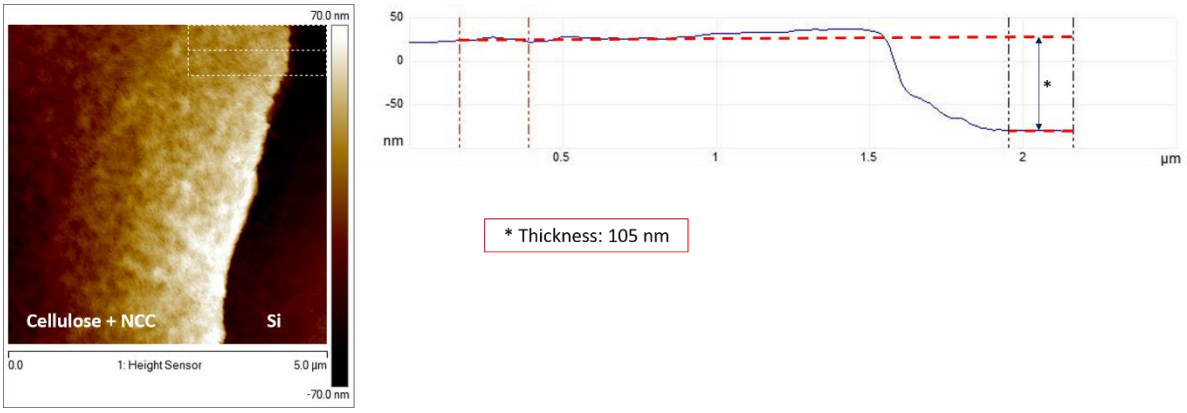

Fig. 2.20. Topography image of the Si-Cellulose + NCC (Control, before washing) after the scratch with a steel needle

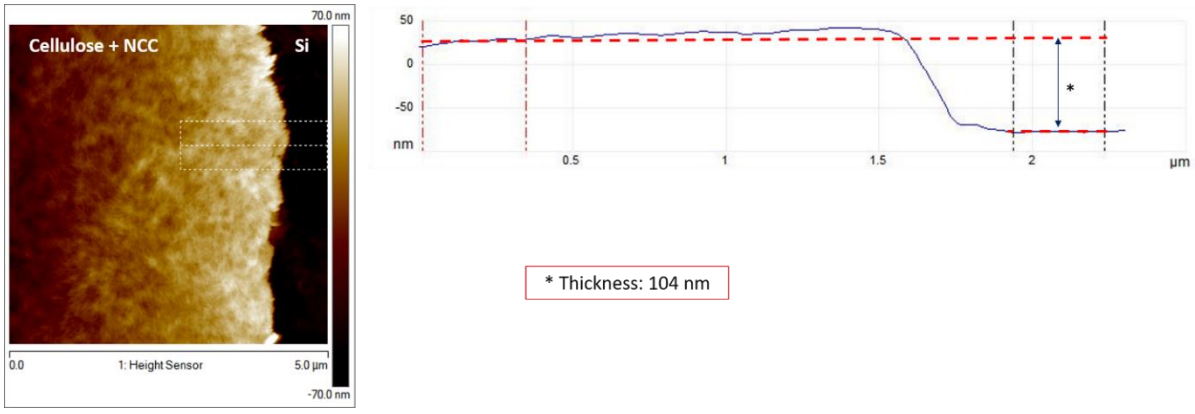

Fig. 2.21. Topography image of the Si-Cellulose + NCC (Control, after washing) after the scratch with a steel needle

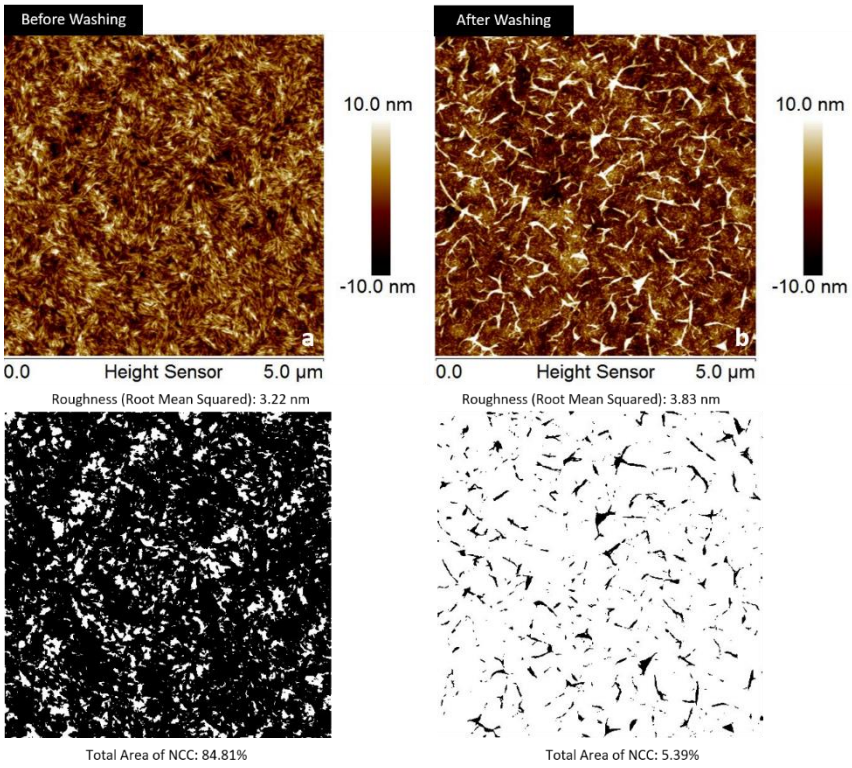

Fig. 2.22. Polyester + NCC (control) before (a) and after washing (b)

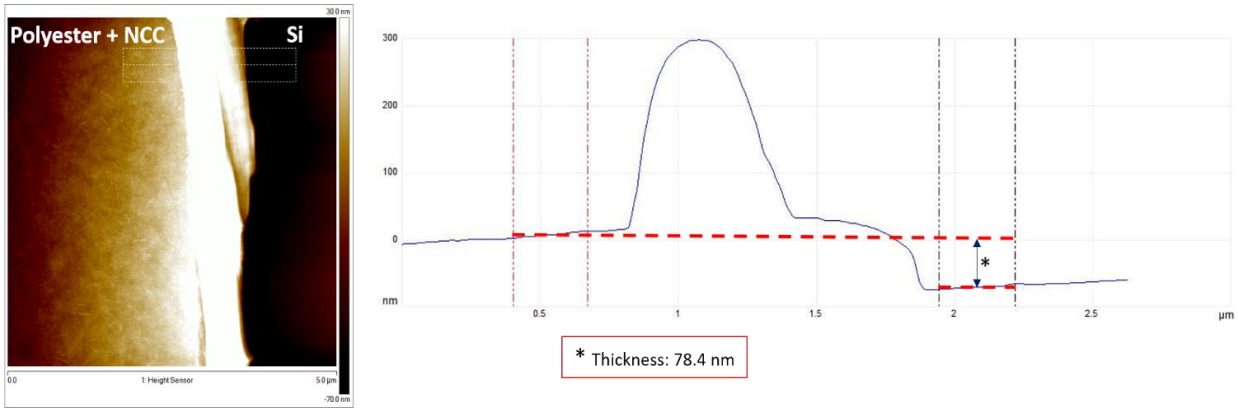

Fig. 2.23. Topography image of the Si-Polyester + NCC (Control, before washing) after the scratch with a steel needle

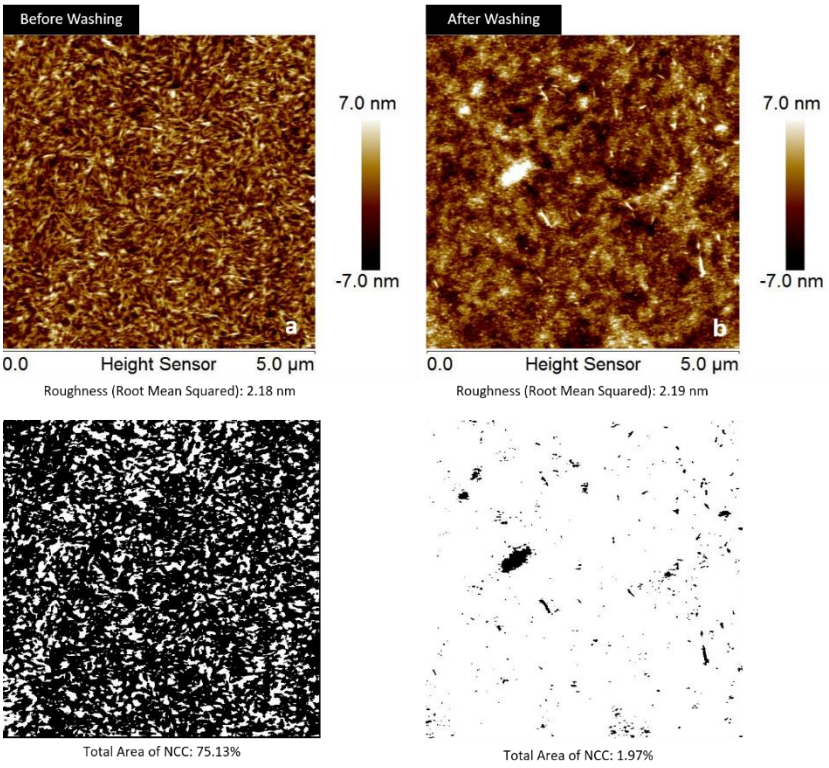

Fig. 2.24. Nylon + NCC (control) before (a) and after washing (b)

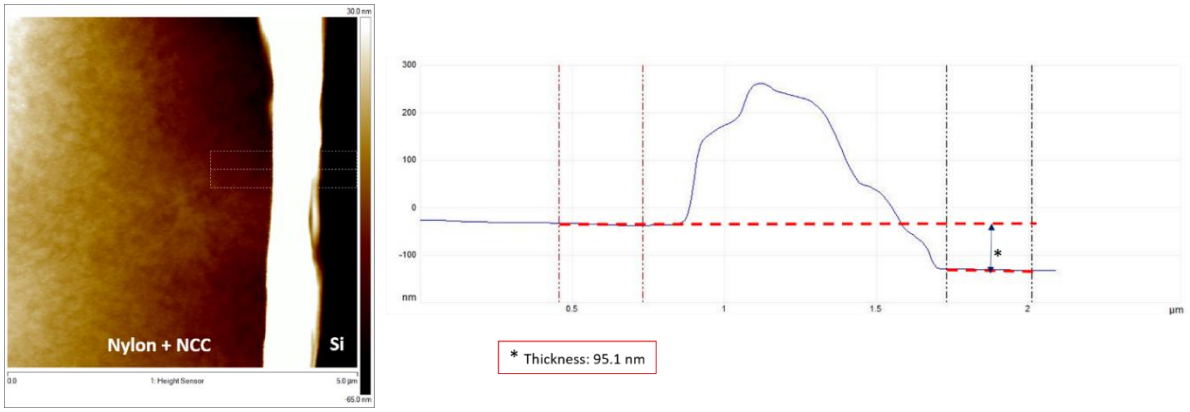

Fig. 2.25. Topography image of the Si-Nylon + NCC (Control, before washing) after the scratch with a steel needle

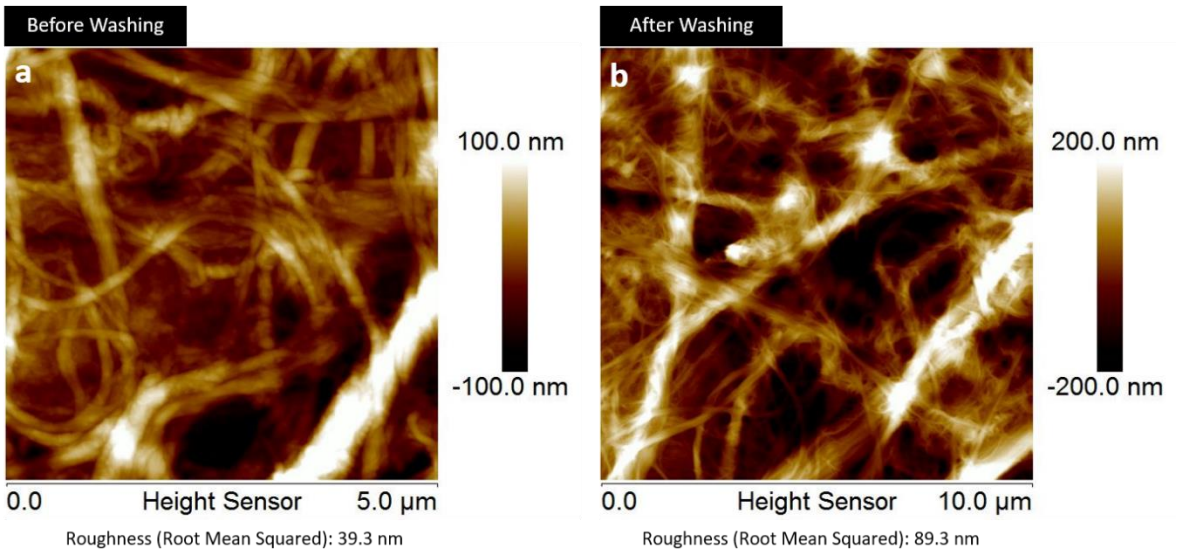

Fig. 2.26. Regenerated cellulose + PEI-NFC before (a) and after washing (b)

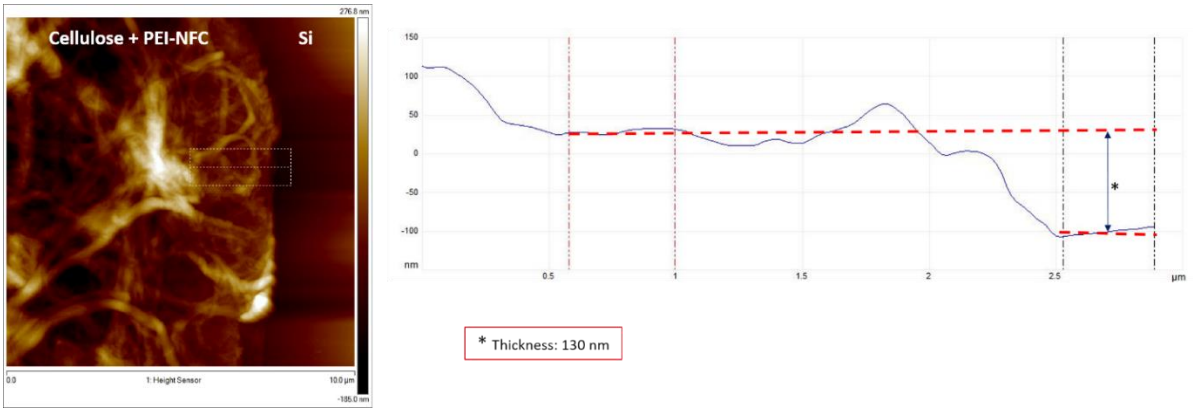

Fig. 2.27. Topography image of the Si-Cellulose + PEI-NFC (before washing) after the scratch with a steel needle

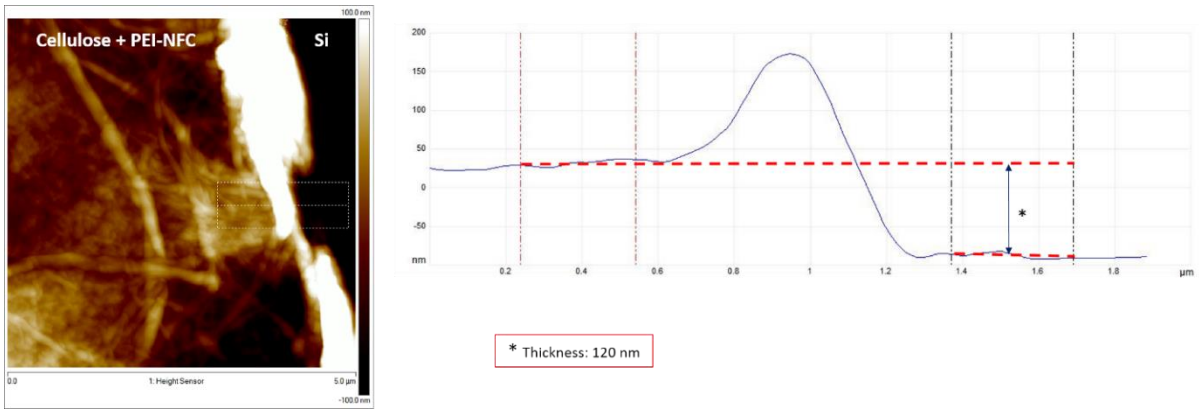

Fig. 2.28. Topography image of the Si-Cellulose + PEI-NFC (after washing) after the scratch with a steel needle

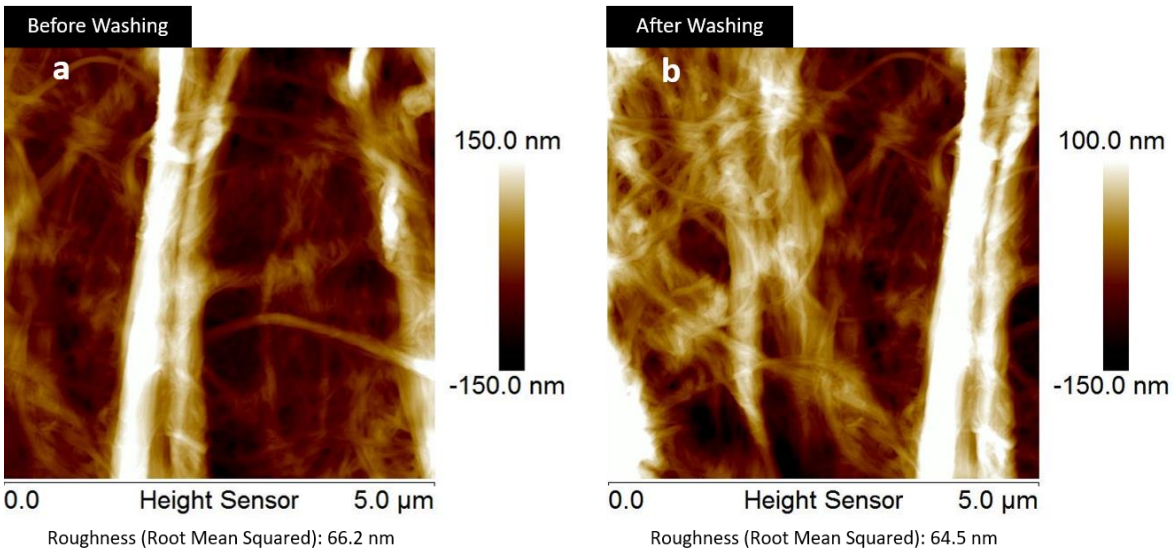

Fig. 2.29. Polyester + PEI-NFC before (a) and after washing (b)

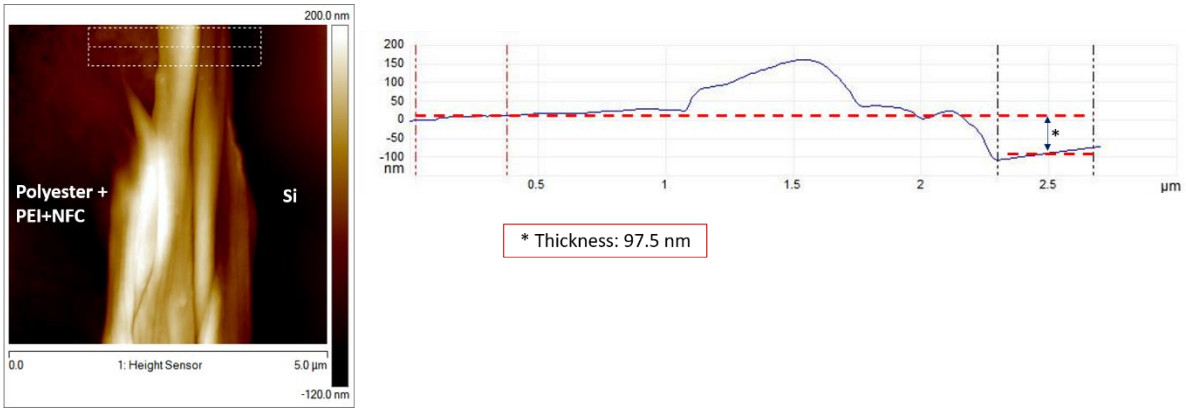

Fig. 2.30. Topography image of the Si-Polyester + PEI-NFC (before washing) after the scratch with a steel needle

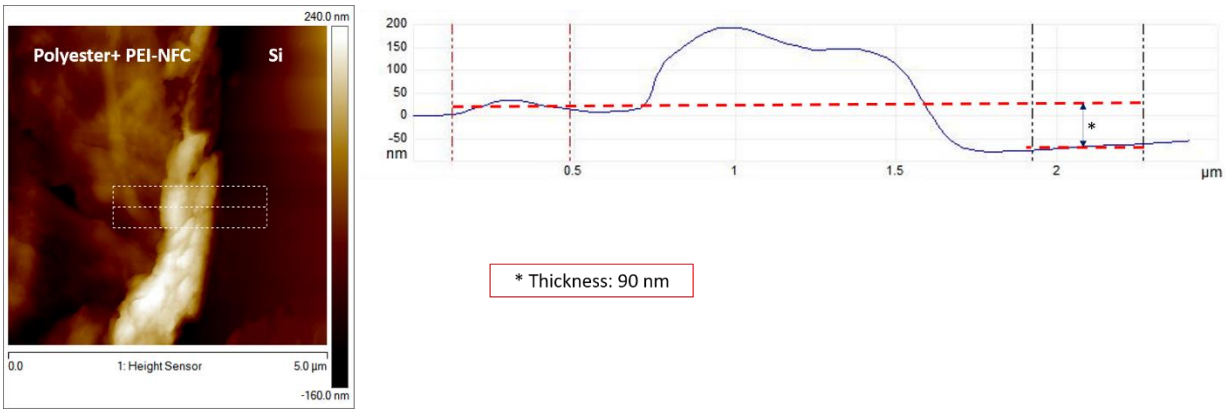

Fig. 2.31. Topography image of the Si-Polyester + PEI-NFC (after washing) after the scratch with a steel needle

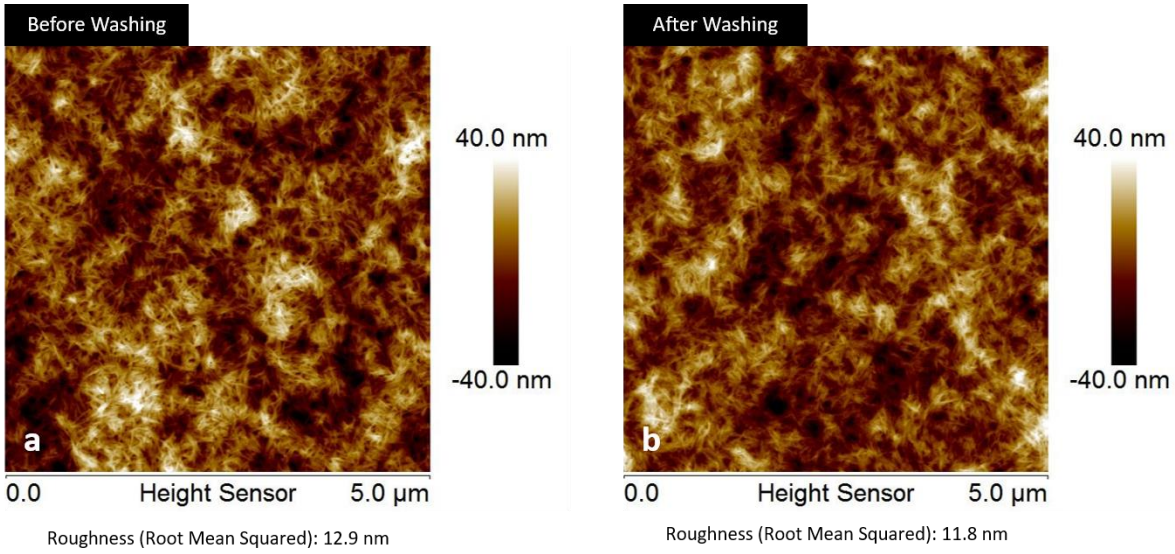

Fig. 2.32. Regenerated cellulose + PEI-NCC before (a) and after washing (b)

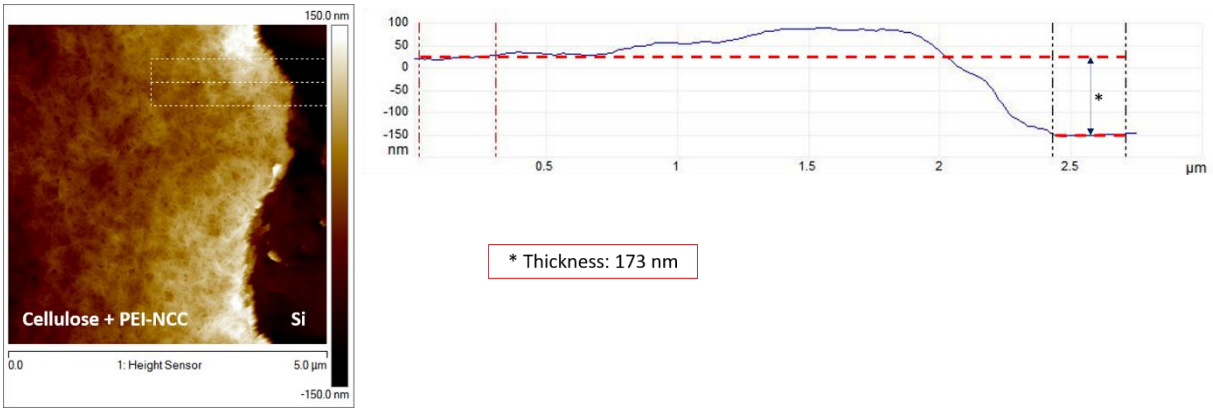

Fig. 2.33. Topography image of the Si-Cellulose + PEI-NCC (before washing) after the scratch with a steel needle

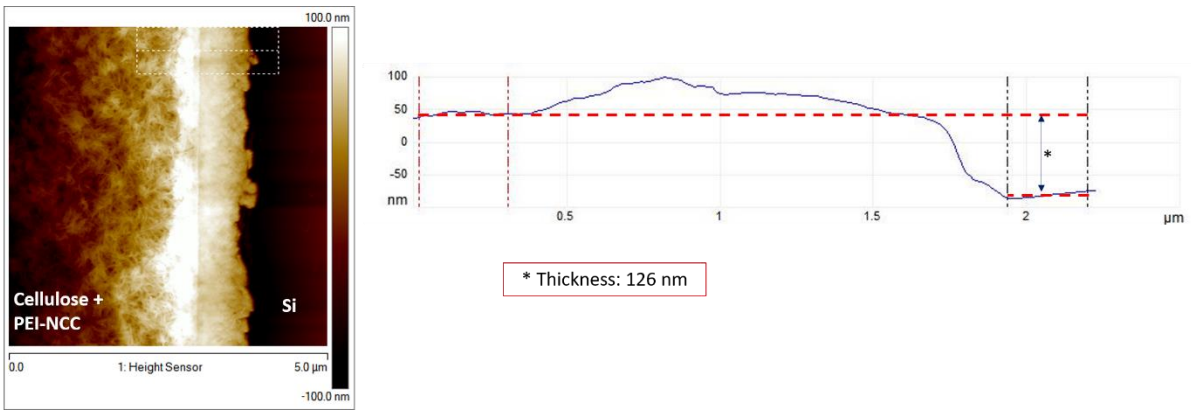

Fig. 2.34. Topography image of the Si-Cellulose + PEI-NCC (after washing) after the scratch with a steel needle

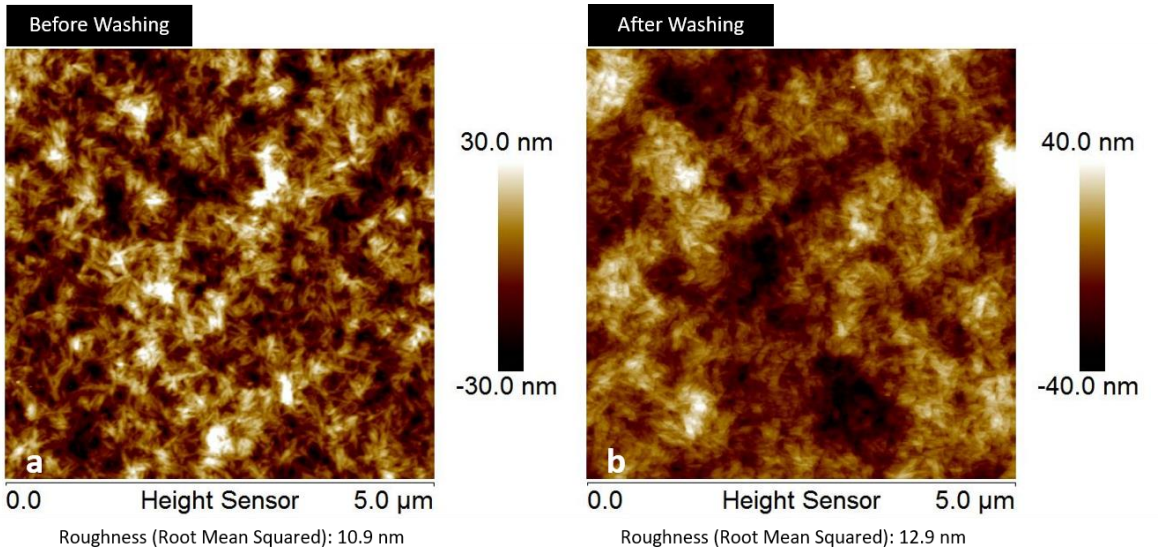

Fig. 2.35. Polyester + PEI-NCC before (a) and after washing (b)

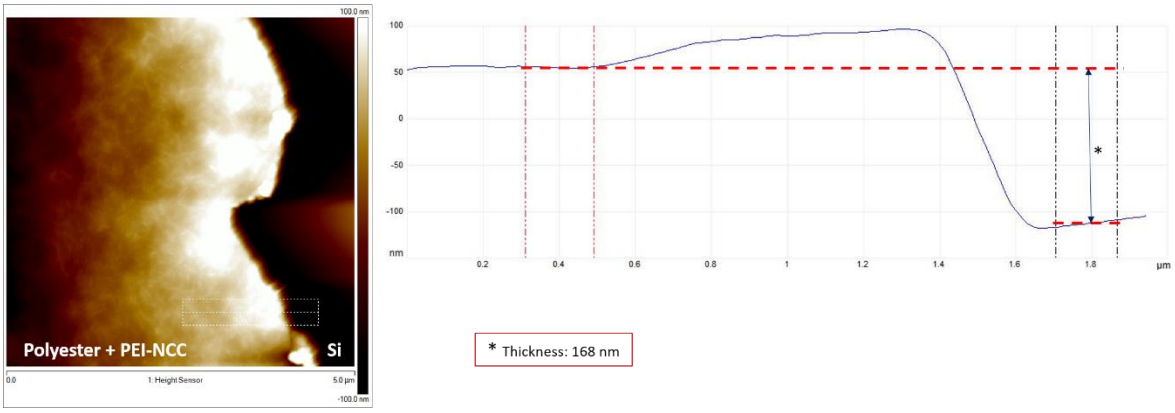

Fig. 2.36. Topography image of the Si-Polyester + PEI-NCC (before washing) after the scratch with a steel needle

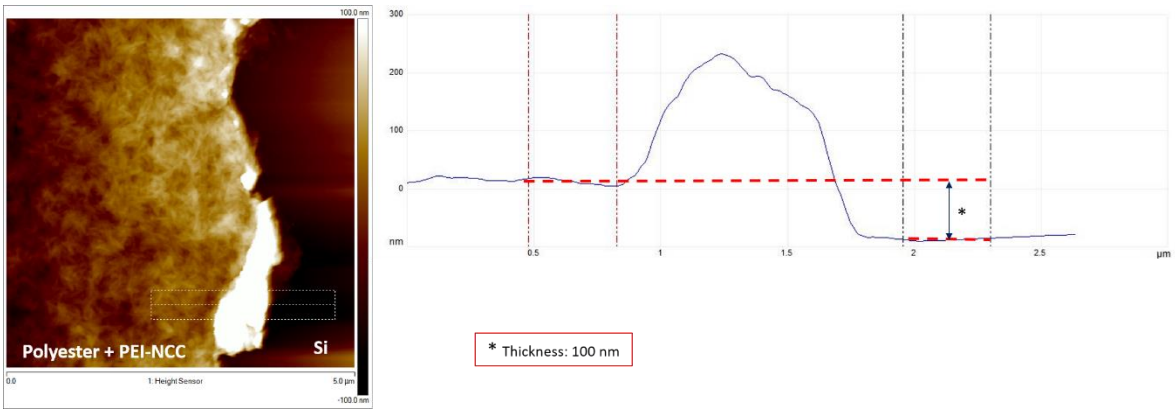

Fig. 2.37. Topography image of the Si-Polyester + PEI-NCC (after washing) after the scratch with a steel needle

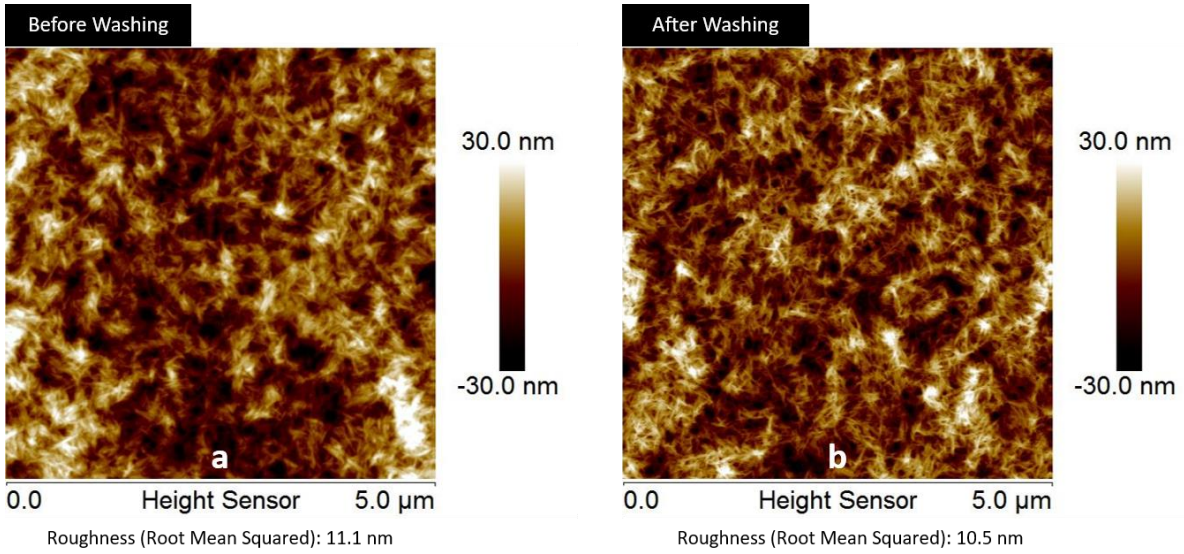

Fig. 2.38. Nylon + PEI-NCC before (a) and after washing (b)

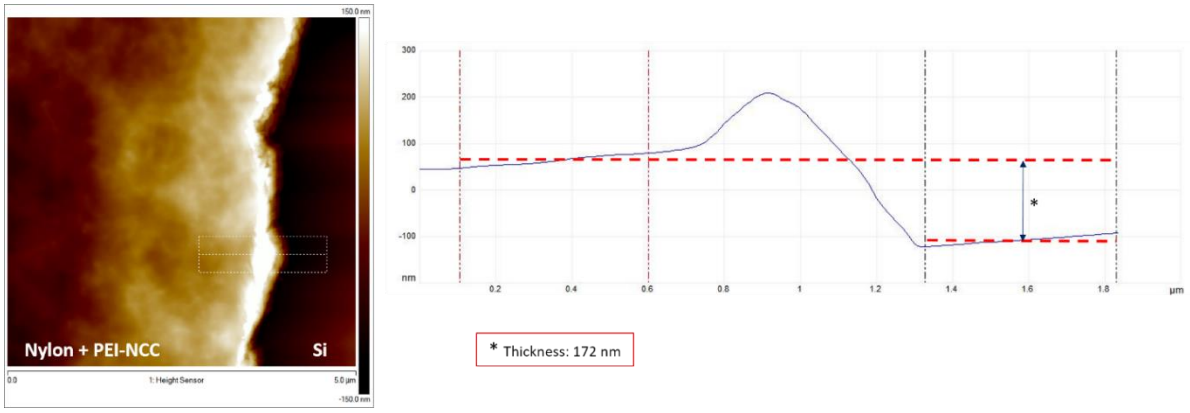

Fig. 2.39. Topography image of the Si-Nylon + PEI-NCC (after washing) after the scratch with a steel needle

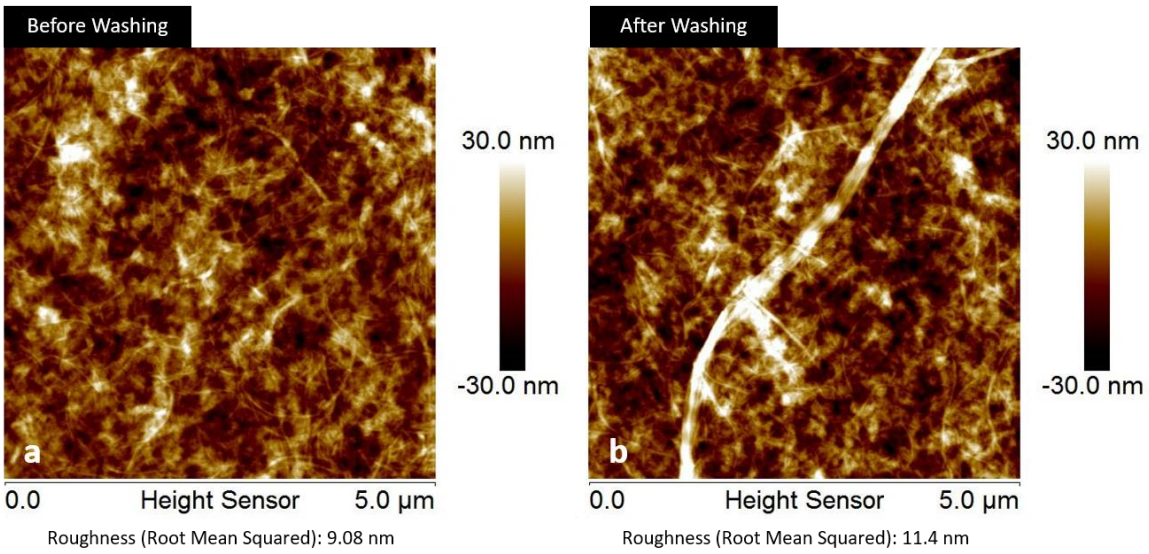

Fig. 2.40. Regenerated cellulose + PEI+NFC before (a) and after washing (b)

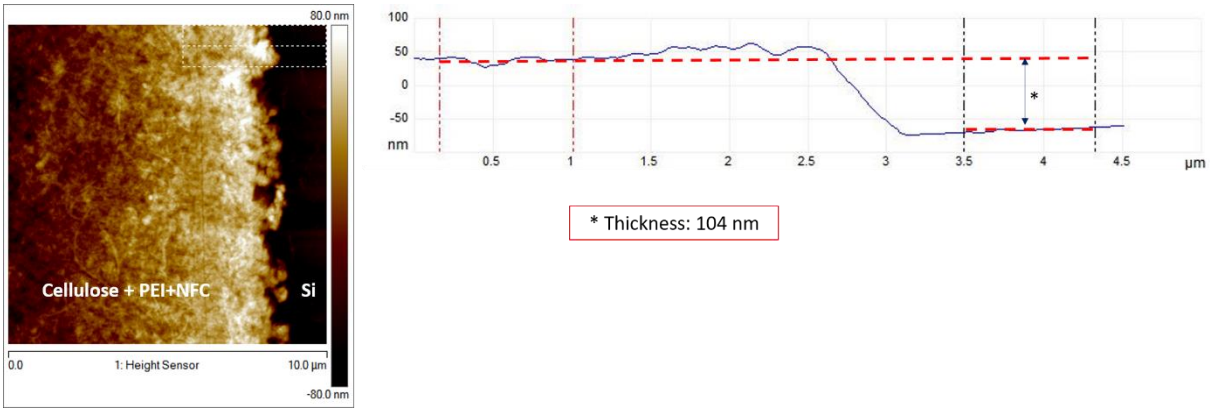

Fig. 2.41. Topography image of the Si-Cellulose + PEI+NFC (before washing) after the scratch with a steel needle

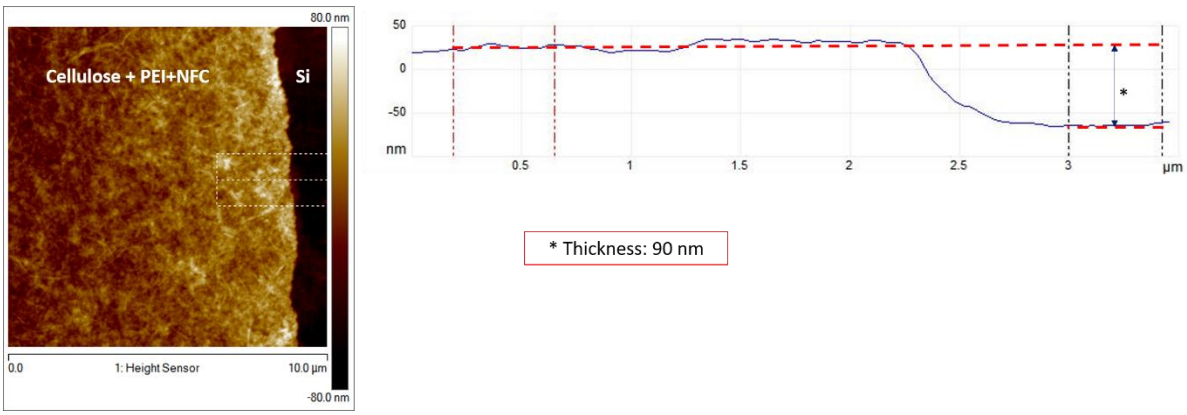

Fig. 2.42. Topography image of the Si-Cellulose + PEI+NFC (after washing) after the scratch with a steel needle

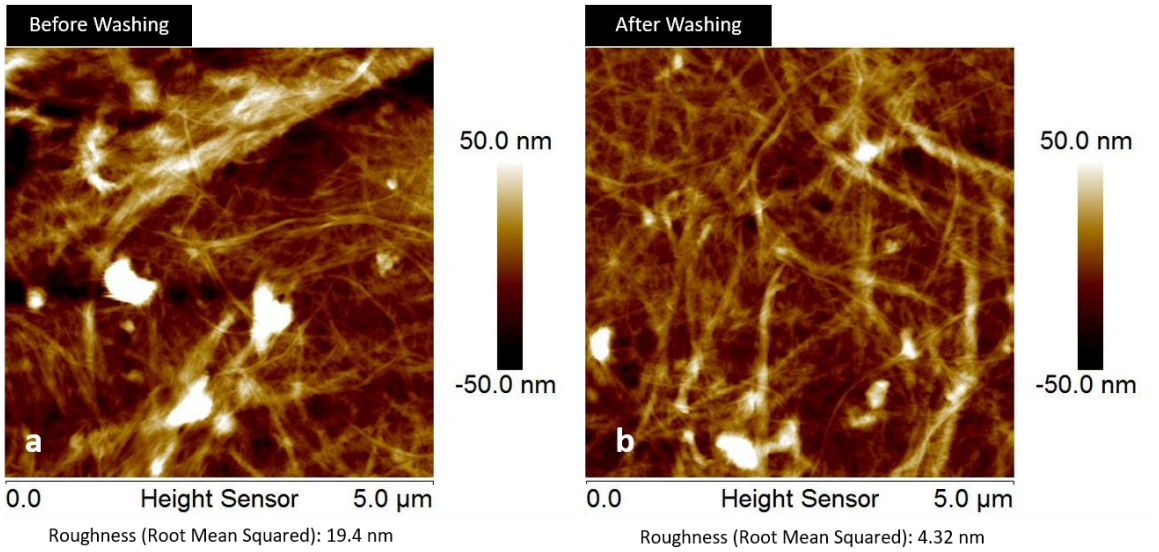

Fig. 2.43. Polyester + PEI+NFC before (a) and after washing (b)

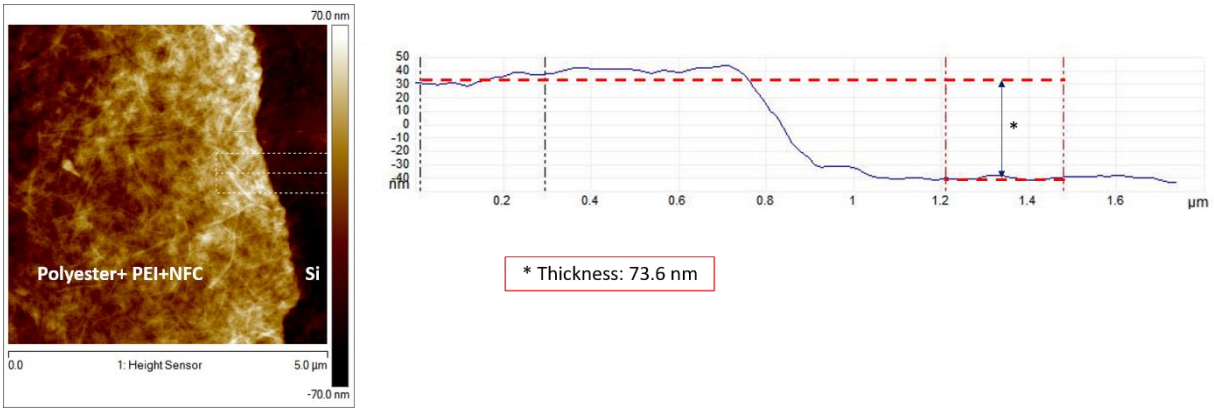

Fig. 2.44. Topography image of the Si-Polyester + PEI+NFC (before washing) after the scratch with a steel needle

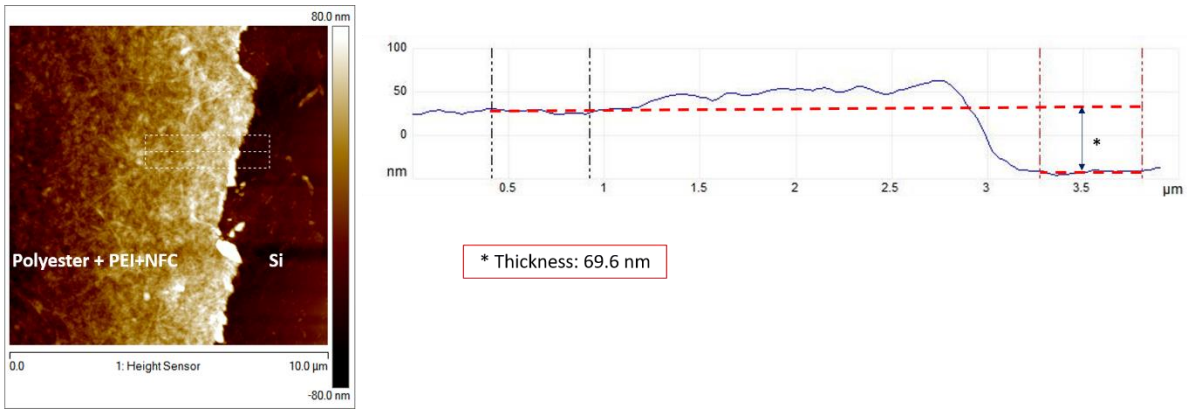

Fig. 2.45. Topography image of the Si-Polyester + PEI+NFC (after washing) after the scratch with a steel needle

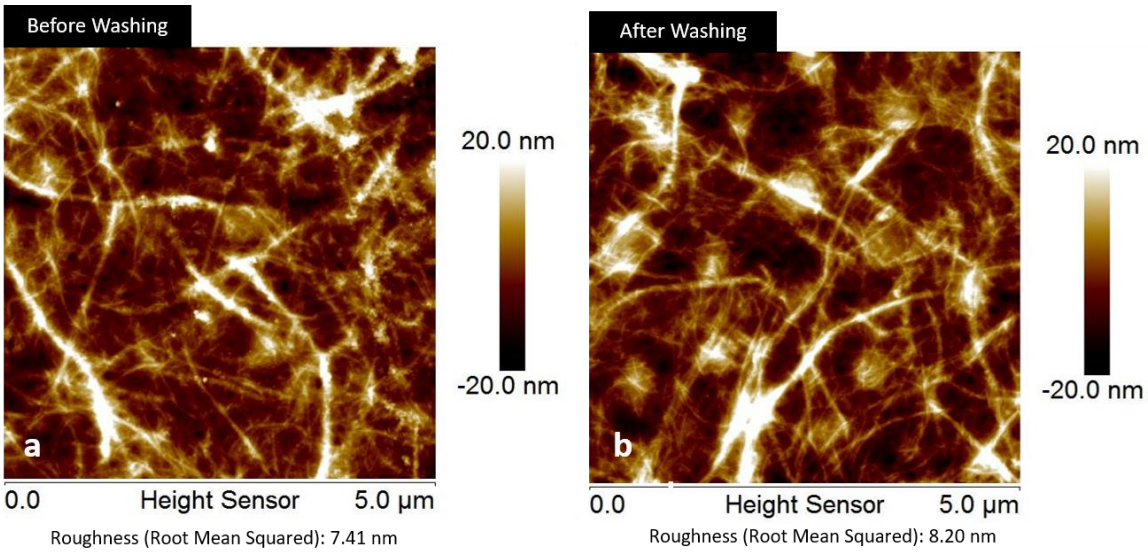

Fig. 2.46. Nylon + PEI+NFC before (a) and after washing (b)

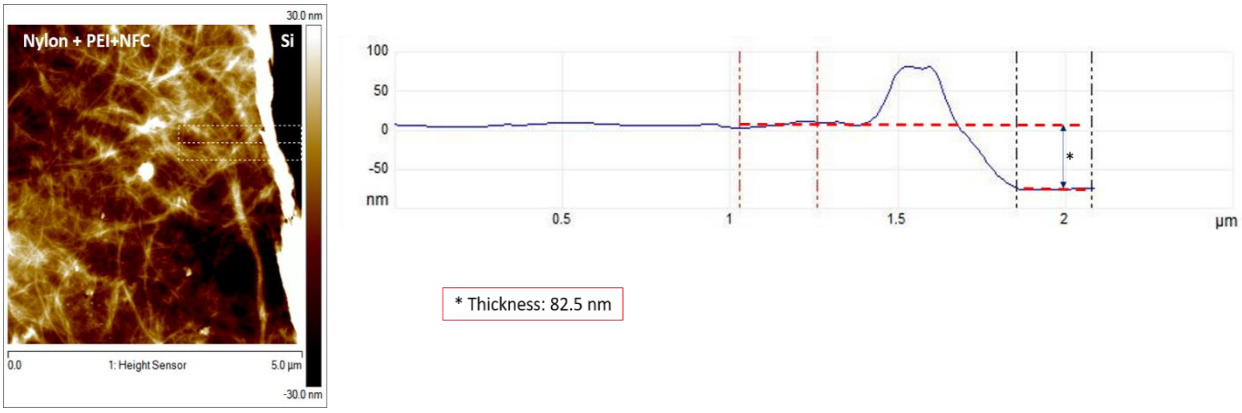

Fig. 2.47 .Topography image of the Si-Nylon + PEI+NFC (before washing) after the scratch with a steel needle

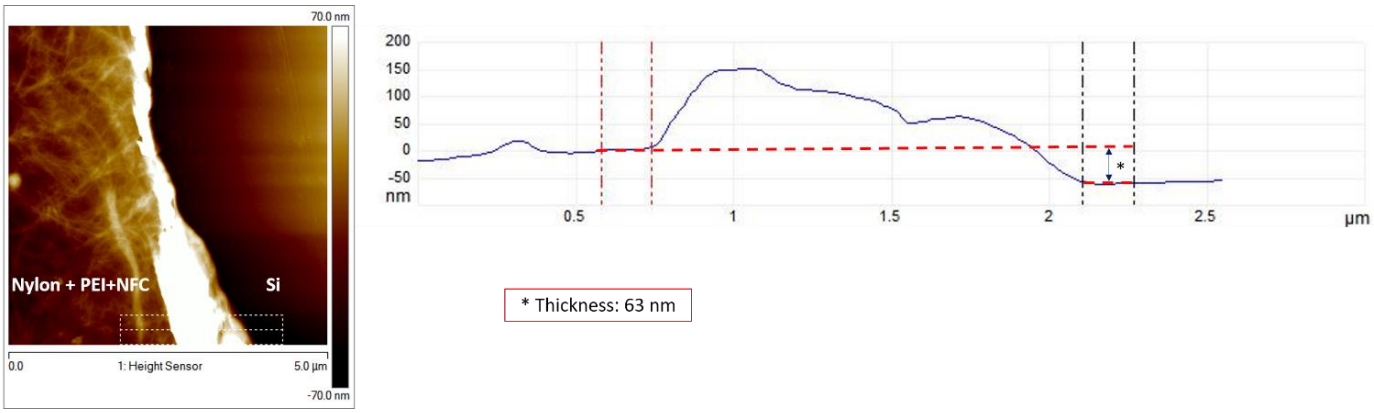

Fig. 2.48. Topography image of the Si-Nylon + PEI+NFC (after washing) after the scratch with a steel needle

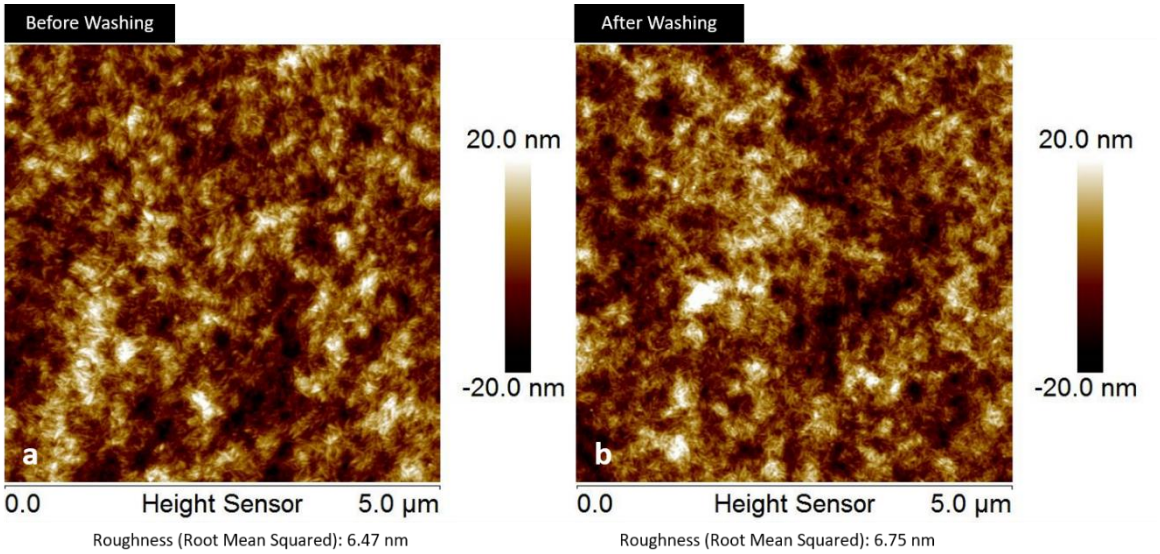

Fig. 2.49. Regenerated cellulose + PEI+NCC before (a) and after washing (b)

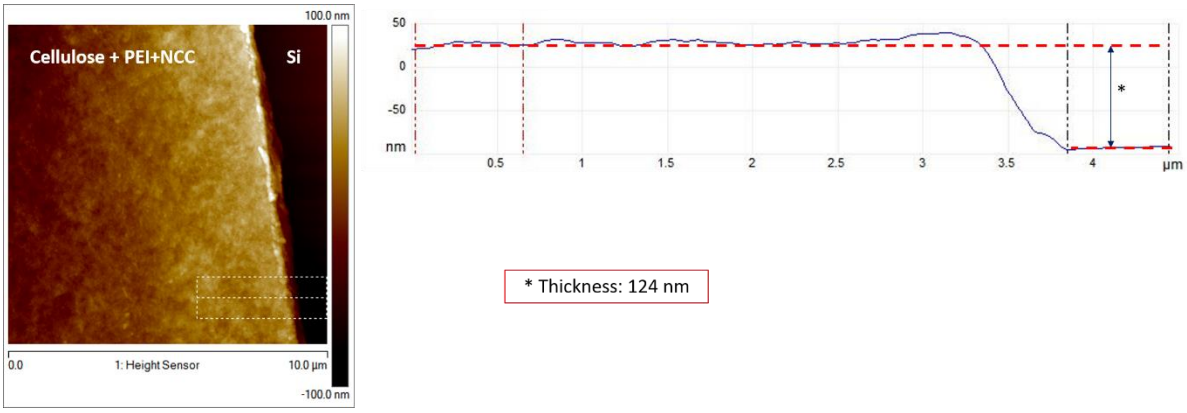

Fig. 2.50. Topography image of the Si-Cellulose + PEI+NCC (before washing) after the scratch with a steel needle

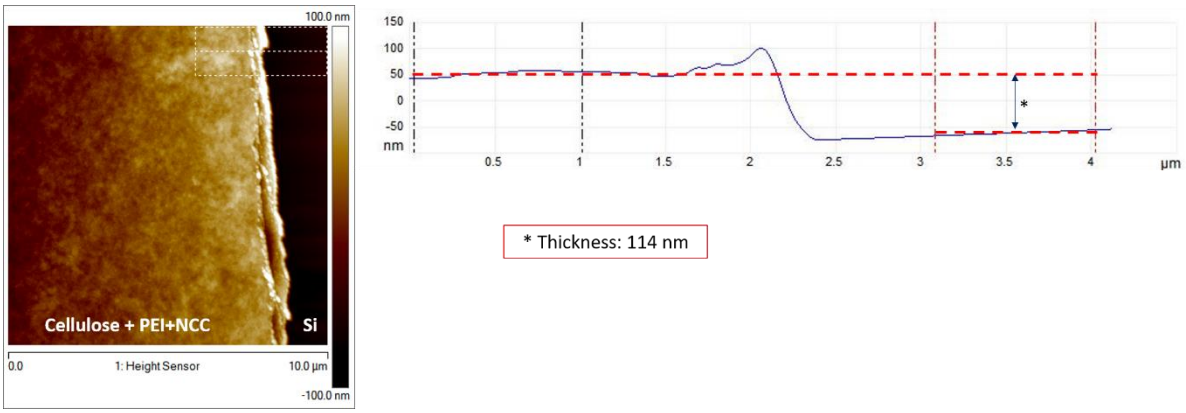

Fig. 2.51. Topography image of the Si-Cellulose + PEI+NCC (after washing) after the scratch with a steel needle

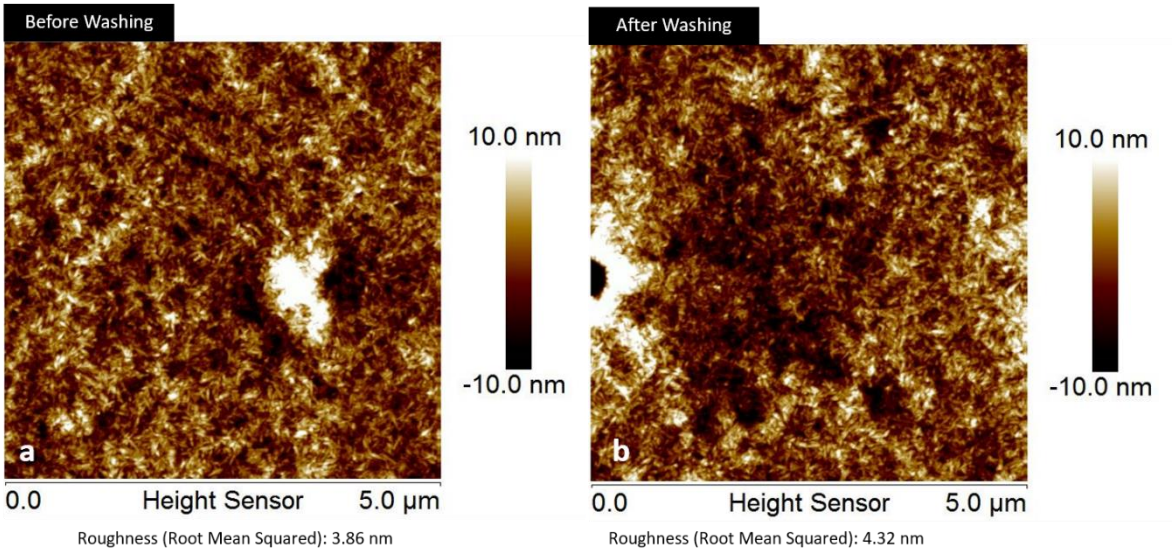

Fig. 2.52. Polyester + PEI+NCC before (a) and after washing (b)

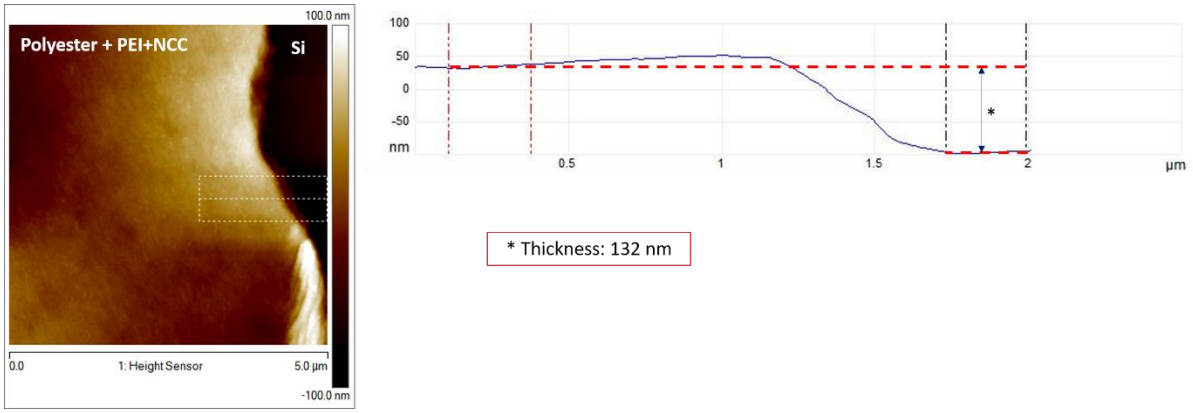

Fig. 2.53. Topography image of the Si-Polyester + PEI+NCC (before washing) after the scratch with a steel needle

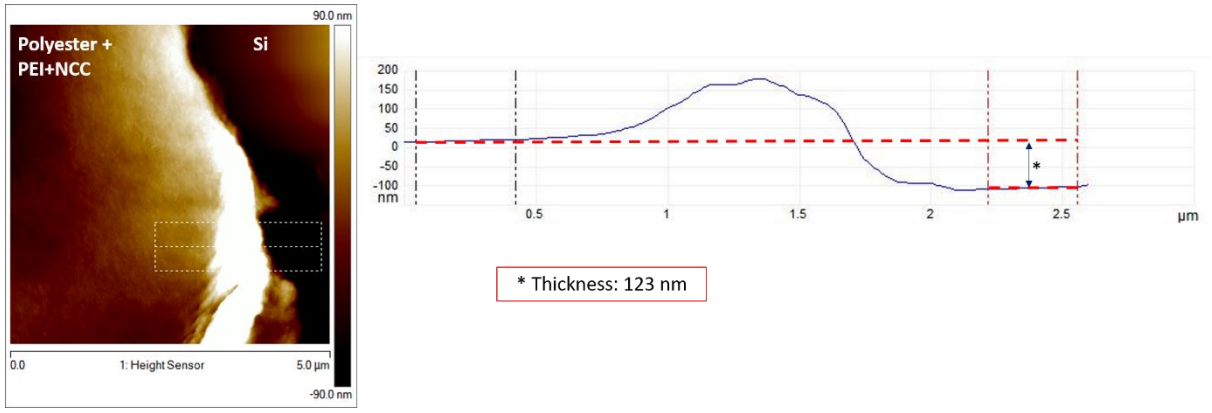

Fig. 2.54. Topography image of the Si-Polyester + PEI+NCC (after washing) after the scratch with a steel needle

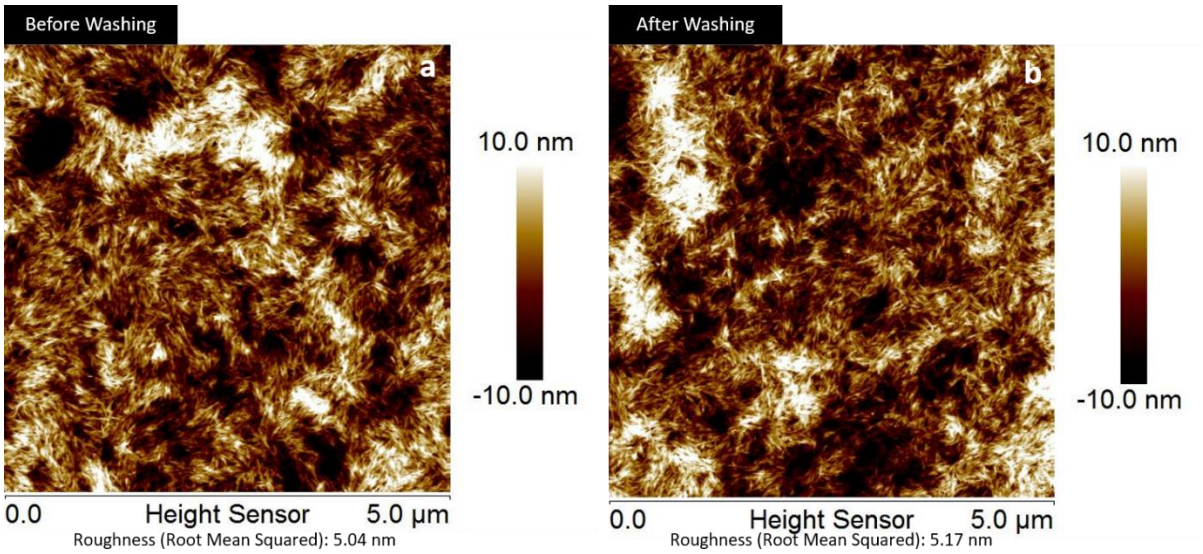

Fig. 2.55. Nylon + PEI+NCC before (a) and after washing (b)

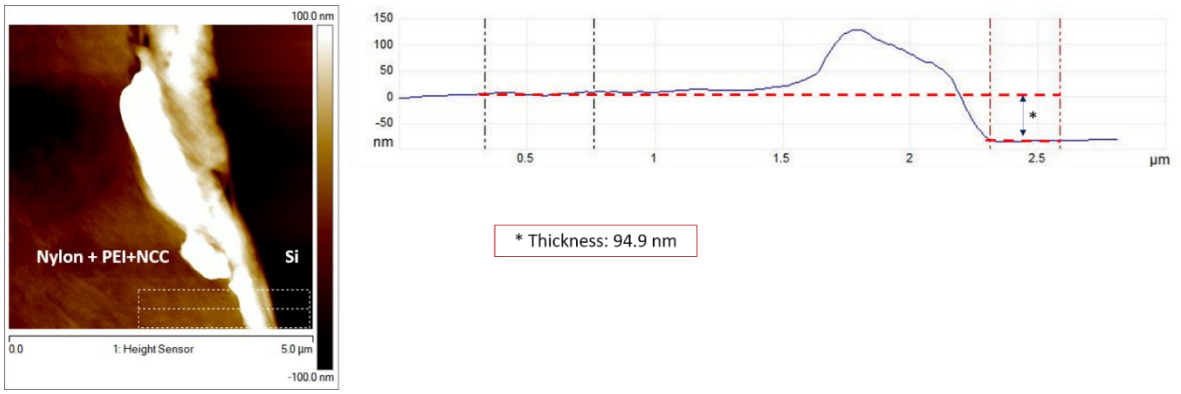

Fig. 2.56. Topography image of the Si-Nylon + PEI+NCC (before washing) after the scratch with a steel needle

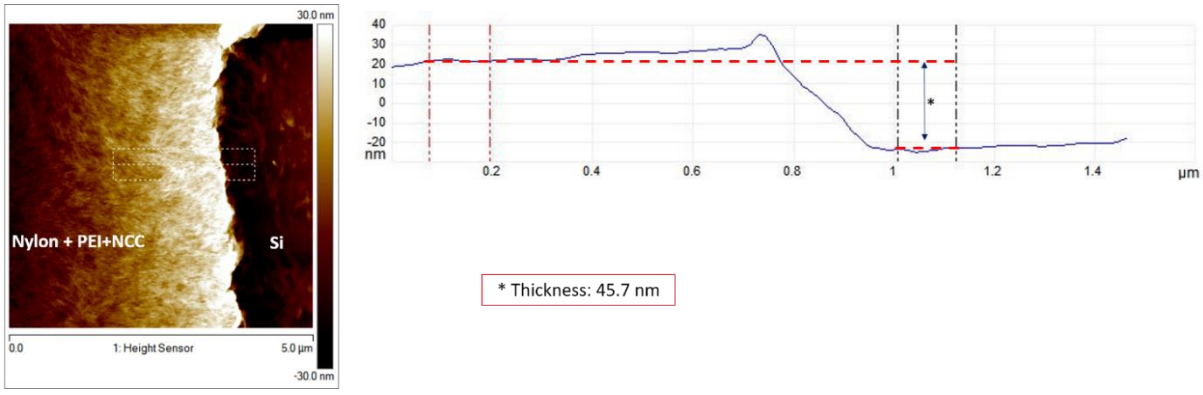

Fig. 2.57. Topography image of the Si-Nylon + PEI+NCC (after washing) after the scratch with a steel needle

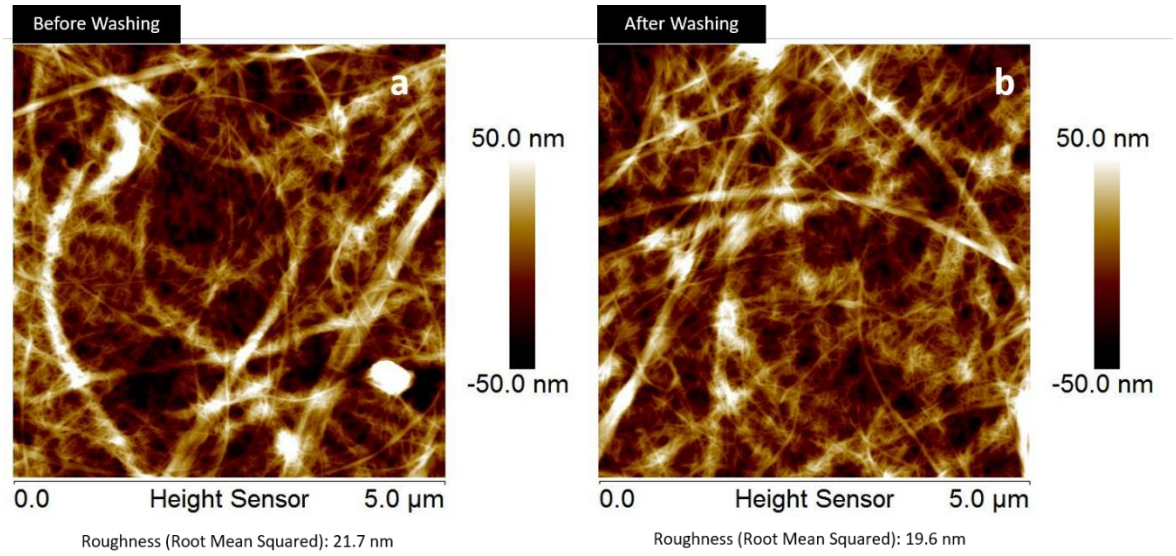

Fig. 2.58. Regenerated cellulose + P(GMA-OEGMA)-NFC before (a) and after washing (b)

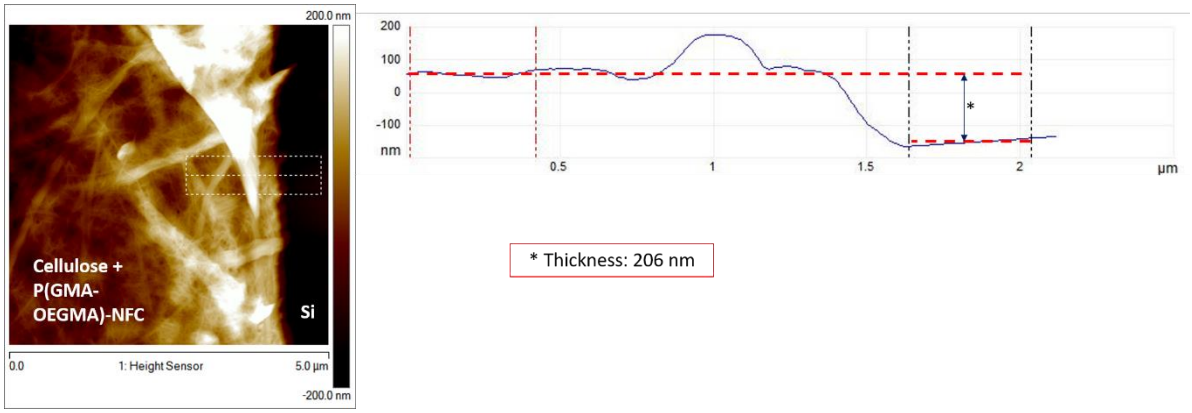

Fig. 2.59. Topography image of the Si-Cellulose + P(GMA-OEGMA)-NFC (before washing) after the scratch with a steel needle

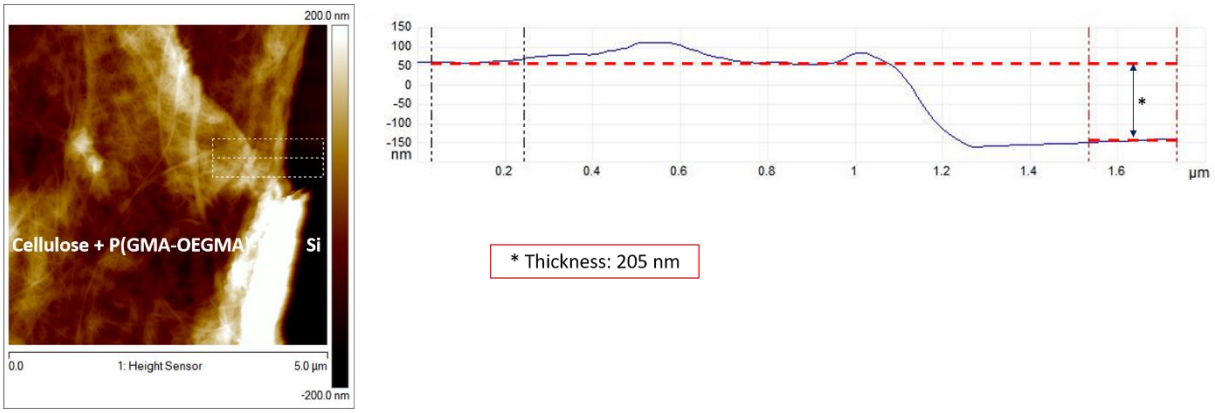

Fig. 2.60. Topography image of the Si-Cellulose + P(GMA-OEGMA)-NFC (after washing) after the scratch with a steel needle

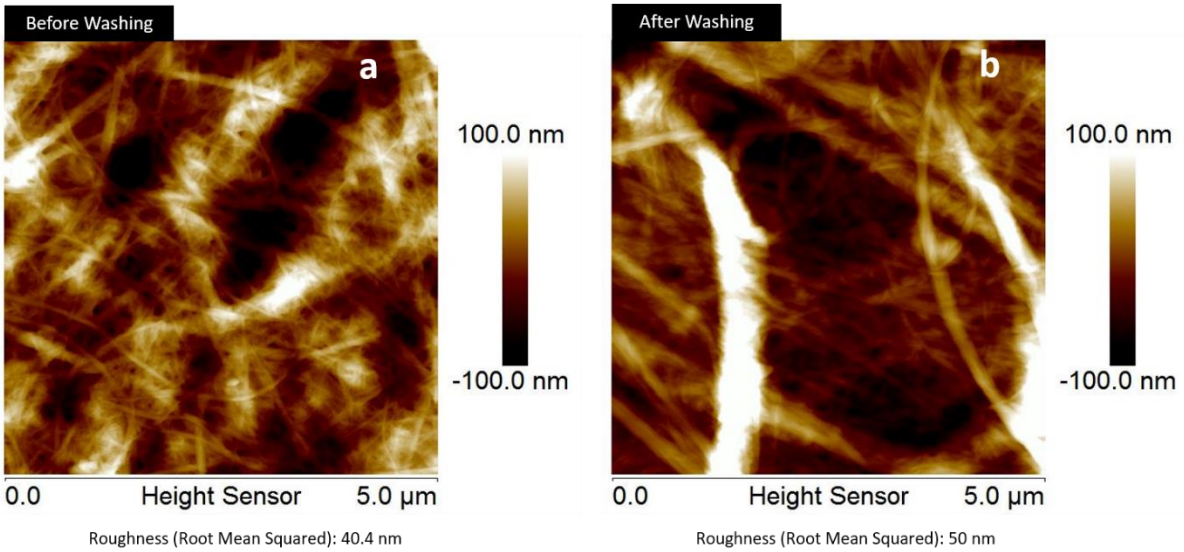

Fig. 2.61. Polyester + P(GMA-OEGMA)-NFC before (a) and after washing (b)

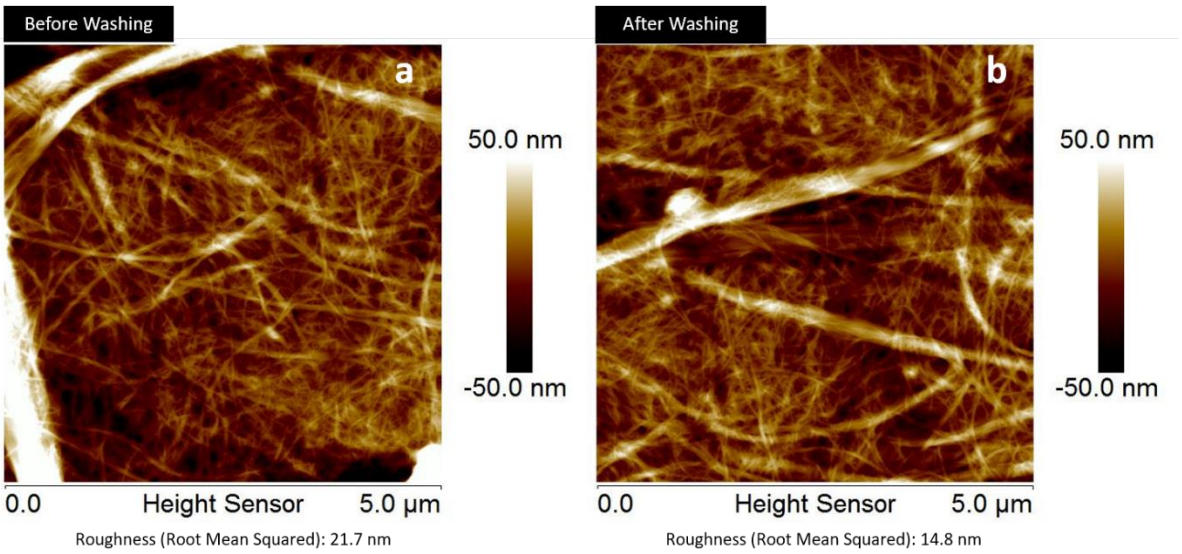

Fig. 2.62. Nylon + P(GMA-OEGMA)-NFC before (a) and after washing (b)

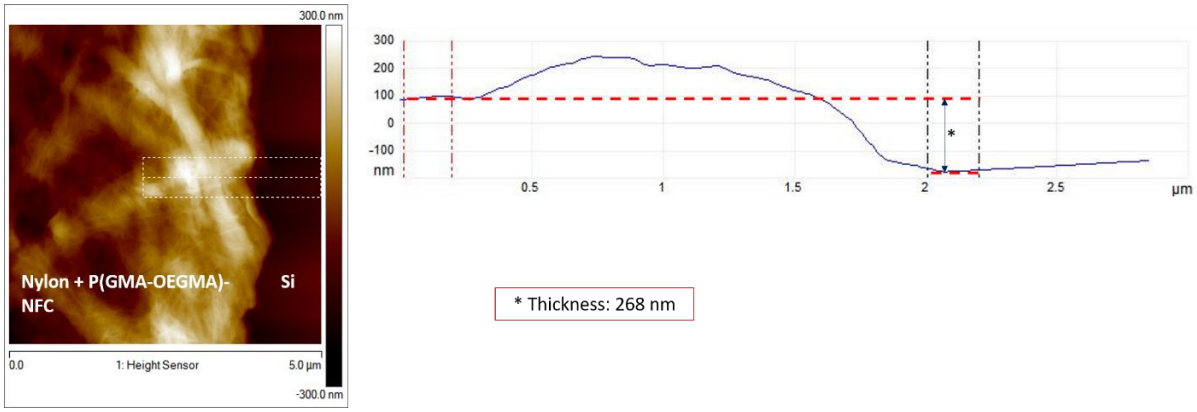

Fig. 2.63. Topography image of the Si-Polyester + P(GMA-OEGMA)-NFC (after washing) after the scratch with a steel needle

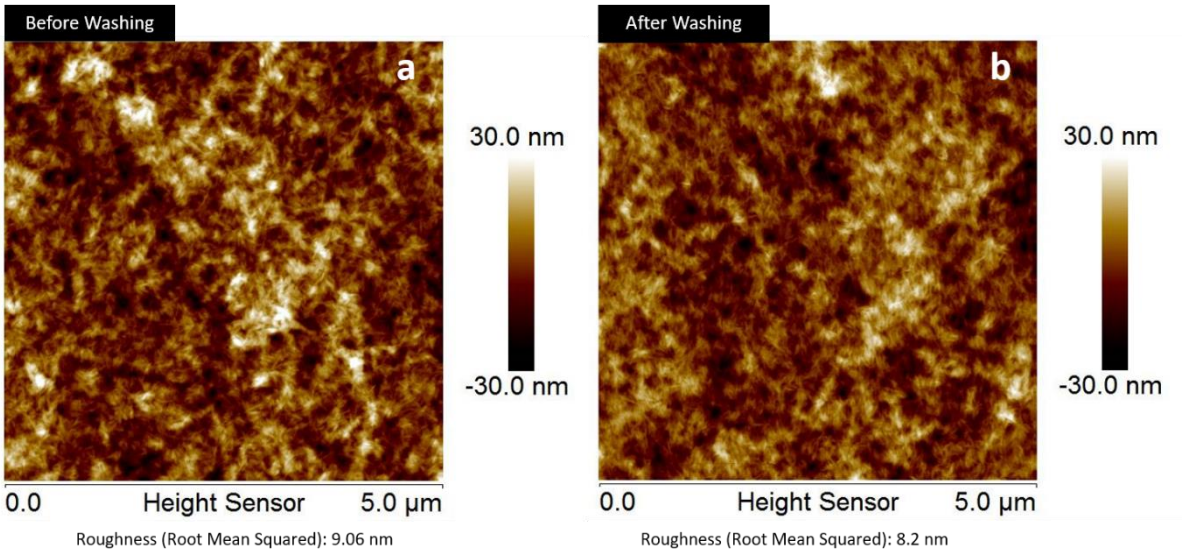

Fig. 2.64. Regenerated cellulose + P(GMA-OEGMA)-NCC before (a) and after washing (b)

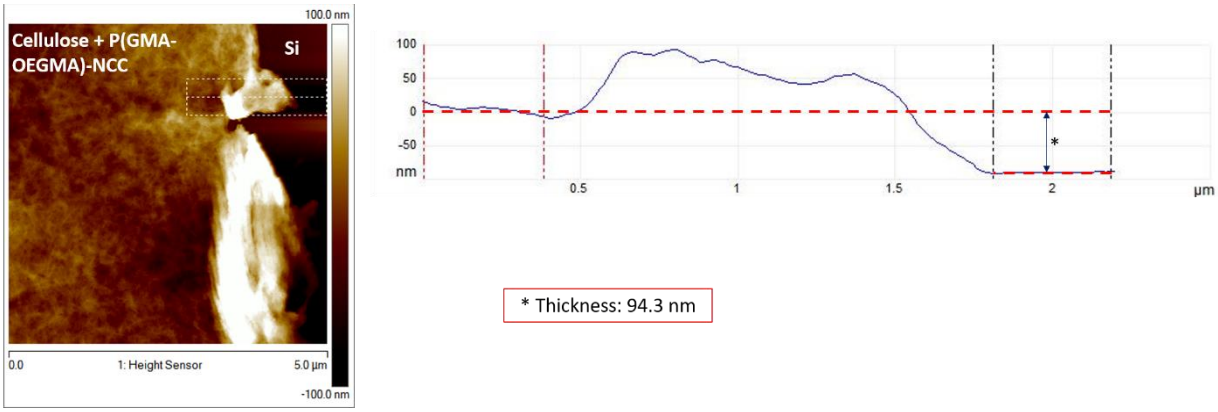

Fig. 2.65. Topography image of the Si-Cellulose + P(GMA-OEGMA)-NCC (before washing) after the scratch with a steel needle

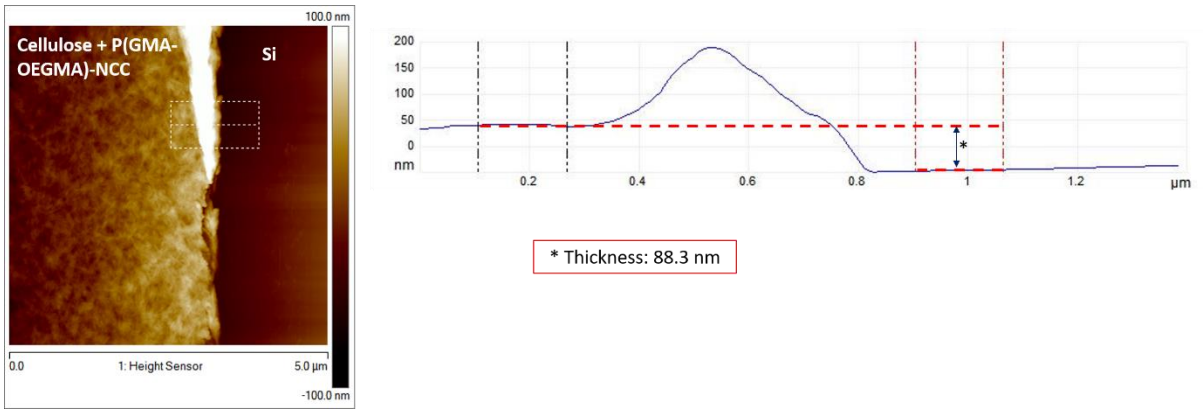

Fig. 2.66. Topography image of the Si-Cellulose + P(GMA-OEGMA)-NCC (after washing) after the scratch with a steel needle

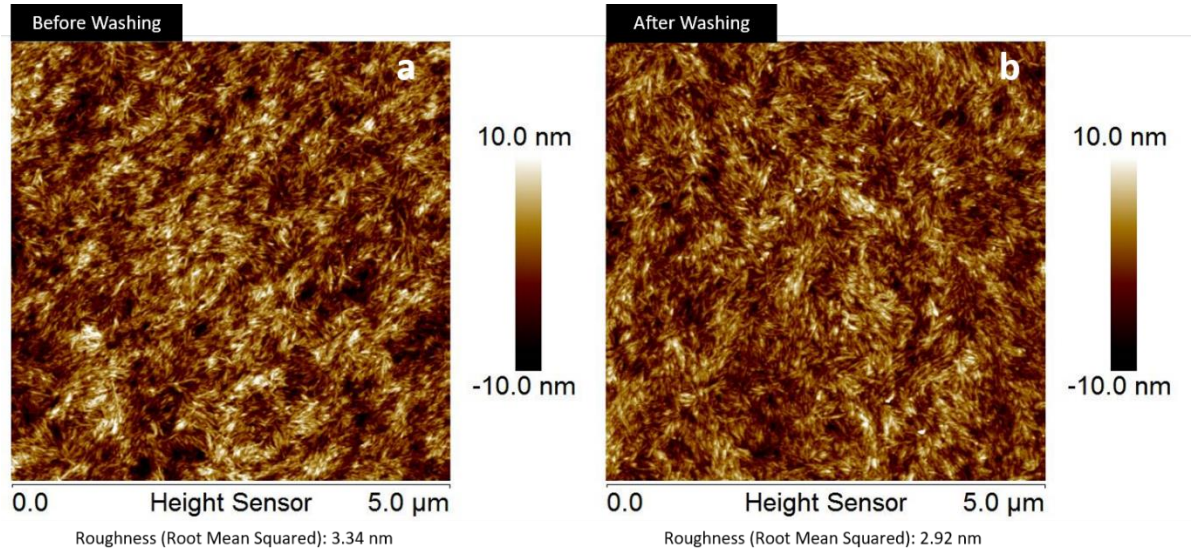

Fig. 2.67. Polyester + P(GMA-OEGMA)-NCC before (a) and after washing (b)

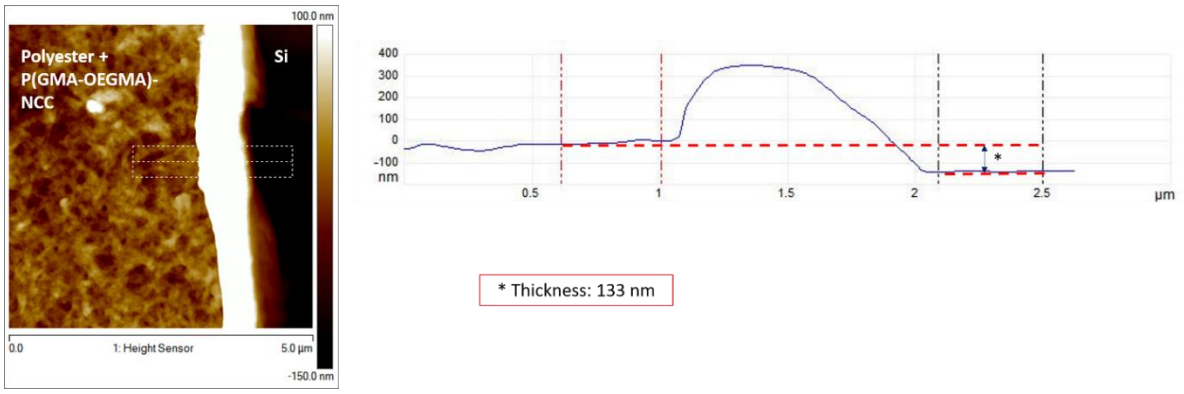

Fig. 2.68. Topography image of the Si-Polyester + P(GMA-OEGMA)-NCC (before washing) after the scratch with a steel needle

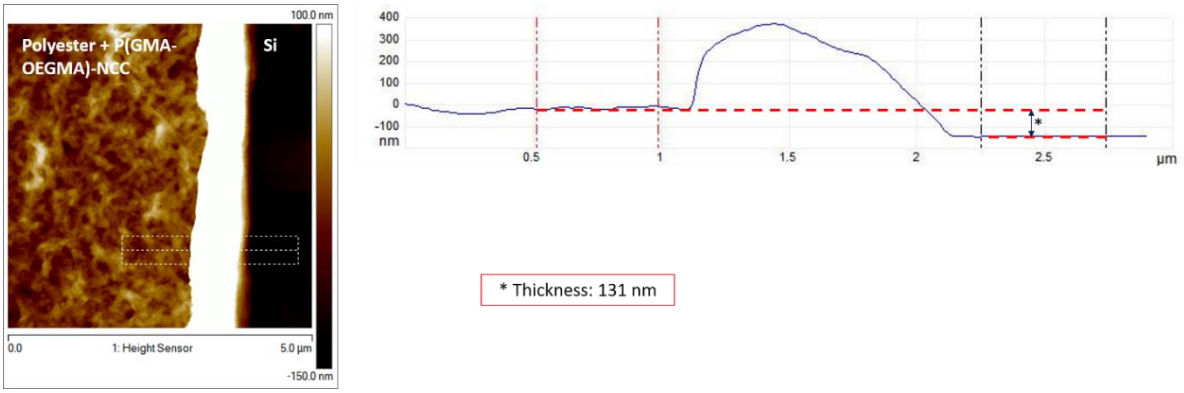

Fig. 2.69. Topography image of the Si-Polyester + P(GMA-OEGMA)-NCC (after washing) after the scratch with a steel needle

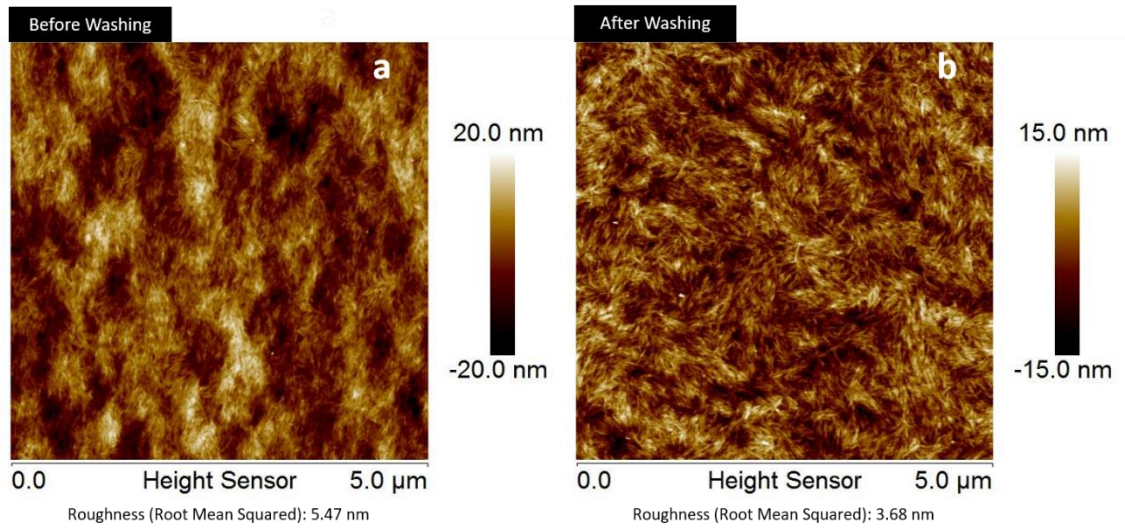

Fig. 2.70. Nylon + P(GMA-OEGMA)-NCC before (a) and after washing (b)

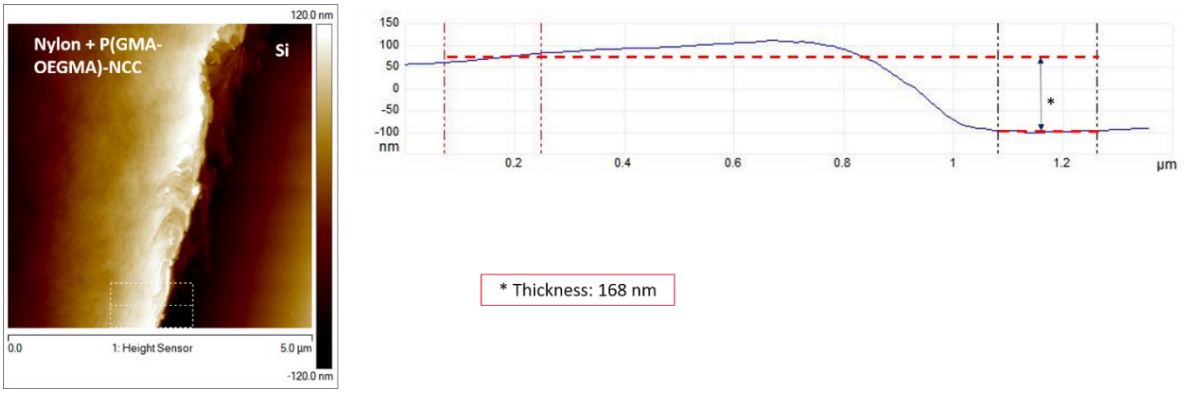

Fig. 2.71. Topography image of the Si-Nylon + P(GMA-OEGMA)-NCC (after washing) after the scratch with a steel needle

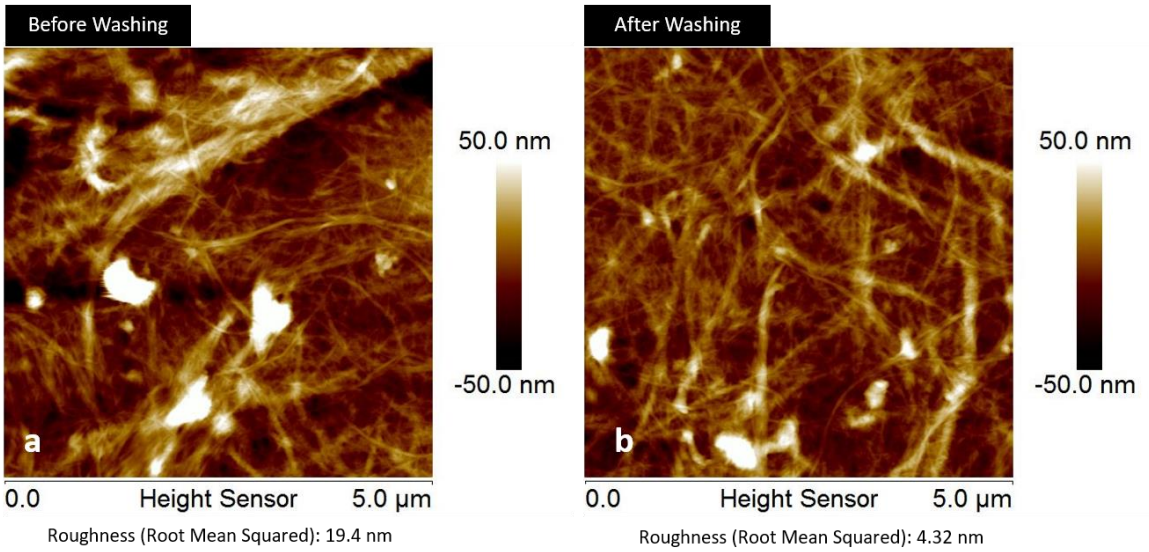

Fig. 2.72. Regenerated cellulose + P(GMA-OEGMA)+NFC before (a) and after washing (b)

Fig. 2.73. Topography image of the Si-Cellulose + P(GMA-OEGMA)+NFC (before washing) after the scratch with a steel needle

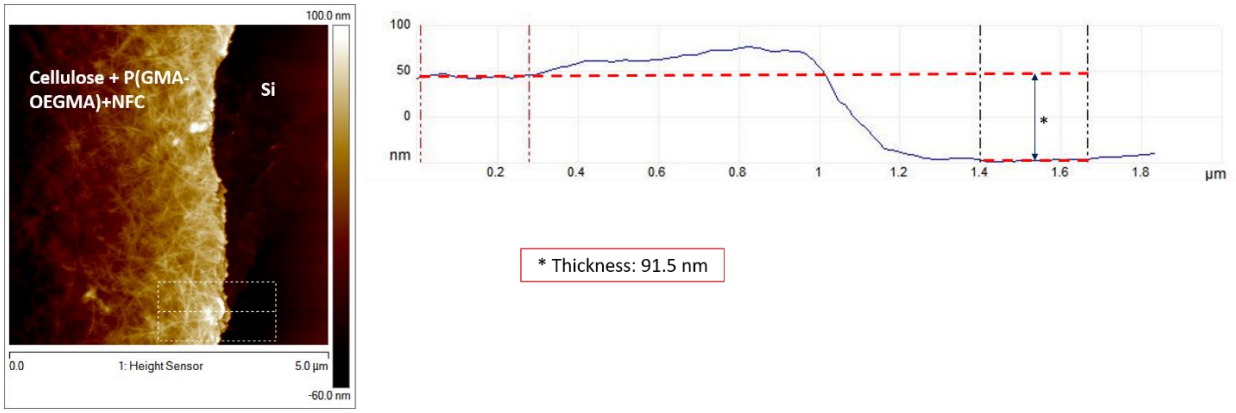

Fig. 2.74. Topography image of the Si-Cellulose + P(GMA-OEGMA)+NFC (after washing) after the scratch with a steel needle

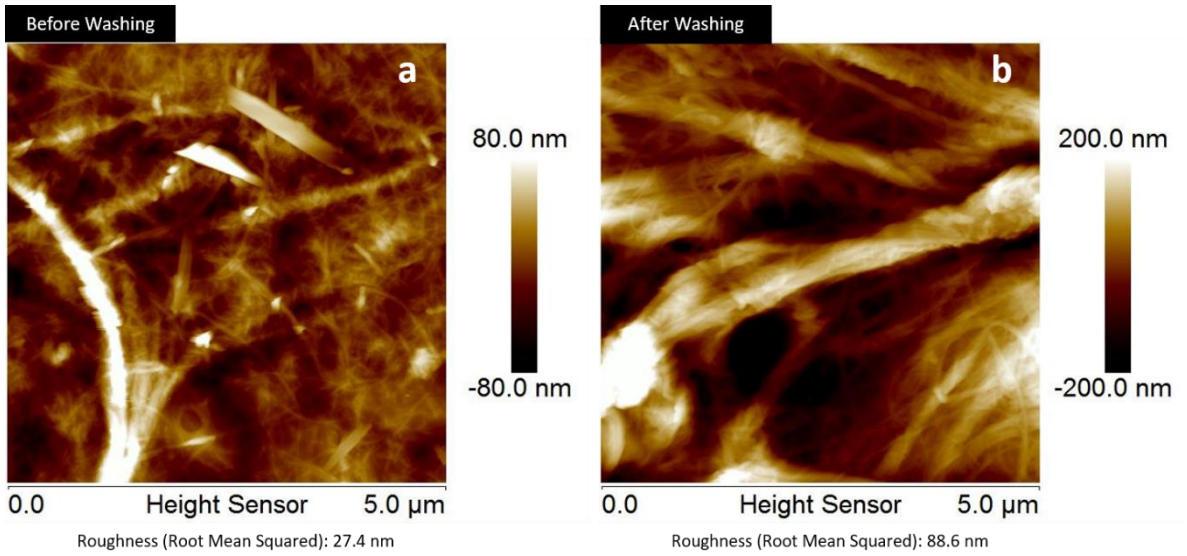

Fig. 2.75. Polyester + P(GMA-OEGMA)+NFC before (a) and after washing (b)

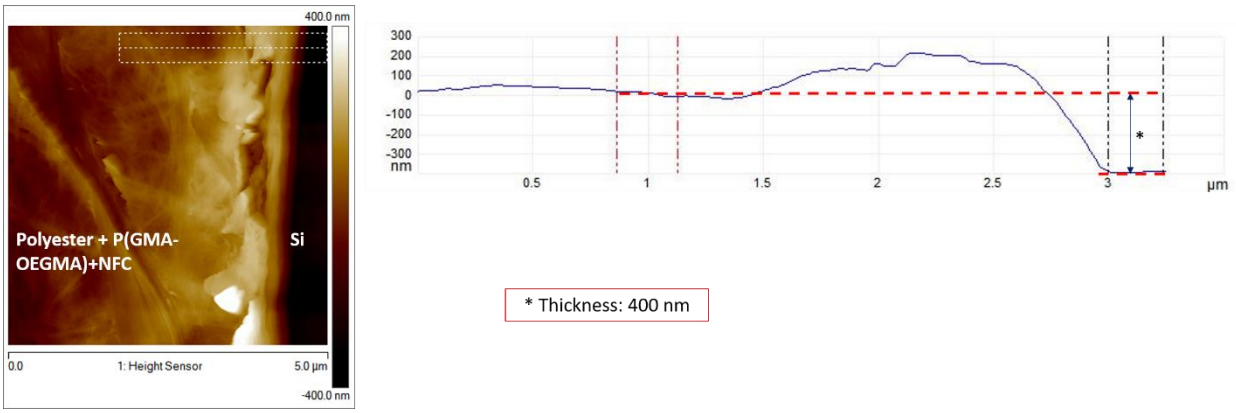

Fig. 2.76. Topography image of the Si-Polyester + P(GMA-OEGMA)+NFC (after washing) after the scratch with a steel needle

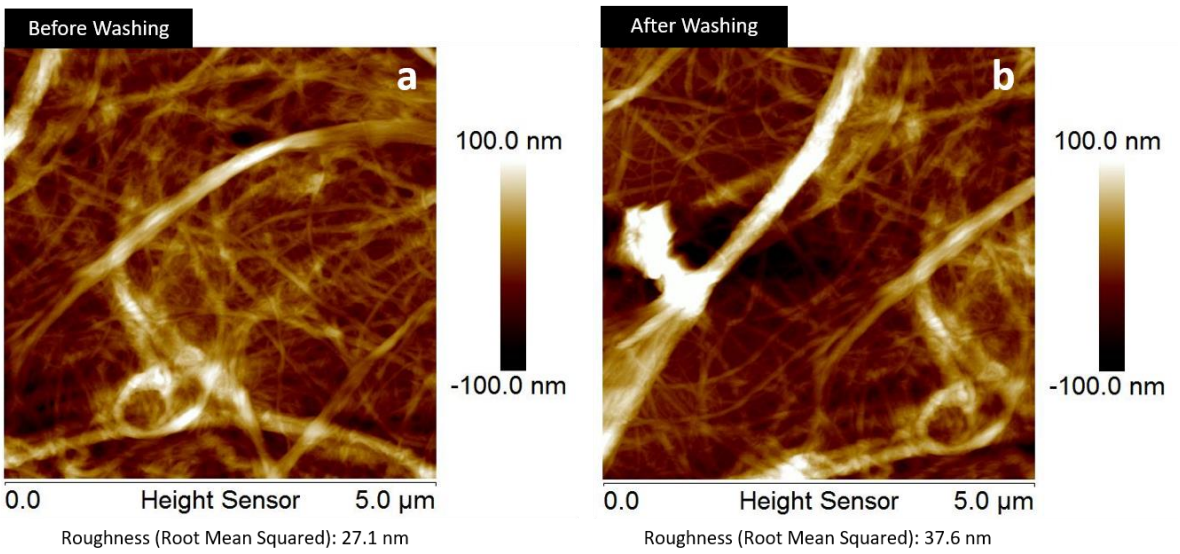

Fig. 2.77. Nylon + P(GMA-OEGMA)+NFC before (a) and after washing (b)

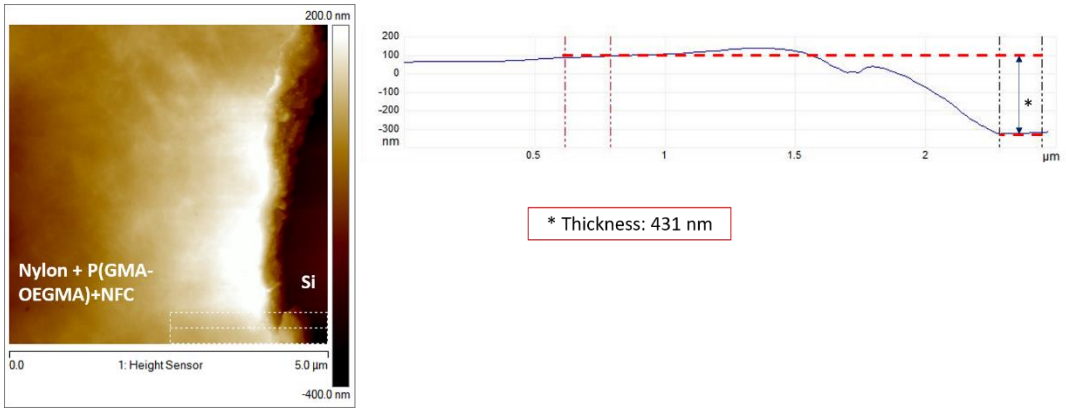

Fig. 2.78. Topography image of the Si-Nylon + P(GMA-OEGMA)+NFC (before washing) after the scratch with a steel needle

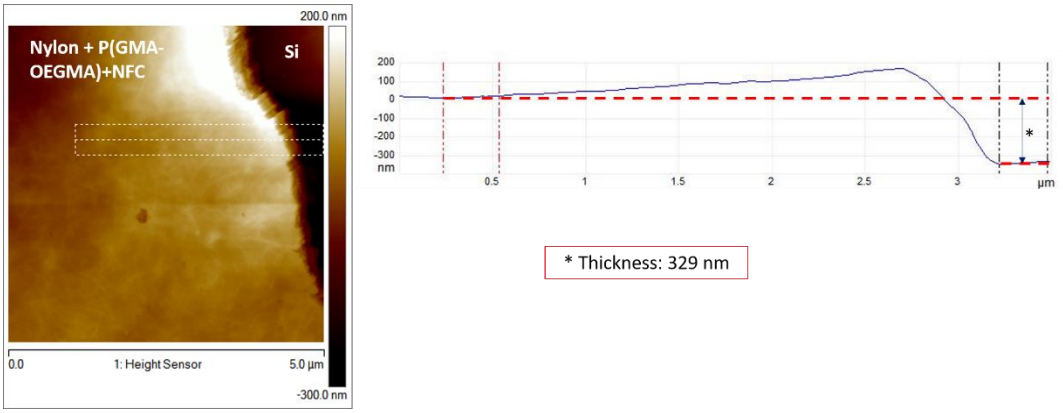

Fig. 2.79. Topography image of the Si-Nylon + P(GMA-OEGMA)+NFC (after washing) after the scratch with a steel needle

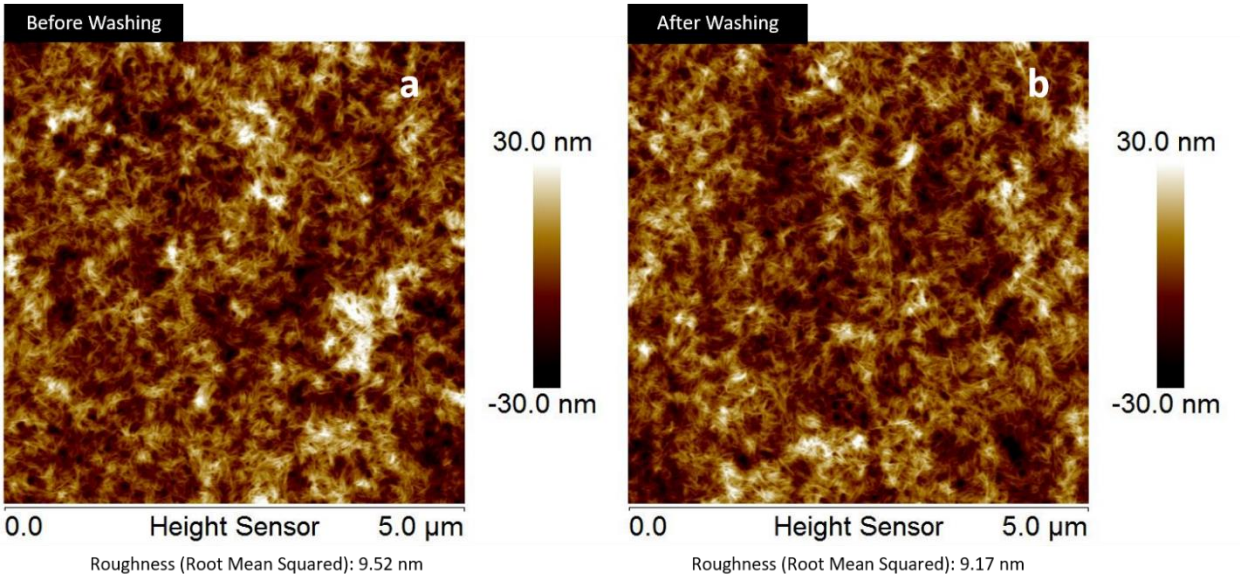

Fig. 2.80. Regenerated cellulose + P(GMA-OEGMA)+NCC before (a) and after washing (b)

Fig. 2.81. Topography image of the Si-Cellulose + P(GMA-OEGMA)+NCC (before washing) after the scratch with a steel needle

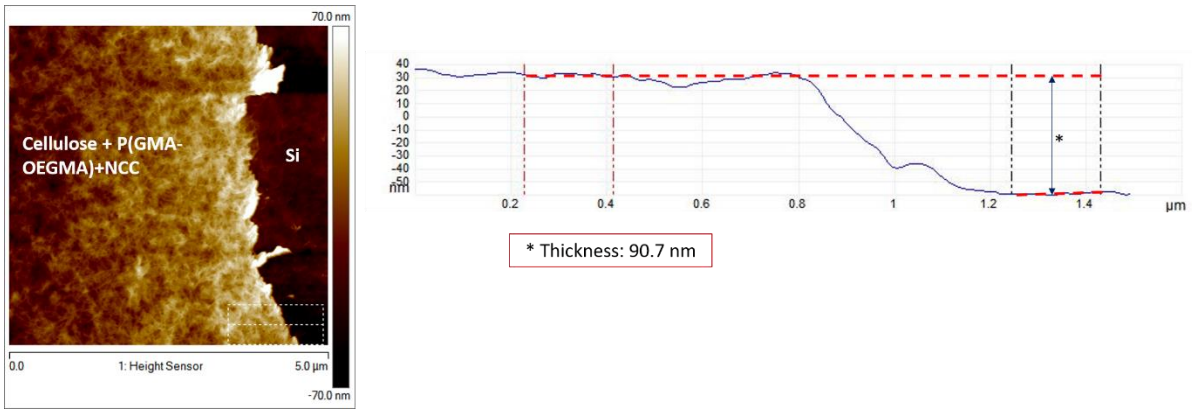

Fig. 2.82. Topography image of the Si-Cellulose + P(GMA-OEGMA)+NCC (after washing) after the scratch with a steel needle

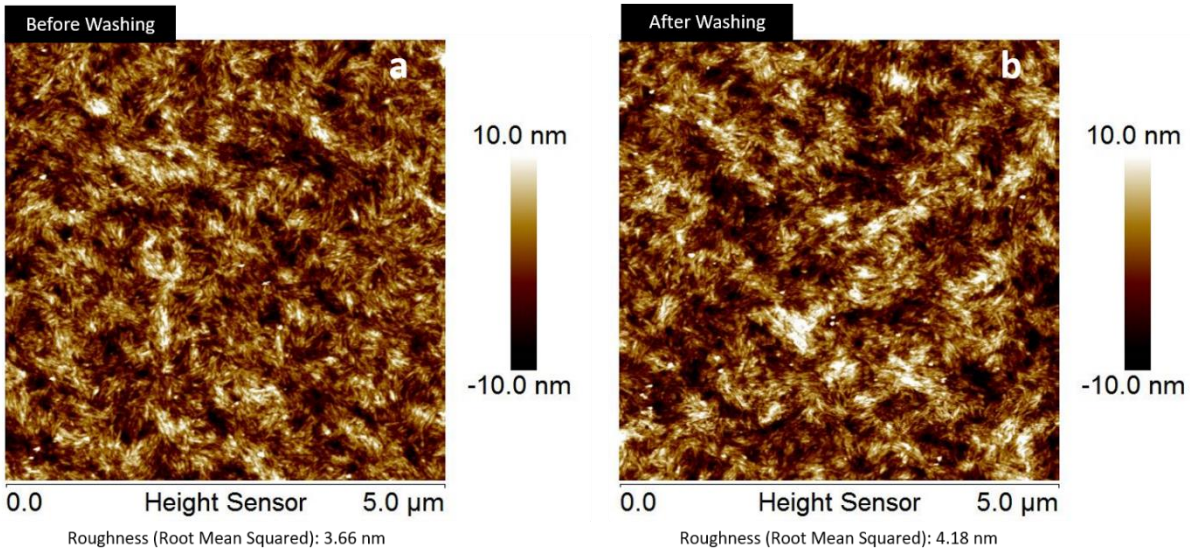

Fig. 2.83. Polyester + P(GMA-OEGMA)+NCC before (a) and after washing (b)

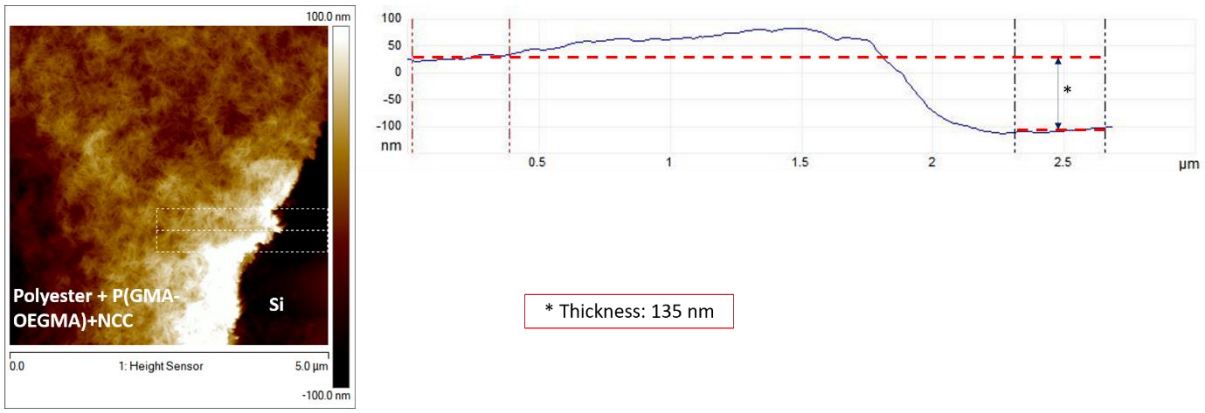

Fig. 2.84. Topography image of the Si-Polyester + P(GMA-OEGMA)+NCC (before washing) after the scratch with a steel needle

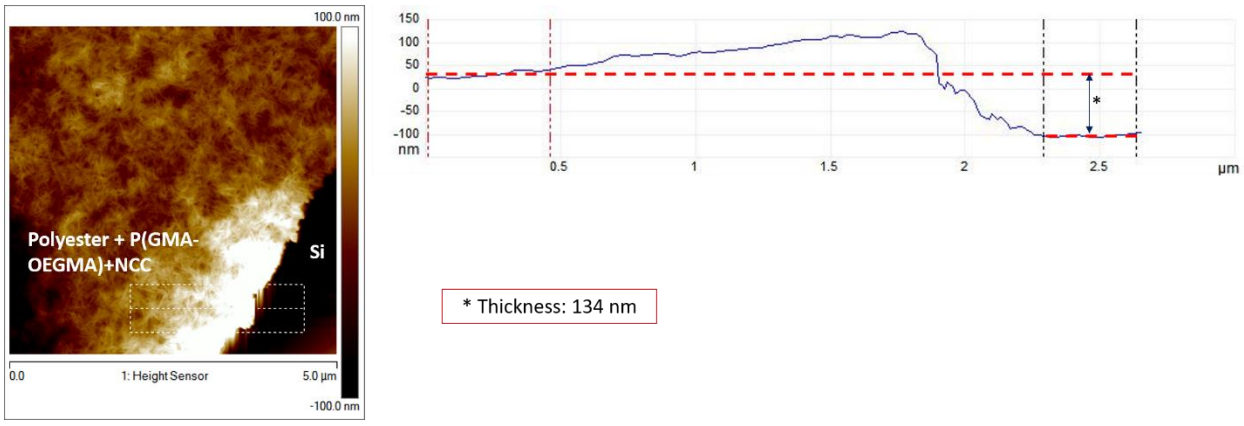

Fig. 2.85. Topography image of the Si-Polyester + P(GMA-OEGMA)+NCC (after washing) after the scratch with a steel needle

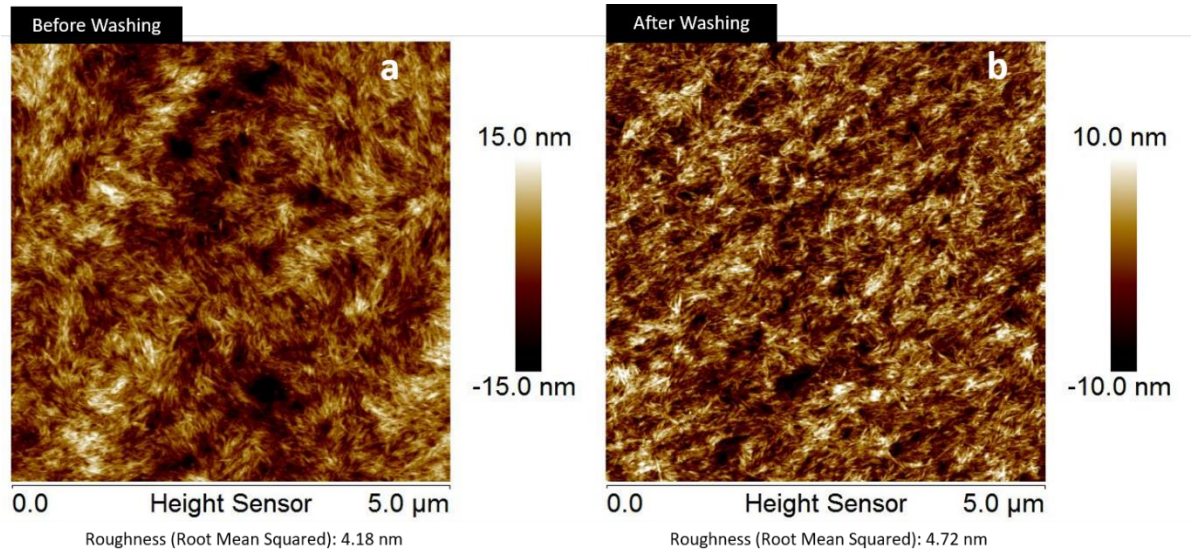

Fig. 2.86. Nylon + P(GMA-OEGMA)+NCC before (a) and after washing (b)

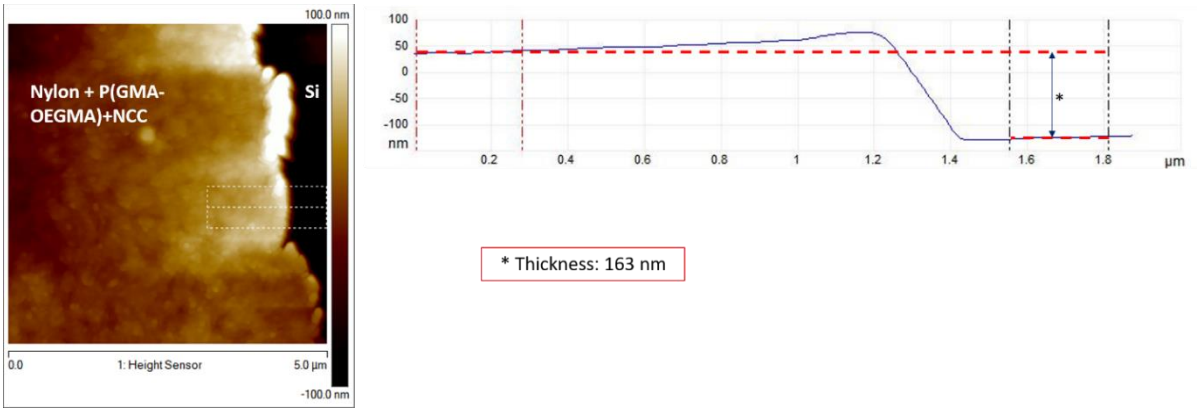

Fig. 2.87. Topography image of the Si-Nylon + P(GMA-OEGMA)+NCC (before washing) after the scratch with a steel needle

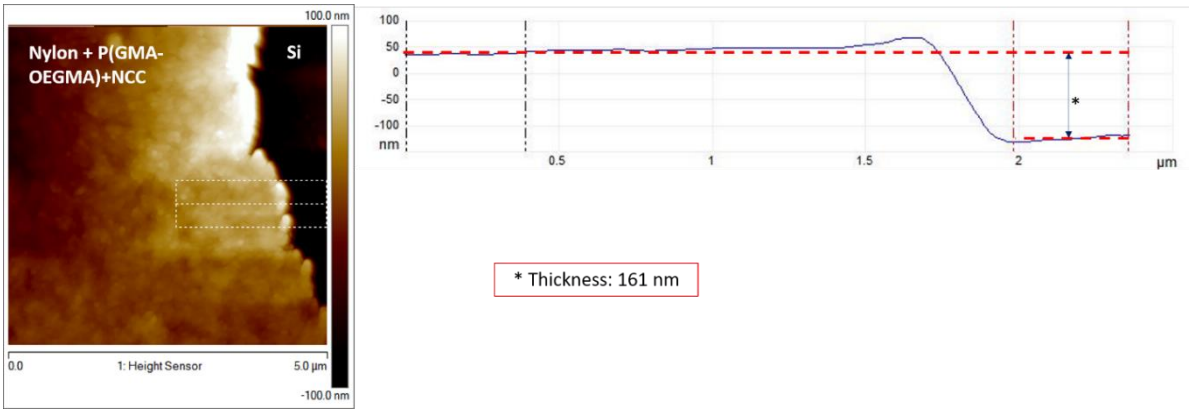

Fig. 2.88. Topography image of the Si-Nylon + P(GMA-OEGMA)+NCC (after washing) after the scratch with a steel needle

CHAPTER 3

ENZYMATIC TREATMENTS OF NANOCELLULOSE HYDROGELS FOR SUSTAINABLE DYEING TECHNOLOGY[2]

[2] Saremi, R., S., Larson, A., Zakharchenko, S., Sharma, and S., Minko. To be submitted to Green Chemistry.

Abstract

Herein, we incorporated dye molecules to the nanocellulose coating that we developed in our previous work to create a sustainable and environmentally friendly dyeing technology with comparable dyeing performance to conventional dyeing technique. To enhance dyeability of nanocellulose, they were treated with cellulases from *Trichoderma reesei* and enzymogel nanoparticles. The enzyme and enzymogel treatments change the surface area and crystallinity of the hydrogels by slowly degrading crystalline region and improving dyeability of nanocellulose without excessively damaging the structure and properties.

3.1 Introduction

Traditional dyeing process requires enormous amounts of water (30 - 50 liters per kg of cloth depending on the type of dye used)[1] and produces large volumes of wastewater. The textile dyeing industry considering the volume and composition of discharge is the number one generator of wastewater among all industrial sectors.[1-3] Environmental concerns related to the harmful effect of textile wastewater and huge consumption of water in textile wet processing industry provide reasons for ongoing interest in the development of sustainable and cleaner production methods.[4] Many approaches have been proposed to improve the efficiency of dyeing process such as surface and chemical modification of textile surfaces to increase dye uptake and reduce the amount of dye and salt in the process.[5-6] Enzymatic treatments that activate and accelerate chemical reaction and as a result, reduce the amount of water needed for the rinsing steps and saves energy. Ultrasonic treatments that reduced consumption of dyes and chemicals and consumes around 20% less water.[7] Waterless dyeing technology such as ColorZen[8] and DyeCoo[9] to tackle wastewater problem of the textile dyeing process. Approaches to improve the efficiency of the rinsing step to save time, reduce the amount of water used in the process, and consequently decrease the cost and environmental impact.[10-11]. And, decolorizing of wastewater to remove color-causing compounds from the wastewater. However, because of a synthetic origin of dyes and their complex aromatic molecular structures, it is tough to remove the colored waste completely, and in this process mostly the decoloration happens rather than the degradation of the dye molecules. Furthermore, new intermediate compounds are generated in different treatment processes of decolorization that in some cases are more toxic than the colored waste.[12] Therefore, there is a need to develop more environmentally and sustainable techniques to reduce the amount of wastewater and eventually eliminates the toxic chemicals in the production methods rather than investing in the treatment of

wastewaters. Although there have been some improvements in the production methods, the problems of toxicity and environmental impacts still exists. Therefore, there is a need to develop new sustainable textile dyeing methods.

Dyeing technique using nanocellulose hydrogels is environmentally friendly and eliminates the need for vast amounts of water in the dyeing process (one-tenth of the amount of water needed in the conventional dyeing process).[13] Nanocellulose either in the form of fibrils (nanofibrillated cellulose-NFC) or the form of whiskers or crystals (nanocrystalline cellulose-NCC)[14-15] are widely used to develop environmentally friendly materials[16] due to their abundant natural resources[17-18] and their unique properties such as low density, high length-to-width ratio, and high mechanical stability. Nanocellulose has crystalline and amorphous regions.[19] Amorphous region and surface area of nanocellulose are two critical parameters in increasing dye uptake and dye fixation in nanocellulose based dyeing.

Cellulases have been widely used for the treatment of cellulose-based materials.[20-21] Cellulases are multi-components enzymes secreted by various groups of microorganisms such as fungi and bacteria. Cellulases from *Trichoderma reesei* contains exoglucanases and endoglucanases which attack crystalline and amorphous regions of cellulose respectively.[22] Hydrolyzed cellulose fibers showed significant difference in dyeability compared to untreated cellulose fibers.[23-25] Cellulase by slowly degrading impurities and crystalline region of nanocellulose improve the accessibility of amorphous regions to dye molecules without excessively damaging cellulose structures and properties. Therefore, in this study, enzymatic treatments with pure enzyme and enzymogel nanoparticles on NFC and NCC fibers were performed before the dyeing process. The effects of cellulase enzyme on dyeability as well as

structural and thermal properties of nanocellulose were investigated using color, weight loss, thermogravimetric, specific surface area, and X-ray measurements.

3.2 Experimental Section

3.2.1 Materials

Nanocellulose Hydrogels. Nanofibrillated cellulose gel (NFC) (2%) was prepared in our previous study,[13] and nanocrystalline cellulose gel (NCC) (11.9%) was purchased from the Process Development Center, University of Maine.

Enzymes. Cellulase from *Trichoderma reesei* (aqueous solution, ≥700 units/g) purchased from Sigma-Aldrich.

Dye, Alkali, and Salt. Reactive Red 120 (MW 1469.98), and Sodium carbonate (MW 105.99) were purchased from Sigma Aldrich. Sodium sulfate Anhydrous (MW 142.04, ≥99.0 %) was obtained from Fisher Scientific.

Methylene Blue. Methylene blue (C16H18N3SCl, 1 g/mL) was purchased from Ward's Science.

3.2.2 Enzymatic Treatments

Cellulases are multi-components enzymes mainly produced by various groups of microorganisms. They synergistically hydrolyze cellulose by cleaving the β (1→4) linkages between D-glucose units. Cellulases from *Trichoderma reesei* (a filamentous fungus) contains, exoglucanases or cellobiohydrolases, endoglucanases, and β-glucosidase. The endoglucanases catalyze the random cleavage of internal bonds of the cellulose chain, while exoglucanase attack the chain ends, releasing cellobiose and glucose as the reaction products. The cellobiose is then hydrolyzed into glucose by β-glucosidase.[26-28] The efficiency of enzymatic hydrolysis of nanocellulose hydrogels depends on the different

physical parameters such as temperature, and PH.[29] *T. ressei cellulases* have a maximum activity at the temperature below 50℃, and PH 5 and almost no activity found over 70℃.[29-31] In this study, NFC and NCC were subjected to the cellulase enzyme secreted by *Trichoderma reesei* under the condition of a liquor-to-sample ratio of 1:100, 0.1% enzyme concentration, pH 4.5 at 40±2 °C for 20 min. Then to stop enzyme activity and to wash off proteins, NFC and NCC were washed in 0.1% aqueous ammonia at 70°C for 20 min, and finally rinsed thoroughly with deionized water.

3.2.3 Enzymogel Treatment

Enzymogel nanoparticles consist of a core-shell structure with an inorganic core (100±10 nm silica core), and a polymer brush shell (30±5 nm (in the dry state) poly(acrylic acid) (PAA)) loaded with enzymes were prepared as previously reported.[32] The PAA brush was synthesized by surface-initiated polymerization of tert-butyl acrylate and the subsequent hydrolysis of poly(tert-butyl acrylate). The enzyme remains encapsulated and active in the polymer brush even when it is residing in the brush until the enzymogel nanoparticles attach to the surface of cellulose.[32] Cellulose substrates like nanocellulose hydrogels can adsorb enzymogel nanoparticles when both the substrate and enzymogel are negatively charged in water at pH around 5. Enzymogel nanoparticles actively interact with the nanocellulose surfaces by hydrogen bonding between hydroxyl groups of cellulose and carboxyl groups of PAA brushes. The previous study[32] showed that enzymogel nanoparticles have more significant degradation effects on cellulose compared to the pure cellulase enzyme. Therefore, they may provide more favorable results regarding the surface modification of NFC and NCC to increase the uptake of functional molecules. In this study, we used enzymogel nanoparticles to treat NFC and NCC and compared the results to

enzyme treated NFC and NCC. Here, cellulase which is positively charged was loaded and encapsulated into the negatively charged polymer brush at a pH around 5 (PAA is negatively charged at a pH range of 4 to 8). This enzyme catalyzes the hydrolysis of the nanocellulose particles attached to the enzymogel core-shell nanoparticle.[32] Fig. *3.5* shows the schematic of the enzymogel nanoparticle consists of a silica core, and a PAA brush shell loaded with enzymes at PH 4.5 and PH 7. The NFC and NCC were treated under the condition of a liquor-to-sample ratio of 1:100, 0.1% enzymogel concentration, pH 4.5 at 40±2 °C for 20 min. The enzyme was deactivated in 0.1% aqueous ammonia at 70°C for 20 min. Finally, the NFC and NCC were rinsed thoroughly with deionized water.

3.2.4 Dyeing Method

Reactive dye because of the straightforward method of application, and good color fastness is the most common dye used for dyeing of cellulose fibers. Dye and salt are first added to the dyebath following with alkali after a period in the process. Salt helps to increase dye exhaustion and alkali with the functional groups in dye results in the covalent bonding between dye and fibers which causes good color fastness.[11] In this study, control, enzyme and enzymogel treated NFC and NCC were dyed with a Reactive Red 120 dye stock solution and salt under the conditions of a liquor-to-sample ratio of 1:100 at 75±5 °C (Fig. *3.2*). The dyed nanocellulose gels were collected by centrifugation at approximately 13000 revolutions per minute for 30 minutes. After fixation, NFC and NCC were thoroughly washed with boiling water to make sure there is no unfixed dye in the nanocellulose gels.

3.2.5 Characterizations

Spectrophotometer. Color strength (K/S) of died NFC and NCC gels before and after washing with deionized water were measured using a spectrophotometer (Macbeth Color-Eye 7000A, illuminant D65, aperture size 75 mm^2, specular included).

UV-Vis spectrophotometer. UV-Vis spectrophotometer (UV-2401PC, Shimadzu) were used to analyze the concentration of methylene blue solutions to measure the specific surface area of NFC and NCC gels before and after the enzymatic treatments.

Thermogravimetric analysis (TGA). Thermal gravimetric analysis (TGA) was performed using a Mettler Toledo TGA/SDTA851e to evaluate the thermal stability of nanocellulose before and after the enzymatic treatment of freeze-dried NFC and NCC.

X-ray Diffraction Measurement. The crystalline structures of the enzymatic treated and control nanocellulose hydrogels were characterized by a PANalytical X'Pert PRO MRD x-ray diffractometer (XRD). The XRD patterns were recorded with a Cu Kα1 radiation (λ = 1.541 Å) in the 2θ range from 5°–50° with a step size of 0.03°.

3.2.6 Adsorption Behavior of Methylene Blue Dye on Nanocellulose Hydrogels

Methylene blue (MB) dye, 3,7-bis(Dimethylamino)phenazathionium chloride, $C_{16}H_{18}ClN_3S.3H_2O$ C16H18ClN3S (Fig. *3.3*) for surface area determination has been used in many studies because of the MB strong adsorption onto solids [33-35]. In this study, adsorption of MB dye on the surface of nanocelloluse hydrogels (NFC and NCC) was used as a method of specific surface area measurement before and after the enzymatic treatments. MB with a molecular weight of 373.9 $gmol^{-1}$ (which corresponds to methylene blue hydrochloride with three groups of water ($C_{16}H_{18}ClN_3S.3H_2O$)) was dried at 110℃ for 2 hours.[34] Calibration curve of absorbance against concentration of MB was obtained at

various known concentrations of the solutions (from 1 μM to 30 μM) (Fig) and was used to measure the concentrations of MB after adsorption onto the NFC and NCC. Adsorption measurements for the control and enzymatic treated NFC and NCC were carried out by adding 5 g of NFC (2%) and 0.84 g of NCC (11.9 %) to 40 ml of methylene blue solution of known concentration. It was previously reported that MB adsorption onto solids reaches its maximum capacity and complete equilibrium in about 24 hours.[34] Therefore, the mixture was shaken continuously for 24 hours. After adsorption, the concentrations of MB in the residual solutions were analyzed by measuring their absorbance at 660 nm by a UV-Vis spectrophotometer.

3.3 Results and Discussion

3.3.1 Color Measurement

Color strength (C) of dyed NFC and NCC gels were measured by a color spectrophotometer at the wavelength of maximum adsorbance (510 nm) before and after washing with deionized water from Kubelka-Munk equation:

$$C = \frac{K}{S} = \frac{(1-R)^2}{2R} \qquad (3.1)$$

Where K is adsorption coefficient, S is the scattering coefficient, and R is the reflectance value. Higher K/S value shows the greater color depth and more significant dye uptake.

Dye fixation, a number of dye molecules that are fixed on the textile surfaces, were calculated using the following equation:

$$F = \frac{C_s}{C_o} \qquad (3.2)$$

Where F is the dye fixation (%), C_s is the color strength after washing, and C_o is the color strength before washing.

Table *3.1* shows higher values for color strength of NFC after the enzyme and enzymogel treatments which consequently resulted in an increase of dye fixation for both treatments. Color strength after washing and dye fixation of enzyme and enzymogel treated NCC also increased significantly compared to the control NCC while for NFC the difference between the control and the enzyme treated samples is not very huge. This difference could be related to the difference in the structure of NFC compared to NCC, which we will discuss in the following sections. It is important to note that the color strength and dye fixation show higher values for nanocellulose based textile dyeing (10.57 to 10.93, 86% to 97%) compared to the conventional dyeing method (5.6 ± 0.1, 78 ± 3%).[13]

3.3.2 Weight Loss Measurement

Weight loss (%) was calculated from the following equation by weighing the freeze-dried samples before and after the enzymatic treatments:

$$W_L = \frac{(W_1 - W_2)}{W_1} \times 100 \qquad (3.3)$$

Where W_1 and W_2 are weights of the samples before and after the enzymatic treatments respectively. The results show 10.79% and 10.17% weight loss for NFC and NCC samples caused by the cellulase treatment and 11.24% and 15.77% weight loss for NFC and NCC after the enzymogel treatment (Table *3.2*). These weight loss values correspond to the impurities such as polysaccharides in the primary wall and the matrix between fibrils in the secondary wall that were removed by the enzyme. These areas because of the impurities

are also less active toward reactive dyes.[24, 36] Therefore, after the cellulase treatments, we observed the increase in color strength and dye fixation for all the samples.

3.3.3 Thermogravimetric Analysis (TGA)

TGA was used to evaluate the thermal stability of NFC and NCC before and after the enzyme treatment with *T. ressei cellulases*. Fig. *3.8* and Fig. *3.9* show the thermogravimetric (a) and differential thermogravimetry (b) curves of NFC and NCC before and after the treatment respectively. The NFC samples (both treated and untreated) show primary decomposition reactions around 100°C followed by a sharp weight loss of 30% starting at 150°C and 200°C for NFC samples before and after the enzyme treatments respectively. For NCC, an initial weight loss (onset of degradation) was observed for treated and untreated samples upon heating to 200°C and 260°C respectively, followed by a sharp weight loss of 55% and 37% for treated and untreated NCC respectively.

It should also be noted that NFC sample shows the decrease in thermal stability (the temperature at the maximum weight loss rate)[37] after the enzyme treatments which can be due to the changes in crystallinity of NFC while the maximum weight loss rate happens at a higher temperature for NCC samples after the enzyme treatment. However, the rate of weight loss is much lower after the enzyme treatment for both NFC and NCC samples.

Specific Surface Area Measurement

A calibration curve was plotted and fitted by a straight line for MB absorbance at 660 nm vs. MB concentration (up to 30 μM) with a slope of 0.071 and a correlation coefficient of 0.99 (Fig. *3.10*). From this plot, the residual concentrations of MB in the solutions were calculated. The Langmuir adsorption isotherm plots (Fig. *3.11* and Fig. *3.12*) shows MB adsorption (q) vs. equilibrium concentration of MB in the solutions (C_2). The adsorption capacity of MB on NFC

and NCC corresponds to the reduction of MB adsorption intensity at 660 nm after 24 hours and was calculated from the following equation:

$$q = \frac{(C_1 - C_2)MV}{1000\, w} \tag{3.4}$$

Where q is the amount of MB adsorbed on the adsorbent (mg/g), V is the solution volume (mL), C_1 is the initial MB concentration (M), C_2 is the final MB concentration in the residual solution (M), M is the molecular weight of MB ($mgmol^{-1}$), and w is the amount of adsorbent (g).

The specific surface area was calculated using the following equation:[38-39]

$$S_{MB} = \frac{q_{MB} \times a_{MB} \times N_A \times 10^{-20}}{M_{MB}} \tag{3.5}$$

Where (S_{MB}) is the specific surface area (m^2/g), q_{MB} is the number of adsorbed molecules of MB at the monolayer of adsorbent (g/g). a_{MB} is the occupied surface area of one molecule of MB (197.2 Å^2), N_A is Avogadro's number (6.02 x 1023 mol^{-1}), and M_{MB} is the molecular weight of MB ($gmol^{-1}$).

Table 3.3 the amount of MB adsorbed on the control and enzymatically treated samples. The quantity of methylene blue adsorbed, and specific surface area for NFC samples show the higher values than NCC samples. This discrepancy explains the higher value for color strength and dye performance of NFC compared to NCC. Because NFC has the higher specific surface area, it can adsorb more reactive dye molecules than NCC. We also observed that the enzyme increases the MB adsorption and specific surface area of NFC and NCC by 13% while enzymogel treated NFC and NCC show 16% and 25% increase respectively.

3.3.4 XRD measurement

X-ray diffraction patterns were obtained (Fig. *3.13* and Fig. *3.14*) for control, enzyme and enzymogel treated NFC and NCC to investigate the effect of enzyme and enzymogel treatments on their crystallinity due to the cellulase-cellulose interactions. Both untreated and treated samples display similar diffraction patterns, and cellulase-cellulose interactions caused almost no change in the position of 2θ for 101, 10$\bar{1}$, 002 and 040 crystal planes for NFC and crystal planes of 101, 10$\bar{1}$, 021, 002 and 040 for NCC. NCC shows both celluloses I and II crystal planes due to the alkali pulping and acid hydrolysis processes which transform cellulose I to II during NCC production.[40-42] NFC has broadened and merged peaks because of the high-pressure mechanical process used in NFC manufacturing that could deform and destruct cellulose crystals to form amorphous regions resulted in broadened and shifted diffraction peaks.[40-42]

The degree of crystallinity was determined using a peak fitting program (PeakFit; www.systat.com) to subtract the baselines. Crystalline peaks were extracted by a curve-fitting process assuming Gaussian functions[43-45] from the diffraction intensity profiles using the OriginPro software. The degree of crystallinity was then calculated from the ratio of the area of all crystalline peaks to the total area.

Apparent crystal size (ACS) was calculated using the Scherrer equation:[29, 46]

$$ACS = 0.9 \times \lambda/\beta cos\theta \qquad (3.6)$$

Where λ is the X-ray wavelength (1.541 Å), β is the full width at half maximum corresponding to 002 crystal plane in radian, θ 002 crystal plane peak position in degrees.

The XRD results including crystallinity (%), apparent crystal size (ACS), and full width at half maximum (FWHM) are summarized in Table 3.4. The degree of crystallinity of NFC decreased from 69.33% to 51.12% and 57.98% after the enzyme and enzymogel treatments

respectively. The apparent crystal size of enzyme and enzymogel treated NFC also show lower values (19.67 Å and 25.01 Å) compared to the control NFC (28.14 Å). For NCC, the degree of crystallinity slightly decreased from approximately 77% to 71% after the treatments. However, the apparent crystal size did not present any significant change after both treatments. It probably means that the NFC crystals were damaged by the two treatments compared to the NCC crystals that show no difference after the enzyme treatment and show a slight decrease after the enzymogel treatment. Cellulase from *Trichoderma reesei* contains exoglucanases which preferably attacks crystalline regions, while endoglucanases attack isolated amorphous regions. The higher reduction in the degree of crystallinity of NFC compared to NCC indicates that the crystalline regions of NFC were more accessible to exoglucanases than NCC.

3.3.5 Summary

The decrease in the degree of crystallinity increased the color strength and dye performance of NFC and NCC after the enzymatic treatments. These results are consistent with the previous studies on dyeability of cellulose fibers after cellulase treatments.[23-25] Cellulases digest impurities such as polysaccharides that are inactive towards the reactive dye which results in the increase of the weight loss and consequently increases the color strength and dye fixation of NFC and NCC. The enzyme and enzymogel treatments also increased the specific surface areas of NFC and NCC resulting in higher color strength and dye fixation of both samples.

3.4 References

1. Kant, R., Textile dyeing industry an environmental hazard. Natural science **2012,** 4 (1), 22-26.

2. Vandevivere, P. C.; Bianchi, R.; Verstraete, W., Treatment and reuse of wastewater from the textile wet-processing industry: Review of emerging technologies. Journal of Chemical Technology and Biotechnology **1998,** 72 (4), 289-302.

3. Reid, R., Go green-a sound business decision (part 1). Coloration Technology **1996,** 112 (4), 103-105.

4. Shahid-ul-Islam; Mohammad, F., Emerging Green Technologies and Environment Friendly Products for Sustainable Textiles. In Roadmap to Sustainable Textiles and Clothing: Environmental and Social Aspects of Textiles and Clothing Supply Chain, Muthu, S. S., Ed. Springer Singapore: Singapore, 2014; pp 63-82.

5. Kitkulnumchai, Y.; Ajavakom, A.; Sukwattanasinitt, M., Treatment of oxidized cellulose fabric with chitosan and its surface activity towards anionic reactive dyes. Cellulose **2008,** 15 (4), 599-608.

6. Wang, H.; Lewis, D., Chemical modification of cotton to improve fibre dyeability. Coloration Technology **2002,** 118 (4), 159-168.

7. Hasanbeigi, A.; Price, L., A technical review of emerging technologies for energy and water efficiency and pollution reduction in the textile industry. Journal of Cleaner Production **2015,** 95, 30-44.

8. ColorZen, 2012. ColorZen: How it Works/the Benefits. Available at: http://www.colorzen.com/.

9. DyeCoo CO2 Dyeing Technology. Available at: http://www.dyecoo.com/.

10. Bradbury, M.; Collishaw, P.; Moorhouse, S., Smart Rinsing: A Step Change in Reactive Dye Application Technology. AATCC Review **2001,** 1 (11).

11. Muthu, S. S., Roadmap to Sustainable Textiles and Clothing: Eco-friendly Raw Materials, Technologies, and Processing Methods. Springer: 2014.

12. Hao, O. J.; Kim, H.; Chiang, P.-C., Decolorization of wastewater. Critical reviews in environmental science and technology **2000,** 30 (4), 449-505.

13. Kim, Y.; McCoy, L. T.; Lee, E.; Lee, H.; Saremi, R.; Feit, C.; Hardin, I. R.; Sharma, S.; Mani, S.; Minko, S., Environmentally sound textile dyeing technology with nanofibrillated cellulose. Green Chemistry **2017,** 19 (17), 4031-4035.

14. Atalla, R. H.; Brady, J. W.; Matthews, J. F.; Ding, S. Y.; Himmel, M. E., Structures of plant cell wall celluloses. Biomass recalcitrance: deconstructing the plant cell wall for bioenergy **2008**, 188-212.

15. Klemm, D.; Kramer, F.; Moritz, S.; Lindström, T.; Ankerfors, M.; Gray, D.; Dorris, A., Nanocelluloses: A new family of nature-based materials. Angewandte Chemie International Edition **2011,** 50 (24), 5438-5466.

16. Azzam, F.; Moreau, C. l.; Cousin, F.; Menelle, A.; Bizot, H.; Cathala, B., Cellulose nanofibril-based multilayered thin films: Effect of ionic strength on porosity, swelling, and optical properties. Langmuir **2014,** 30 (27), 8091-8100.

17. Henriksson, M.; Berglund, L. A., Structure and properties of cellulose nanocomposite films containing melamine formaldehyde. Journal of Applied Polymer Science **2007,** 106 (4), 2817-2824.

18. Iwamoto, S.; Nakagaito, A.; Yano, H., Nano-fibrillation of pulp fibers for the processing of transparent nanocomposites. Applied Physics A **2007,** 89 (2), 461-466.

19. Kumar, R.; Singh, S.; Singh, O. V., Bioconversion of lignocellulosic biomass: biochemical and molecular perspectives. Journal of industrial microbiology & biotechnology **2008,** 35 (5), 377-391.

20. Hall, M.; Bansal, P.; Lee, J. H.; Realff, M. J.; Bommarius, A. S., Cellulose crystallinity–a key predictor of the enzymatic hydrolysis rate. The FEBS journal **2010,** 277 (6), 1571-1582.

21. Himmel, M. E.; Ruth, M. F.; Wyman, C. E., Cellulase for commodity products from cellulosic biomass. Current opinion in biotechnology **1999,** 10 (4), 358-364.

22. Haigler, C. H., Biosynthesis and biodegradation of cellulose. CRC Press: 1990.

23. Mori, R.; Huga, T.; Takagishi, T., Relationship between cellulase treatment and the dyeability with a direct dye for various kinds of cellulosic fibers. Journal of applied polymer science **1993,** 48 (7), 1223-1227.

24. Mori, R.; Haga, T.; Takagishi, T., Changes in dyeability and morphology of cotton fiber subjected to cellulase treatment. Journal of applied polymer science **1997,** 65 (1), 155-164.

25. Mori, R.; Haga, T.; Takagishi, T., Reactive dye dyeability of cellulose fibers with cellulase treatment. Journal of applied polymer science **1996,** 59 (8), 1263-1269.

26. Wood, T. M.; Garcia-Campayo, V., Enzymology of cellulose degradation. Biodegradation **1990,** 1 (2-3), 147-161.

27. Reinikainen, T.; Henriksson, K.; Siika-aho, M.; Teleman, O.; Poutanen, K., Low-level endoglucanase contamination in a Trichoderma reesei cellobiohydrolase II preparation affects its enzymatic activity on β-glucan. Enzyme and microbial technology **1995,** 17 (10), 888-892.

28. Béguin, P.; Aubert, J.-P., The biological degradation of cellulose. FEMS microbiology reviews **1994,** 13 (1), 25-58.

29. Cao, Y.; Tan, H., Effects of cellulase on the modification of cellulose. Carbohydrate Research **2002,** 337 (14), 1291-1296.

30. Baker, J.; Tatsumoto, K.; Grohmann, K.; Woodward, J.; Wichert, J.; Shoemaker, S.; Himmel, M., Thermal denaturation ofTrichoderma reesei cellulases studied by differential scanning calorimetry and tryptophan fluorescence. Applied biochemistry and biotechnology **1992,** 34 (1), 217-231.

31. Andreaus, J.; Azevedo, H.; Cavaco-Paulo, A., Effects of temperature on the cellulose binding ability of cellulase enzymes. Journal of molecular catalysis B: Enzymatic **1999,** 7 (1), 233-239.

32. Kudina, O.; Zakharchenko, A.; Trotsenko, O.; Tokarev, A.; Ionov, L.; Stoychev, G.; Puretskiy, N.; Pryor, S. W.; Voronov, A.; Minko, S., Highly efficient phase boundary biocatalysis with enzymogel nanoparticles. Angewandte Chemie International Edition **2014,** 53 (2), 483-487.

33. Froix, M. F.; Nelson, R., The interaction of water with cellulose from nuclear magnetic resonance relaxation times. Macromolecules **1975,** 8 (6), 726-730.

34. Hequet, E.; Abidi, N.; Gourlot, J., Application of methylene blue adsorption to cotton fiber specific surface area measurement: Part 1 methodology. J. of Cotton Science **1998,** 2, 164-173.

35. Ardizzone, S.; Gabrielli, G.; Lazzari, P., Adsorption of methylene blue at solid/liquid and water/air interfaces. Colloids and Surfaces A: Physicochemical and Engineering Aspects **1993,** 76, 149-157.

36. Sakurai, N.; Yamamoto, R.; Kato, Y., Plant cell wall and polysaccharides. Baifukan, Tokyo **1991,** 161.

37. Agustin, M. B.; Nakatsubo, F.; Yano, H., The thermal stability of nanocellulose and its acetates with different degree of polymerization. Cellulose **2016,** 23 (1), 451-464.

38. Eric, H.; Chongrak, K.; Noureddine, A.; Jean, P., Application of methylene blue adsorption to cotton fiber specific surface area measurement. J Cotton Sci **1998,** 2, 164-173.

39. Gregg, S.; Sing, K. S., Adsorption, surface area, and porosity. **1983**.

40. Brown Jr, R. D.; Jurasek, L., Hydrolysis of cellulose: mechanisms of enzymatic and acid catalysis. ACS Publications: 1979.

41. El Oudiani, A.; Chaabouni, Y.; Msahli, S.; Sakli, F., Crystal transition from cellulose I to cellulose II in NaOH treated Agave americana L. fibre. Carbohydrate polymers **2011,** 86 (3), 1221-1229.

42. Xu, X.; Liu, F.; Jiang, L.; Zhu, J.; Haagenson, D.; Wiesenborn, D. P., Cellulose nanocrystals vs. cellulose nanofibrils: a comparative study on their microstructures and effects as polymer reinforcing agents. ACS applied materials & interfaces **2013,** 5 (8), 2999-3009.

43. Garvey, C. J.; Parker, I. H.; Simon, G. P., On the interpretation of X-ray diffraction powder patterns in terms of the nanostructure of cellulose I fibres. Macromolecular Chemistry and Physics **2005,** 206 (15), 1568-1575.

44. Hult, E.-L.; Iversen, T.; Sugiyama, J., Characterization of the supermolecular structure of cellulose in wood pulp fibres. Cellulose **2003,** 10 (2), 103-110.

45. Park, S.; Baker, J. O.; Himmel, M. E.; Parilla, P. A.; Johnson, D. K., Cellulose crystallinity index: measurement techniques and their impact on interpreting cellulase performance. Biotechnology for biofuels **2010,** 3 (1), 10.

46. Segal, L.; Creely, J.; Martin Jr, A.; Conrad, C., An empirical method for estimating the degree of crystallinity of native cellulose using the X-ray diffractometer. Textile Research Journal **1959,** 29 (10), 786-794.

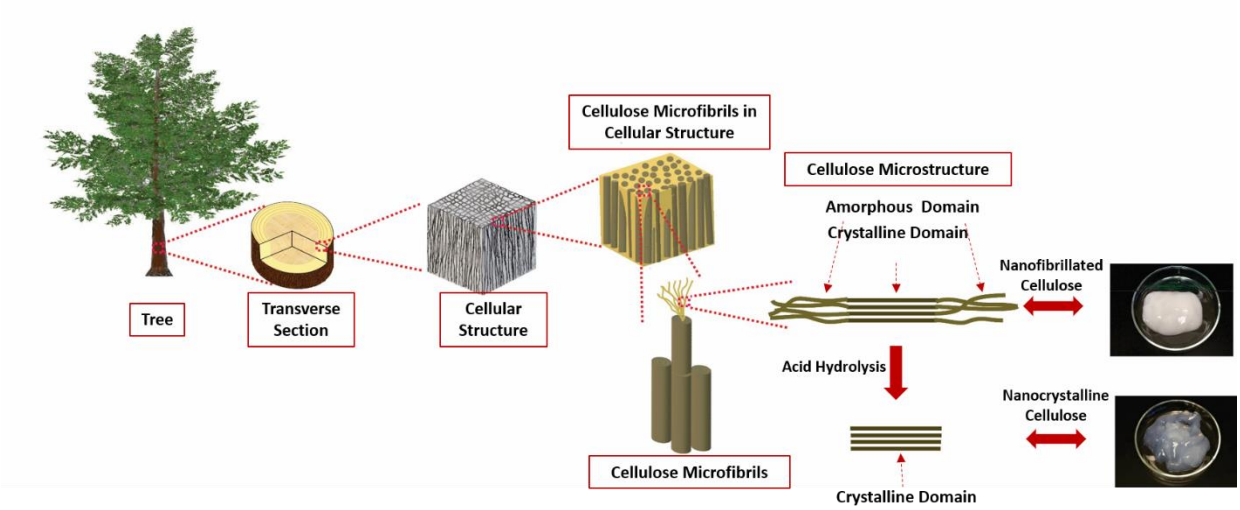

Fig. 3.1. Hierarchical morphology of cellulose fiber and schematic illustration of NFC and NCC production

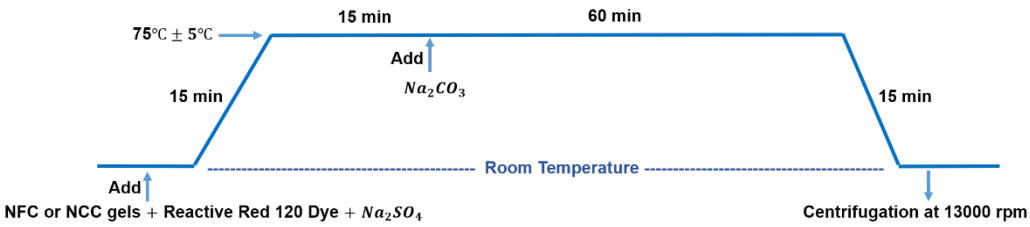

Fig. 3.2. Dyeing protocol of NFC and NCC with reactive red 120

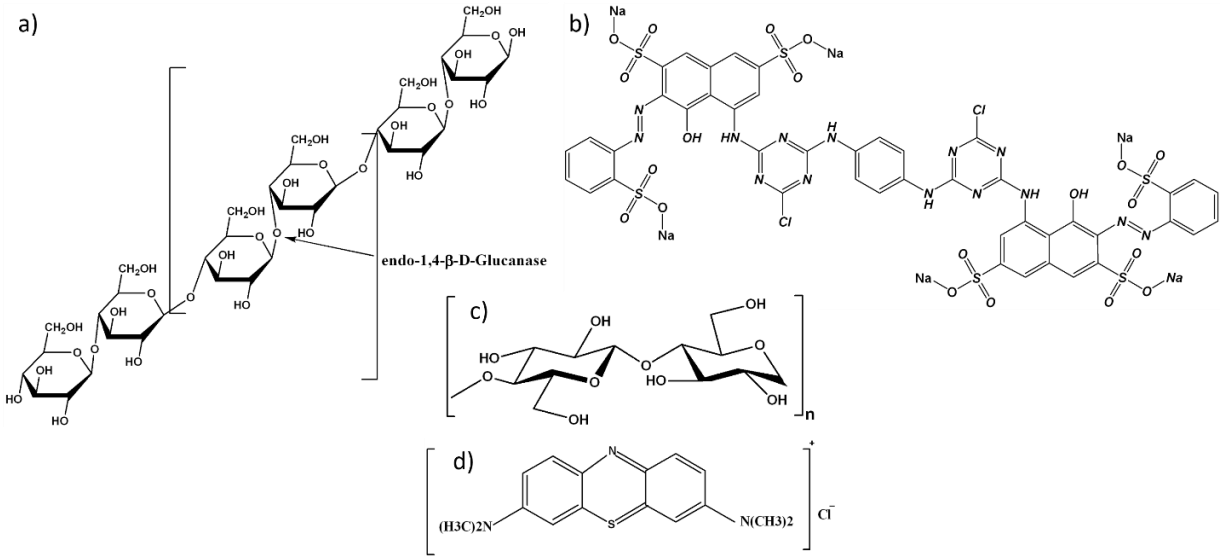

Fig. 3.3. Chemical structure of cellulase from Trichoderma reesei ATCC 26921 (a), reactive red dye 120 (b), cellulose (c), and methylene blue (d)

Fig. 3.4. Dyed enzyme-treated NFC and NCC (a) dyed cotton fabric with enzyme-treated NFC (b), and dyed cotton fabric with enzyme-treated NCC (c)

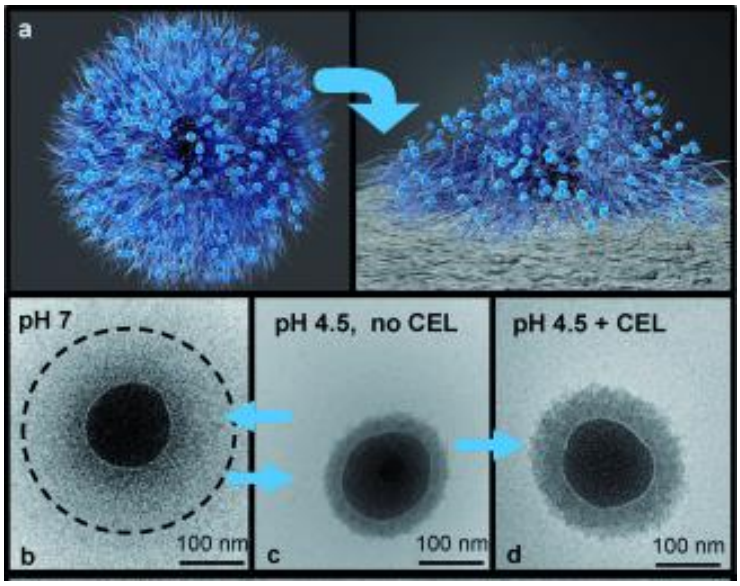

Fig. 3.5. (a) Schematic of the enzymogel nanoparticle consists of a silica core, and a PAA brush shell loaded with cellulase enzyme; (b, c, d) cryo-TEM images of the particle with a silica core (b) swollen, (c) shrunken PAA brush, and (d) uniformly loaded with enzymes at pH 4.5 reproduced with permission from[32]

Table 3.1. Color Strength and dye Fixation of NFC and NCC samples before and after washing

	Color strength before washing (K/S)	**Color strength after washing (K/S)**	**Dye fixation (%)**
NFC	10.33	8.72	85
Enzyme-Treated NFC	11.94	10.57	89
Enzymogel-Treated NFC	12.14	11.01	91
NCC	12.57	6.84	54
Enzyme-Treated NCC	12.61	10.90	86
Enzymogel-Treated NCC	11.28	10.93	97

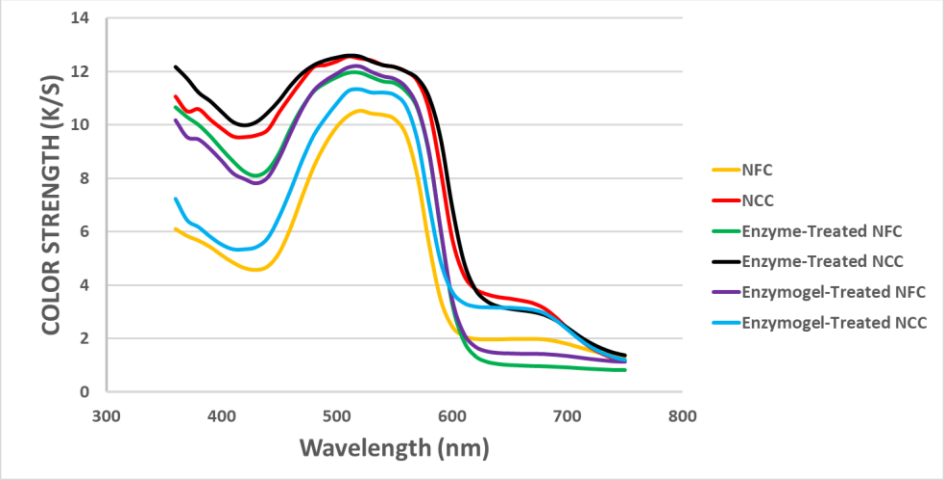

Fig. 3.6. Color strength spectra of NFC and NCC before washing

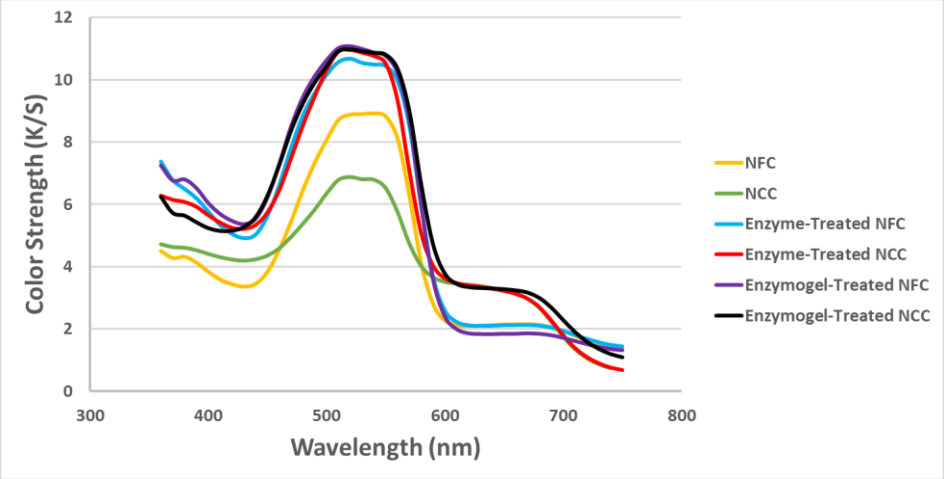

Fig. 3.7. Color strength spectra of NFC and NCC after washing

Table 3.2. Measurements of weight loss (%) after the enzyme and enzymogel treatments

Average (n=5)	NFC Weight Loss (%)	NCC Weight Loss (%)
Enzyme Treatment	10.79 (0.53)	10.17 (0.61)
Enzymogel Treatment	11.24 (1.22)	15.77 (0.88)

Standard deviations are shown in parenthesis.

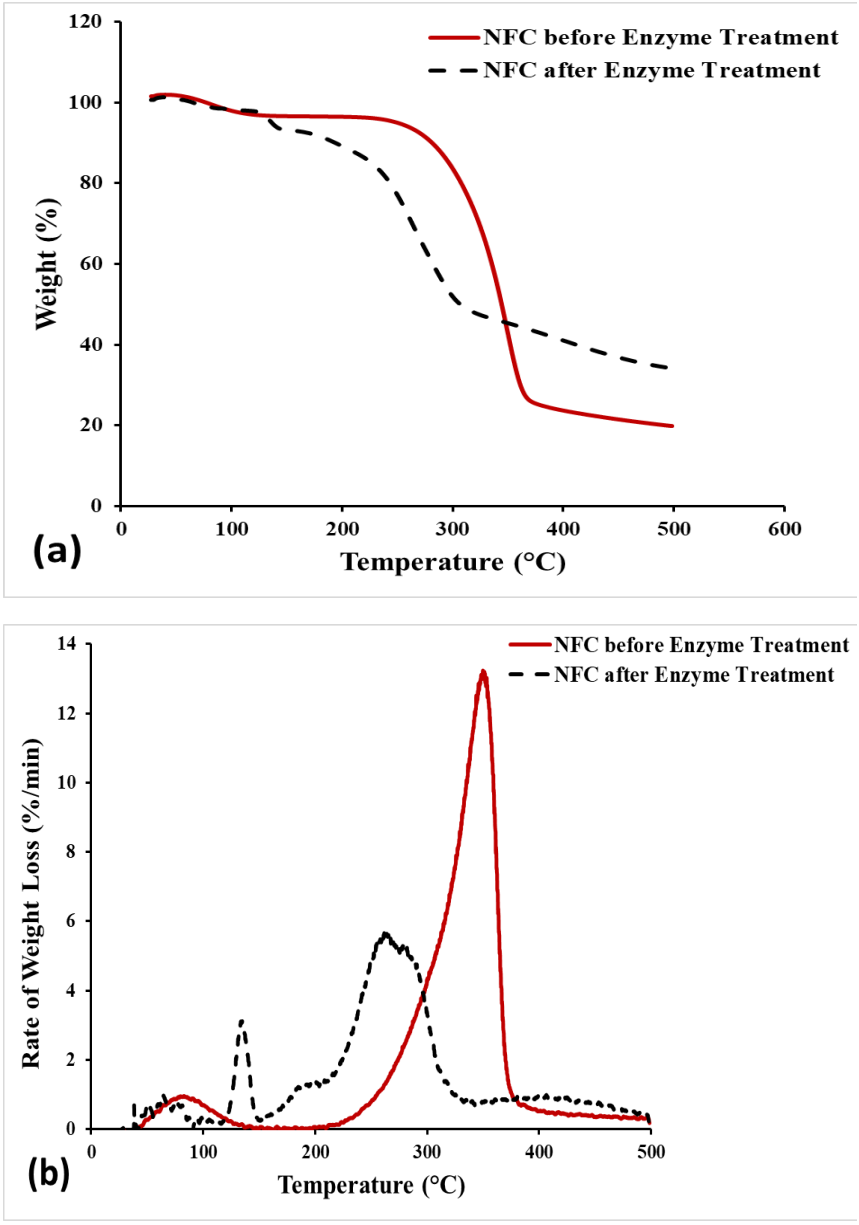

Fig. 3.8. TGA (a) and DTG (b) curves of NFC before and after the enzyme treatment

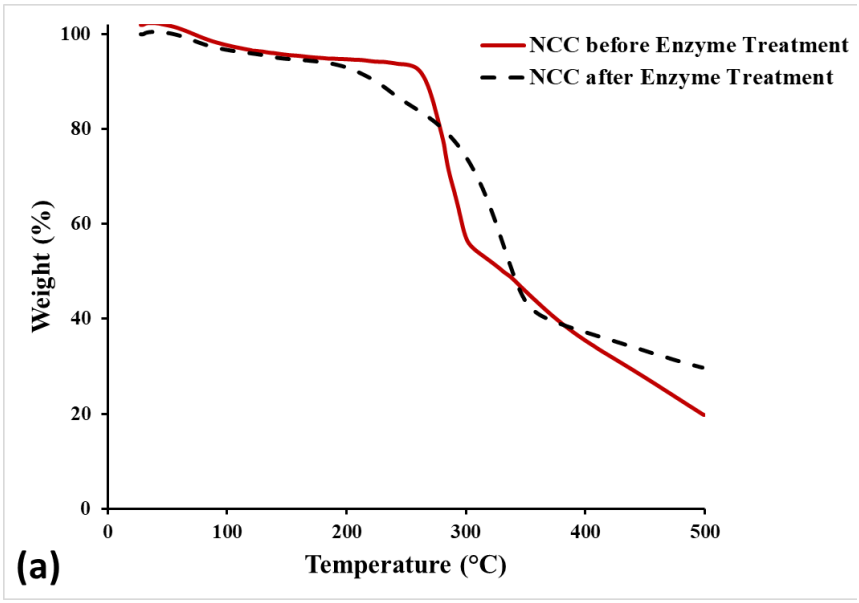

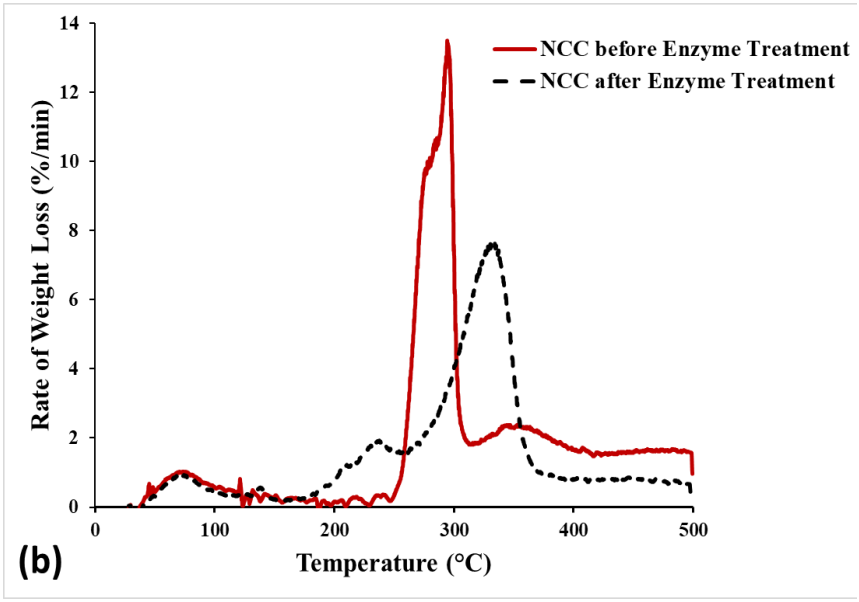

Fig. 3.9. TGA (a) and DTG (b) curves of NCC before and after the enzyme treatment

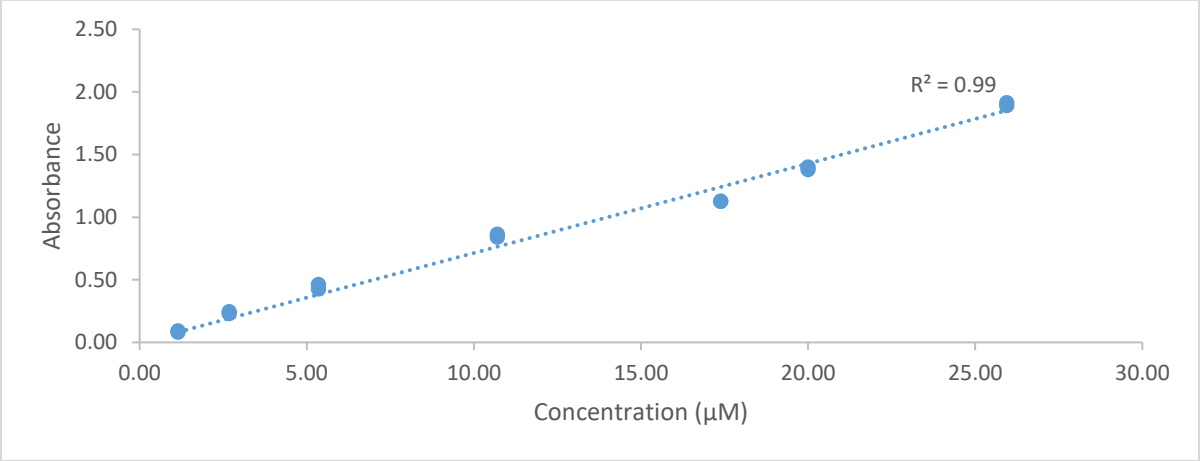

Fig. 3.10. Calibration curve of absorbance vs. concentration of methylene blue

Table 3.3. Methylene blue adsorption and specific surface areas of NFC and NCC samples

	MB Adsorption (mg/g)	S (m2/g)
NFC	257.41	817.28
Enzyme-Treated NFC	289.28	918.46
Enzymogel-Treated NFC	290.60	922.64
NCC	227.86	723.46
Enzyme-Treated NCC	264.91	841.09
Enzymogel-Treated NCC	283.57	900.33

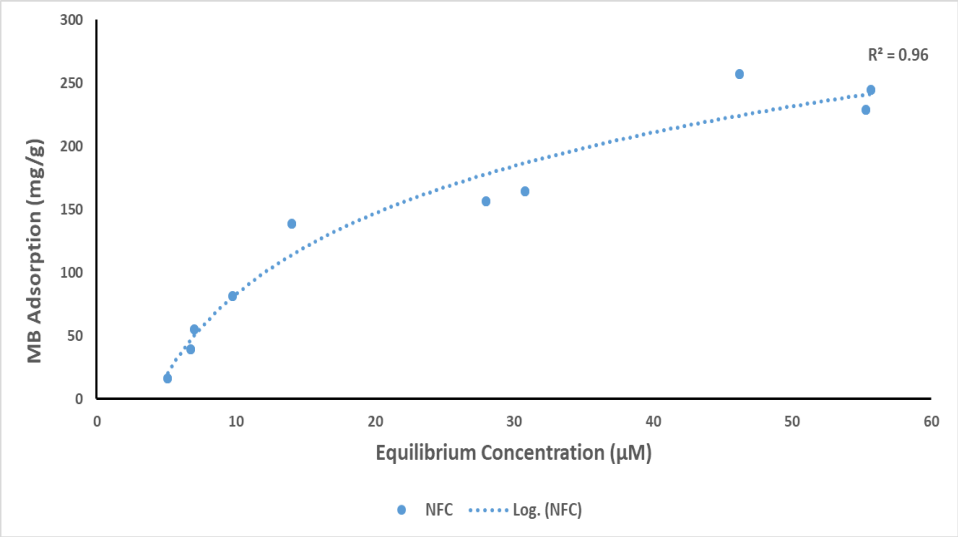

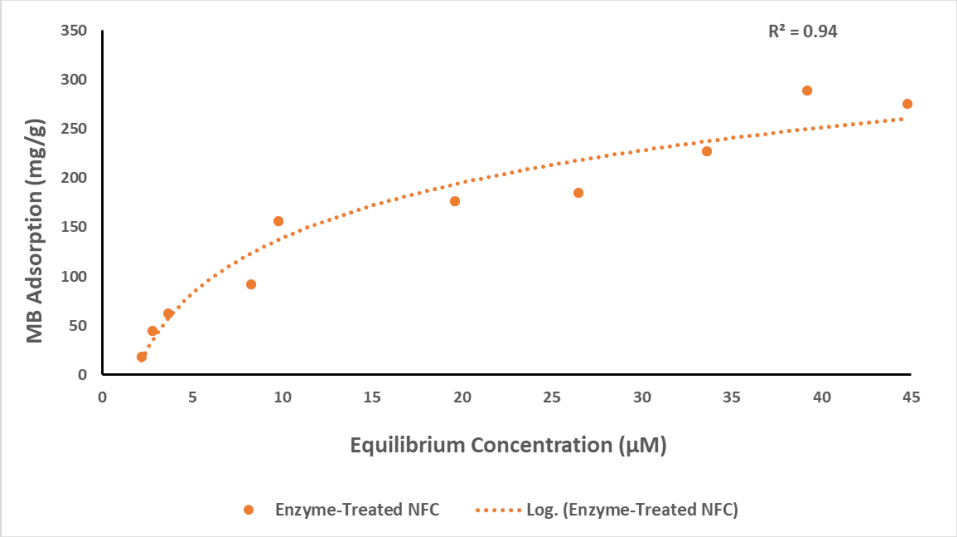

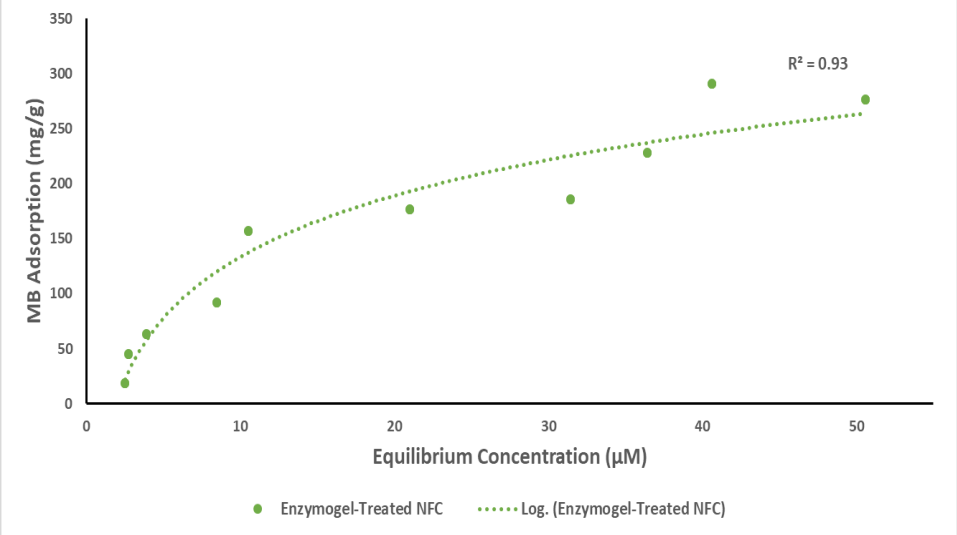

Fig. 3.11. Langmuir adsorption isotherm of Methylene blue on NFC

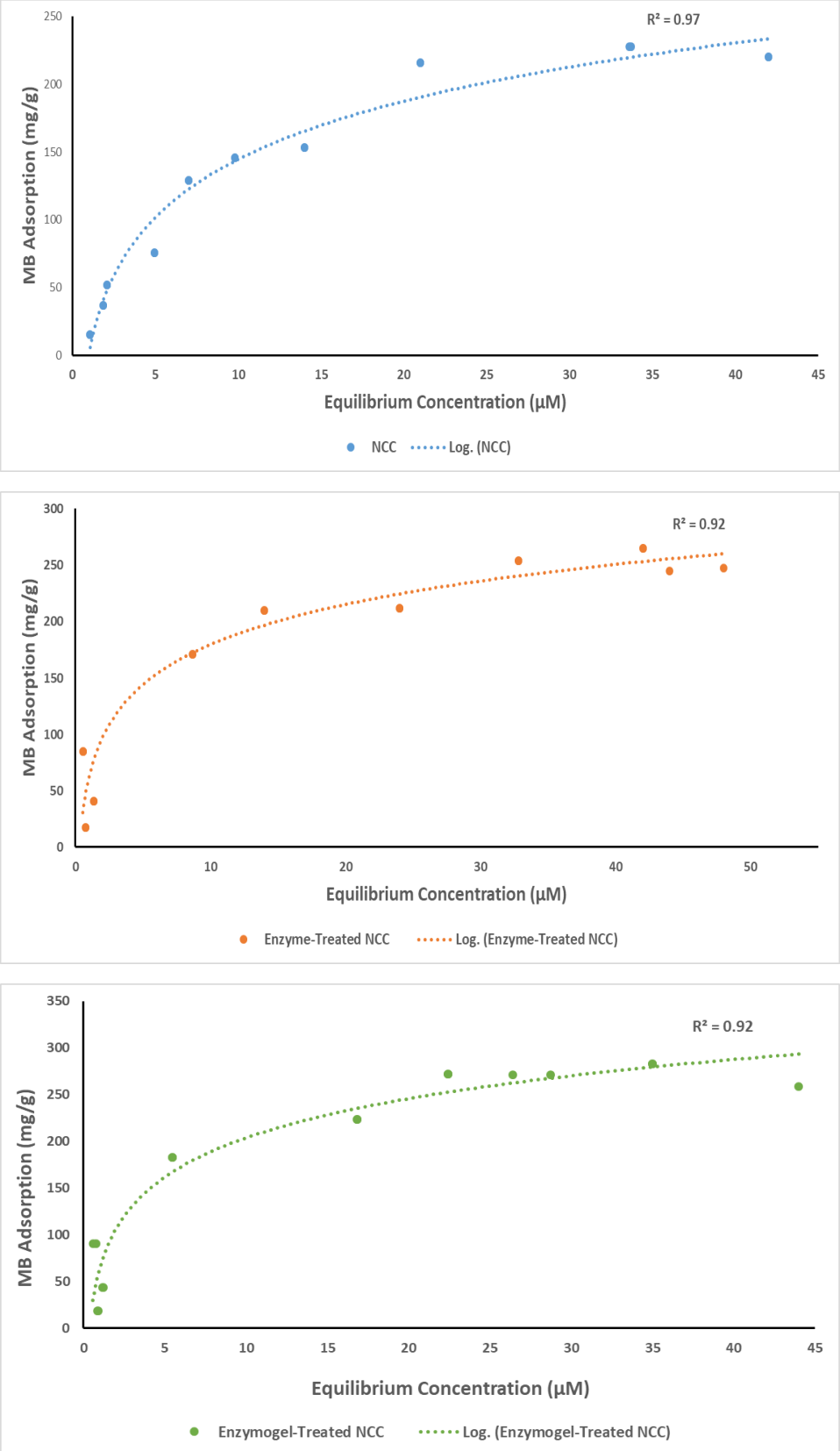

Fig. 3.12. Langmuir adsorption isotherm of Methylene blue on NCC

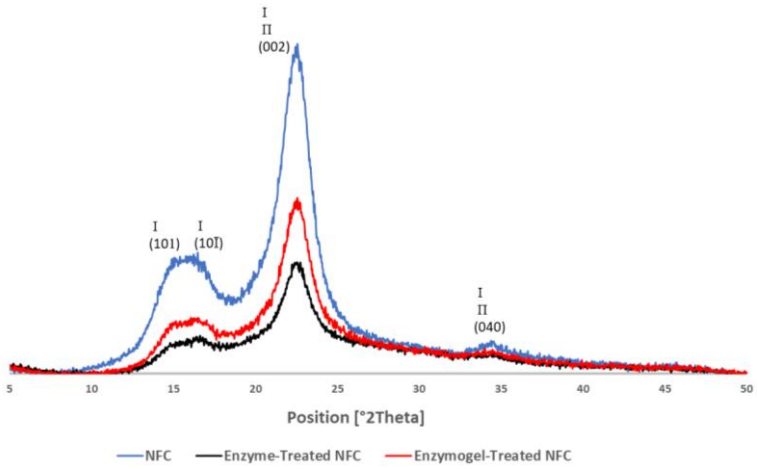

Fig. 3.13. X-ray diffraction patterns of NFC samples

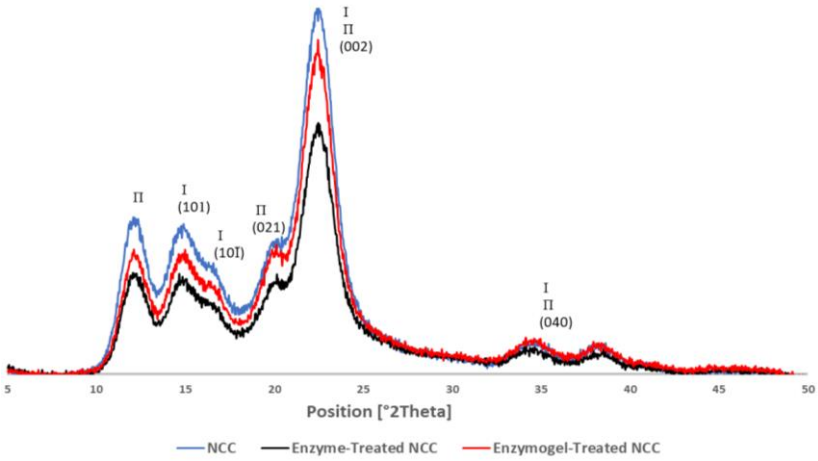

Fig. 3.14. X-ray diffraction patterns of NCC samples

Table 3.4. XRD results of NFC and NCC samples

	Crystallinity (%)	**ACS (Å)**	**FWHM**
NFC	69.33	28.14	2.88
Enzyme-Treated NFC	51.12	19.67	4.12
Enzymogel-Treated NFC	57.98	25.01	3.24
NCC	77.14	33.21	2.44
Enzyme-Treated NCC	71.37	33.76	2.40
Enzymogel-Treated NCC	71.03	32.54	2.49

CHAPTER 4

SUMMARY AND FUTTURE WORK

4.1 Summary

Stable, thin and smooth nanocellulose coatings were developed using two different methods of modifying nanocellulose gels and modifying substrates. The stability of the coatings was analyzed by measuring the thicknesses of the films with AFM and ellipsometry before and after the washing step. Before the modification with the anchoring substances, only cellulose films showed stability after the washing step. After the modification, all the samples had excellent stability, and thicknesses up to 431 nm were achieved. T peel test was conducted to investigate the adhesion between nanocellulose hydrogels and fabrics. And nylon fabrics showed higher peel strength compared to cotton, polyester, and blended fabrics. Then the developed nanocellulose coatings were used to transfer dye molecules to textile surfaces for the development of nanocellulose based sustainable textile dyeing method. Enzyme and enzymogel treatments on nanocellulose were performed before the dyeing step to increase the dyeability of nanocellulose hydrogels. Finally, the effects of cellulase enzymes after enzyme and enzymogel treatments on nanocellulose structure and properties as well as dyeing performance were studied by measuring the weight loss, thermal stability, specific surface area, degree of crystallinity, color strength and dye fixation. The decrease in the degree of crystallinity, increases the amorphous regions of NFC and NCC resulting in the higher values for color strength and dye performance of NFC and NCC after the enzyme and enzymogel treatments. Cellulases by digesting impurities such as polysaccharides as well as making defects in the crystal structures and surface of nanocellulose

that are less active towards the reactive dye, increase the weight loss and consequently increase color strength and dye fixation of NFC and NCC. The enzyme and enzymogel treatments also increased the specific surface areas of NFC and NCC resulting in higher color strength and dye fixation of both samples.

4.2 Future Work

While this dissertation has successfully developed nanocellulose coatings and sustainable dyeing technology for textile materials, there are many ways to improve the quality and properties of final products. Followings are a few examples of future extensions to our work:

Stiffness, resilience, density, thermal characteristics and hand of fabrics after dyeing using the nanocellulose dyeing technique should be investigated and compared to those died with the conventional dyeing method. It can be of interest to investigate the effect of various additives such as poly (ethylene oxide) and poly (ethylene glycol) with different molecular weights on stiffness and hand of fabrics after dyeing with nanocellulose hydrogels. Finally, incorporating other functional molecules or particles such as antimicrobial, flame-retardant and stain-resistant molecules to the nanocellulose coatings will indeed be crucial in designing sustainable and more environmentally friendly functional textiles.